CHARACTERIZATION AND APPLICATION OF TORREFIED MALAYSIA BIOMASS AS A BIOFUEL FOR GASIFICATION

FAKHRUR RAZIL ALAWI BIN ABDUL WAHID

Master of Science

UNIVERSITI MALAYSIA PAHANG

UNIVERSITI MALAYSIA PAHANG

DECLARATION OF THESIS AND COPYRIGHT

Author's Full Name   : FAKHRUR RAZIL ALAWI BIN ABDUL WAHID

Date of Birth   : 02 JUNE 1991

Title   : CHARACTERIZATION AND APPLICATION OF TORREFIED MALAYSIA BIOMASS AS A BIOFUEL FOR GASIFICATION

Academic Session   : SEM 2 2018/2019

I declare that this thesis is classified as:

☐ CONFIDENTIAL   (Contains confidential information under the Official Secret Act 1997)*

☐ RESTRICTED   (Contains restricted information as specified by the organization where research was done)*

☑ OPEN ACCESS   I agree that my thesis to be published as online open access (Full Text)

I acknowledge that Universiti Malaysia Pahang reserves the following rights:

1. The Thesis is the Property of Universiti Malaysia Pahang
2. The Library of Universiti Malaysia Pahang has the right to make copies of the thesis for the purpose of research only.
3. The Library has the right to make copies of the thesis for academic exchange.

Certified by:

_____   _____
(Student's Signature)   (Supervisor's Signature)

FAKHRUR RAZIL ALAWI BIN ABDUL   DR. SURIYATI BINTI SALEH
WAHID   Date:
910602-03-5407
Date:

NOTE : * If the thesis is CONFIDENTIAL or RESTRICTED, please attach a thesis declaration letter.

SUPERVISOR'S DECLARATION

We hereby declare that we have checked this thesis and in our opinion, this thesis is adequate in terms of scope and quality for the award of the degree of Master of Science.

_____

(Supervisor's Signature)

Full name   : DR. SURIYATI BINTI SALEH
Position   : SENIOR LECTURER
Date   :

_____

(Co-supervisor's Signature)

Full name   : DR. NOOR ASMA FAZLI BIN ABDUL SAMAD
Position   : SENIOR LECTURER
Date   :

STUDENT'S DECLARATION

I hereby declare that the work in this thesis is based on my original work except for quotations and citations which have been duly acknowledged. I also declare that it has not been previously or concurrently submitted for any other degree at Universiti Malaysia Pahang or any other institutions.

_____

(Student's Signature)

Full Name   : FAKHRUR RAZIL ALAWI BIN ABDUL WAHID

ID Number   : MKC15027

Date   :

CHARACTERIZATION AND APPLICATION OF TORREFIED MALAYSIA
BIOMASS AS A BIOFUEL FOR GASIFICATION

FAKHRUR RAZIL ALAWI BIN ABDUL WAHID

Thesis submitted in fulfilment of the requirements
for the award of the degree of
Master of Science

Faculty of Chemical and Natural Resources Engineering

UNIVERSITI MALAYSIA PAHANG

APRIL 2019

DEDICATION

In the name of Allah, Most Gracious, Most Merciful
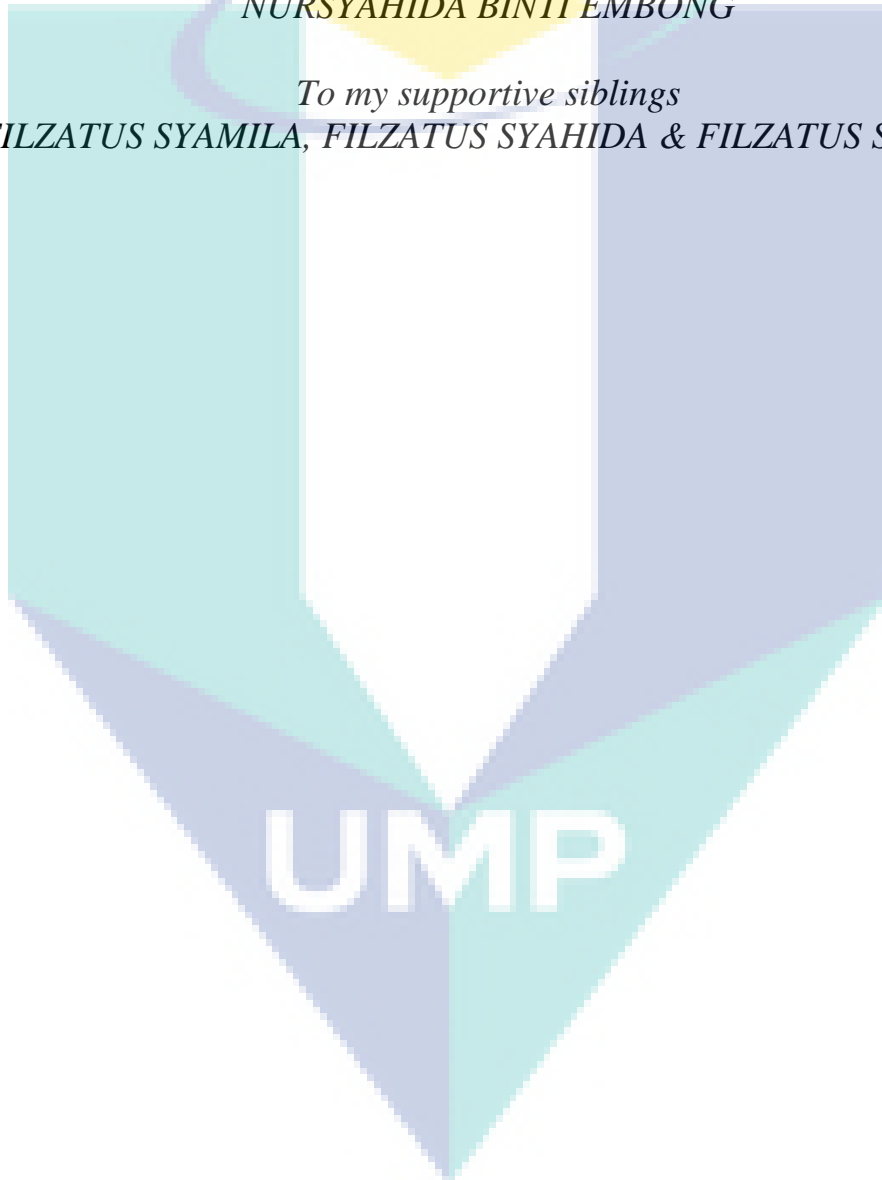

To my beloved parents
ABDUL WAHID BIN MD ALI & JUNIATI BINTI MOHD NOOR

To my lovely wife
NURSYAHIDA BINTI EMBONG

To my supportive siblings
FILZATUS SYAMILA, FILZATUS SYAHIDA & FILZATUS SABIHA

ACKNOWLEDGEMENTS

First and foremost, I would like to express my gratitude to Him, Allah S.W.T for the inspiration, encouragement and strength given to me throughout the completion of this thesis. With His blessing, I finally able to finish this research successfully. I owe my deepest gratitude and heartily thankful to my supervisor, Dr. Suriyati binti Saleh and co-supervisor, Dr Noor Asma Fazli bin Abdul Samad, for constantly guiding and encouraging me throughout this study. Thanks for all the push that are given to me, without it I don't know what will happen and keeps me want to change and do my best in finishing this thesis and do my best in life. Thanks a lot for guiding and teaching me throughout the period when I am in your care.

Heartfelt thanks and appreciation also goes to my lovely parents, Abdul Wahid Bin Md Ali and Juniati Binti Mohd Noor. Not to forget my siblings and Nursyahida Binti Embong who keeps giving moral support when I'm in the slump. My sincere appreciation also extended to Bilal Muslim, Huda Harun, Zakirah Zahari and my fellow colleagues for willingness to help and supported me throughout completion of this research. Their views and tips are very useful indeed. Unfortunately, it is not possible to list all of them in this limited space. Last but not least, I want to thank all the persons who involved in this studies whether it is directly or indirectly in order to complete this thesis successfully. Thank you all very much.

ABSTRAK

Lambakan sisa kelapa sawit dari industri minyak kelapa sawit dan sisa hutan dari aktiviti pembalakan mengakibatkan masalah sisa buangan. Walau bagaimanapun, ia boleh digunakan sebagai sumber tenaga baru dan boleh ditingkatkan bagi menangani kelemahan biojisim dengan menggunakan proses torefaksi. Torefaksi adalah proses pemanasan pada suhu rendah antara 200 °C – 330 °C dalam keadaan lengai. Biojisim yang telah dirawat dengan torefaksi menunjukkan peningkatan ciri-ciri biojisim tersebut dan sesuai untuk proses penggasan. Setiap kumpulan biojisim mempunyai ciri-ciri tersendiri, maka kajian terhadapnya adalah penting. Sebagai sumber tenaga, nilai haba tinggi adalah penting dan untuk menentukan nilai ini memakan masa yang lama dan terdedah kepada ralat. Masalah ini boleh diselesaikan dengan memperkenalkan korelasi nilai haba tinggi. Objektif kajian ini adalah untuk mengkaji kesan proses torefaksi terhadap suhu dan masa yang berlainan kepada beberapa jenis biojisim, membangunkan korelasi untuk meramal nilai haba tinggi berdasarkan ciri-ciri kimia biojisim dan untuk menunjukkan penggunaan penggasan biojisim menggunakan biojisim dalam keadaan mentah dan *torrefied*. Sumber biojisim adalah dari sisa kelapa sawit (pelepah sawit, tandan buah kosong, gentian mesokarpa sawit dan tempurung kelapa sawit) serta sisa hutan (habuk kayu meranti, seraya, kulim dan chengal). Biojisim telah dibakar dalam tiub reaktor pada empat suhu yang berbeza (240, 270, 300 dan 330 °C) dengan kehadiran nitrogen pada tiga masa yang berlainan (15, 30 dan 60 minit). Pencirian biojisim mentah dan *torrefied* seperti nilai haba tinggi, jisim dan hasil tenaga, analisis hampiran dan analisis muktamad telah dijalankan. Data analisis digunakan dalam menganggar korelasi nilai haba tinggi dan simulasi penggasan lapisan terbendalir. Berdasarkan hasil jisim dan tenaga, masa yang sesuai untuk *torrefied* kedua-dua jenis biojisim adalah pada 30 minit. Untuk analisis muktamad, komposisi karbon untuk kedua-dua sisa kelapa sawit dan sisa hutan memperlihatkan kenaikan manakala komposisi hidrogen dan oksigen menunjukkan penurunan. Dalam analisis hampiran, karbon tetap meningkat sehingga 56 wt% untuk sisa kelapa sawit dan 47 wt% untuk sisa hutan. Nisbah hidrogen ke karbon dan oksigen ke karbon menunjukkan penurunan nilai. Akhir sekali, untuk nilai haba tinggi, nilainya meningkat kerana faktor peningkatan HHV dapat mencapai 1.58 dan 1.41 untuk sisa minyak sisa dan sisa hutan. Bagi model yang meramalkan nilai haba tinggi, korelasi linear berdasarkan analisis hampiran menghasilkan anggaran terbaik manakala untuk sisa kelapa sawit (ralat purata mutlak (AAE): 5.37%) dan sisa hutan (AAE: 10.37%). Dengan menggunakan data yang diperoleh dalam simulasi penggasan, dicatatkan bahawa biojisim terbaik untuk sisa kelapa sawit adalah pelepah sawit (OPF) manakala untuk sisa hutan adalah habuk kayu kulim. Analisis lanjut menunjukkan bahawa kedua-dua biojisim menghasilkan hidrogen tertinggi apabila suhu pada 700 °C, mempunyai nilai 0.2 untuk nisbah udara kepada biojisim (ABR) dan 1.0 untuk nisbah wap kepada biojisim (SBR). Menggunakan keadaan operasi tersebut, kecekapan gas sejuk (CGE) dan nilai haba rendah (LHV) untuk gas sintesis dapat dikira. Perubahan CGE untuk pelepah sawit berada dalam lingkungan 0.85% hingga 6.29%, manakala untuk Kulim, kenaikan adalah dari 3.0% hingga 8.6%. Untuk LHV gas sintesis, kedua-dua biojisim mempunyai LHV hampir sama kecuali pada keadaan mentah, *torrefied* pada suhu 240 °C dan *torrefied* pada 270 °C. Pada keadaan tersebut, Kulim menunjukkan perbandingan LHV yang lebih tinggi daripada OPF dengan perbezaan 0.01 MJ/kg. Dengan membandingkan kedua-dua jenis biojisim (OPF dan Kulim), Kulim dipilih menjadi biojisim yang terbaik untuk penggasan dan dalam keadaan *torrefied*.

ABSTRACT

Abundances of oil palm waste from palm oil industry and forestry residue from logging activity leads to disposal problems. However these waste can be used as a renewable energy resources and can be upgraded to tackle biomass disadvantages through torrefaction process. Torrefaction is a process of heating at low temperature ranging from 200 – 300 °C under inert condition. Pre-treated biomass with torrefaction consequently upgrades the properties of biomass making it suitable for gasification. Different group of biomass have different properties thus it is essential to study the biomass characteristic. For biofuel, higher heating value (HHV) is important and the process to determine HHV is time consuming and prone to errors. This problem could be solved by introducing HHV correlations. Thus, the objectives of this study are to investigate the effect of torrefaction process at different temperatures and residence time for several types of biomass, to estimate correlations of higher heating value based on chemical properties of the biomass, and to apply biomass gasification using raw and torrefied biomass. The sources of biomass are from oil palm waste (oil palm frond, empty fruit bunch, palm mesocarp fibre and palm kernel shell) and forestry residue (meranti, seraya, kulim and chengal sawdust). Biomass torrefaction process was conducted in a tubular reactor at four different temperatures (240, 270, 300 and 330 °C), in an inert nitrogen atmosphere at three different residence time (15, 30 and 60 minutes). The torrefied biomass products were characterized in terms of heating value, mass and energy yield, proximate and ultimate analysis. The obtained data were then used to estimate the higher heating value correlations and served as the starting information for a fluidized bed gasification simulation run. Based on the result of mass and energy yields, the optimum residence time used for both biomass are at 30 minute. From the ultimate analysis, the carbon composition for both oil palm waste and forestry residue show an increasing trends while hydrogen and oxygen compositions for both types of biomass show decreasing trends. From proximate analysis, fixed carbon is increased up to 56 wt% for oil palm waste and 47 wt% for forestry residue. For hydrogen to carbon and oxygen to carbon ratios, it showed a decreasing trend. The higher heating value increased as the enhancement factor for HHV reached up to 1.58 and 1.41 for oil palm waste and forestry residue respectively. On model development for the prediction of higher heating value, linear correlation based on proximate analysis gives the best estimate for oil palm waste (average absolute error (AAE): 5.37%) and forestry residue (AAE: 10.37%). Through gasification simulation, it is noted that the best biomass to be used from oil palm waste is oil palm frond (OPF) while for forestry residue is Kulim sawdust. Further analysis shows that both biomass produced the highest hydrogen gas when it is operated at gasification temperature of 700 °C, air to biomass ratio (ABR) of 0.2 and steam to biomass ratio (SBR) of 1.0. Using this operating condition, cold gas efficiency (CGE) and lower heating value (LHV) of the syngas are calculated. CGE changes for OPF is in the range of 0.85% to 6.29%, while for Kulim sawdust, the increment is from 3.0% to 8.6%.Both biomass have almost similar LHV except for the biomass at raw condition, torrefied at 240 °C and torrefied at 270 °C. Kulim sawdust shows a higher LHV than OPF with the different of 0.01 MJ/kg. By comparing both types of biomass (OPF and Kulim sawdust), Kulim sawdust is chosen to be the best biomass to be gasified under torrefied condition.

TABLE OF CONTENT

LIST OF TABLES

LIST OF FIGURES

LIST OF SYMBOLS

α	Mechanism factor
β	Fraction of steam consume by reaction
m_i	Initial mass of biomass
m_f	Final mass of biomass
m_t	Weight of crucible and biomass
m_c	Weight of crucible
N	Total number of sample
i	Specific sample of a biomass
y_e	Mass fraction of experimental biomass
y_p	Mass fraction of predicted biomass
t_{dif}	Temperature different
W	constant value (2409.26 cal/°C)
b_{fuse}	Length of burn fuse wire
m	Mass of biomass
LHV_{PG}	Lower heating value of product gas
LHV_{Bio}	Lower heating value of biomass
$\dot{m}_{PG}$	Mass flow rates of product gas
$\dot{m}_{Bio}$	Mass flow rates of biomass
χ_{CO}	Composition of carbon monoxide
χ_{H2}	Composition of hydrogen
χ_{CH4}	Composition of methane

LIST OF ABBREVIATIONS

OPW   Oil palm waste

FR   Forestry residue

C   Carbon

H   Hydrogen

N   Nitrogen

O   Oxygen

S   Sulphur

FC   Fixed carbon

VM   Volatile matter

MC   Moisture content

HHV   Higher heating value

H/C   Hydrogen to carbon ratio

O/C   Oxygen to carbon ratio

ABR   Air to biomass ratio

SBR   Steam to biomass ratio

CGE   Cold gas efficiency

LHV   Lower heating value

RMSE   Root mean square error

AE   Absolute error

AAE   Average absolute error

CHAPTER 1

INTRODUCTION

1.1   Background

Today, various forms of biomass energy are utilized all over the world to meet the energy demands and as alternative to substitute the depletion of fossil fuel. This is due to the fact that biomass provides a clean, renewable energy source, little or no net carbon dioxide which can help to reduce greenhouse gas (GHG) emission to the atmosphere. In particular, conversion of non-edible biomass such as agriculture residues, wood chips, fruit bunches, stalks, and industrial and municipal solid wastes into fuels and useful chemicals would solve waste disposal and energy issues. Currently Malaysia is the world second largest palm oil producer after Indonesia with production capacity of 18.75 Mt in 2015 (Sabil et al., 2013). The palm oil fruits produce only 10% of palm oil whereas the other 90% remains as biomass waste in the form of mainly Empty Fruit Bunch (EFB), Palm Kernel Shell (PKS) and Mesocarp Fibre (PMF). Approximately the amounts of oil palm waste are 9.66, 5.20, and 17.08 million tonnes of fibres, shell, and EFB, respectively (Sabil et al., 2013). This number is expected to increase yearly due to expansion of oil palm field in order to meet the increase demands of oil palm. In addition, due to the oil palm harvesting activity, the amount of oil palm frond waste is increasing which ultimately led to disposal problem. In order to utilize these oil palm waste, current practices show that the EFB and PKS are used as fuel for steam production at palm oil mills and in some extent as organic fertiliser while oil palm frond (OPF) is usually retained in the plantations and left to decompose naturally for nutrient replacement or mulching purposes. Meanwhile, Malaysia's annual log production in 2010 was estimated to be 24 million m^3 (Malaysian Timber Industry Board, 2012). By multiplying with 0.78 (ratio of wood waste), wood waste generated was estimated to be about 18 million m^3/year (The Japan Institute of Energy, 2008).

Thus the high potential value of this waste to be used for more lucrative purposes is often being ignored and remains untapped.

In order to overcome this problem, thermochemical conversion technologies can be employed to convert oil palm waste for energy recovery while addressing disposal problem. Gasification has emerged as an alternative to traditional combustion applications due to its ability to produce better energy efficiency and lower environmental impact. Technically biomass gasification is a process whereas the biomass undergone chemical conversion to produce fuel gas or syngas which consists of carbon dioxide (CO_2), carbon monoxide (CO), hydrogen (H_2) and traces of methane (CH_4). This process is occurred when there are air; oxygen and/or steam present and involves partial oxidation of the feed in a reduction atmosphere. The hydrogen from syngas after cleaning up or purification step can be used in many ways including heat and gas provider, electricity generation and chemical synthesis. The hydrogen obtained in this way is more sustainable compare to hydrogen produced from fossil fuels because of the low conversion efficiency of fossil fuels. Although hydrogen gas can be produced from those gasifiers, there is a concern on the low energy efficiency and low fuel quality. This is due to the fact that raw oil palm waste particularly empty fruit bunch contains high moisture content between 30 – 40%, low bulk density, high O/C ratio and relatively low calorific value.

One of the ways to improve the fuel properties (characterized by higher heating value, ultimate analysis and proximate analysis) is by using torrefaction process. Torrefaction is a pre-treatment method to upgrade raw biomass to a refined fuel with improved properties such as higher heating value and carbon content. Torrefaction is usually carried out at temperature in the range of 200 – 300 °C for residence time between 30 – 60 minutes under inert environment at atmospheric pressure. As a result of torrefaction, biomass exhibits brittle behaviour and a reduction in mechanical strength thus eliminating poor grindability problem of raw biomass. Besides, torrefaction increases energy value of torrefied biomass due to the increment of carbon content. It also reduces the moisture content and hemicellulose content in biomass so that the shelf life of biomass is increased as no biodegradation occur during the storage. Because of these improved properties, the value in terms of carbon content and heating value of the torrefied biomass as a fuel is significantly higher than the raw biomass.

1.2   Motivation and problem statement

Many of the problems in biomass gasification are related to the properties of the fuel (biomass). For example, oil palm waste contain high moisture content around 30 – 40%. Usually a high moisture level in a raw oil palm waste leads to a high energy loss during the gasification. In addition raw biomass usually have high O/C ratios (high atom O and low atom C in the chemical formula) which lowering the gasification efficiencies. In order to increase the energy efficiency, improve the energy product quality and reduce the emissions in the thermochemical energy conversion process, the reduction of biomass moisture content plays a vital role. Therefore rather than gasifying these biomass directly, a suitable pre-treatment is necessary to modify their properties prior to gasification.

Several studies have been performed related to the efficiency of biomass gasification using torrefied biomass. For example, Kuo et al. (2014) evaluated a two-stage gasification process for raw and torrefied bamboo under isothermal conditions. It was reported that the carbon conversion and synthesis gas yield are higher for torrefied materials than the raw biomass. Their study indicates that torrefied biomass at 250 °C was found to be the most feasible fuel for gasification. Meanwhile Tapasvi et al. (2015) simulated two-stage biomass gasification model in Aspen Plus using raw Leucaena wood and torrefied Leucaena wood as a feedstock. Their study reported the torrefied Leucaena at 300 °C with residence time of 30 minutes produce a higher synthesis gas especially hydrogen gas compared to raw Leucaena. Thus, there is a considerable lack of information on the behaviour of torrefied biomass in terms of the best torrefaction temperature and residence time and the behaviour of torrefied material is then depending on the biomass itself. Uemura et al. (2011), Matali et al. (2016) and Aziz et al. (2012), data for oil palm waste can be used as benchmark, while the data of forestry residue are lacking. As such, the lacks of data for forestry residue mainly from Malaysia origin can be further studied.

Higher heating value (HHV) is an important property of a fuel as a measure of energy content. Bomb calorimeter is usually used to determine the HHV of a fuel. This method of determining HHV is sophisticated and prone to errors. In order to avoid such difficulties, correlations have been developed to estimate the HHV of biomass by using proximate and ultimate analysis to be used as an alternatives. The methods for estimating HHV dates back to the late 1800s where the first correlation is introduced

3

based on the ultimate properties of coal. Ultimate analysis gives elemental composition of biomass and needs special arrangement of the experimentation. Meanwhile proximate analysis gives the information of fixed carbon, volatile matter and ash content of the biomass and the method is relatively simple and cheap compare to ultimate analysis. That is why the popularity of estimating HHV using proximate analysis is on the rise. However, the estimated HHV from published correlations only consider raw biomass and not the torrefied biomass. Although the published correlations by Channiwala & Parikh (2002), Sheng & Azevedo (2005) and Yin (2011) cover wide ranges of biomass from various country, it does not guarantee the accuracy of HHV for torrefied biomass. Using established correlations to estimate the HHV of torrefied biomass often yields a significance error when compare to the measured HHV. Thus, a correlations can be made to estimate the HHV of both raw and torrefied biomass by modifying the established correlations.

1.3   Objectives

The objectives of this study are as follows:

1. To study the effect of different torrefaction temperatures and residence times on the changes of physical and chemical properties using oil palm waste and forestry residue.
2. To develop model for predicting higher heating value based on the ultimate analysis and proximate analysis.
3. To evaluate the effectiveness of torrefied biomass as an input for biomass gasification for producing synthesis gas by using Aspen Plus simulation software.

1.4   Scopes

The scopes of this study are as follows:

1. The biomass used are oil palm waste (oil palm frond, palm mesocarp fibre, palm kernel shell and empty fruit bunch) and forestry residue (meranti, seraya, kulim and chengal sawdust) which are torrefied at different temperatures ranges from 240 to 330 °C and residence times of 15, 30 and 60 minutes. The analysis of raw and torrefied biomass in

terms of ultimate analysis, proximate analysis, higher heating value, oxygen to carbon ratio and hydrogen to carbon ratio.

2. The models development for estimating higher heating value are using the proximate and ultimate analysis of raw and torrefied biomass.

3. The fluidized bed gasification model is simulated using raw and torrefied biomass as the inputs and the Lower Heating Value (LHV) and Cold Gas Efficiency (CGE) are evaluated.

1.5   Thesis organization

The thesis has been arranged as follows:

Chapter 1 provides the purpose of this study by explaining the background of this study as well as the objectives and scopes. Chapter 2 provides general overview of biomass, torrefaction as pre-treatment method, properties for torrefied biomass, review on the published correlation model and biomass gasification technologies.

Chapter 3 includes the overall torrefaction experimental procedures, data analysis procedures for measuring the higher heating value (HHV), proximate analysis and ultimate analysis. In addition the work flow for developing model correlation to estimate HHV using ultimate and proximate analysis as well as gasification based on simulation are explained in Chapter 3.

For Chapter 4, the results obtained from torrefaction experiments are discussed in terms of its physical appearances, mass and energy yields, proximate analysis, ultimate analysis and higher heating value. The new correlation models for predicting HHV using data of proximate analysis and ultimate analysis are presented in Chapter 4.

In Chapter 5, the application of the fluidized bed gasification is highlighted using raw and torrefied oil palm waste and forestry residue where the effects of gasification operating conditions on the synthesis gas production are investigated. Finally, some conclusions and recommendations for future works are summarized in Chapter 6.

CHAPTER 2

LITERATURE REVIEW

2.1   Biomass

Biomass primarily consists of cellulose, hemicellulose, lignin and other compounds such as proteins, minerals, starches, water, hydrocarbons and ash. The composition of these constituents in the biomass varies with species, age and growth conditions. The plant cell wall is tough and sometimes fairly rigid layer that provides structural support and protection from mechanical and thermal stresses (Tumuluru et al., 2011). Cellulose is the main cell wall component in the plant biomass followed by hemicellulose and lignin. The range of cellulose content in the biomass is from 40 – 50 wt%, while hemicelluloses and lignin typically in the ranges from 20 – 30 wt% and 15 – 30 wt% respectively. In Malaysia there are a lot of biomass sources that can be exploited as renewable energy source. Table 2.1 shows the types of renewable energy in Malaysia and its estimated energy value for each types of renewable energy. As shown in Table 2.1, the forestry residue and oil palm waste have been identified as the top renewable energy source with the highest energy value around RM 11,883 million and RM 6,291 million respectively. However the use of both forestry residue and oil palm waste for energy related applications are still not fully exploited and there is plenty room for optimizing the utilization of both biomass into more profitable application.

Table 2.1 Types of renewable energy in Malaysia and its energy value

Renewable Energy Source	Energy Value in RM million (annual)
Forestry residue	11,883
Oil palm	6,291
Mill residues	932
Municipal waste	233

Source: Fazeli et al. (2016)

In order to utilize oil palm waste or forestry residue as alternative biofuel, there are variety of methods can be used such as gasification, pyrolysis, anaerobic digestion, fermentation and transesterification. However, both oil palm waste and forestry residue cannot be used directly as a fuel due to low heating value and low bulk density. Furthermore the high moisture content presents in oil palm waste and forestry residue and their ability to absorb moisture from the surrounding atmosphere increase the costs of thermochemical conversion due to the drying process. As consequence low conversion efficiency is obtained when using oil palm waste and forestry residue directly. For those reasons, biomass needs to be pre-treated before it can be converted into high-value-added products.

Pre-treatment process is used to improve the biomass properties. There are several pre-treatment methods such as physical (comminution), biological, chemical and physicochemical (Agbor et al., 2011). To upgrade the biomass, comminution is not suitable as it involves only on the physical aspects of biomass such as size reduction. As for biological method, the use of fungi takes a lot of time and not suitable for industrial purpose. Chemical pre-treatment involves using the organic solvents, acid, alkali and ionic liquids. By using chemicals, it have significant effect on the structure of the biomass itself. Thus, it is not suitable for all type of biomass. Physicochemical pre-treatment have a wide variety of technologies such as liquid hot water pre-treatment, wet oxidation pre-treatment, ammonia recycle percolation and torrefaction. Among these technologies, torrefaction can be used on the wide ranges of biomass.

2.2 Torrefaction

Torrefaction is a feasible method for improving the properties of biomass as a fuel. As defined in most of studies, torrefaction is a thermal conversion method of biomass which operate at low temperature (200 – 320 °C) under atmospheric conditions in the absence of oxygen (Pimchuai et al., 2010; Almeida et al., 2010; Repellin et al., 2010). This process improves the physical, chemical and biochemical composition of the biomass which improves the performance for combustion and gasification processes (Tumuluru et al., 2011; Medic et al., 2012; Pimchuai et al., 2010). Torrefaction is also known as roasting, slow and mild pyrolysis, wood cooking and high temperature drying (Medic et al., 2012). Torrefaction converts raw biomass into a solid that is suitable for combustion and gasification applications, which has a higher heating value,

hydrophobic, compactable and grindable, and has a lower oxygen-to-carbon (O/C) ratio than the raw biomass (Medic et al., 2012; Pimchuai et al., 2010; van der Stelt et al., 2011). The value of fixed carbon (FC), volatile matter (VM) and higher heating value (HHV) for different types of biomass is shown in Table 2.2. From Table 2.2, it has been observed that torrefaction is definitely able to increase the value of FC and HHV and to decrease the VM value. The increment of FC and HHV usually is preferable for gasification or combustion processes due to the fact that the biomass is more combustible which contributing to the more energy production.

Table 2.2 List of fixed carbon (FC), volatile matter (VM) and higher heating value (HHV) of various type of biomass

Biomass	T (°C)	t (min)	FC (wt%)	VM (wt%)	HHV (MJ/kg)	Reference
Bagasse						
Raw	-	-	14.6	80.7	18.3	Chen et al., (2012)
Torrefied	200	60	25.9	66.8	20.9	
	300	60	42.2	45.9	23.4	
Bamboo						
Raw	-	-	17.8	80.1	18.2	Rousset et al., (2011)
	220	60	22.5	75.2	19.3	
Torrefied	250	60	29.2	67.9	21.0	
	280	60	37.8	58.8	23.1	
Eucalyptus						
Raw	-	-	9.4	89.8	19.4	
	240	30	22.3	77.0	22.2	
	240	60	23.4	75.6	21.8	Arias et al., (2008)
	240	180	23.9	75.1	21.9	
Torrefied	280	30	30.6	68.3	23.4	
	280	60	35.5	62.8	25.0	
	280	180	37.0	61.4	25.9	

During torrefaction, mass loss of biomass is dominantly based on the decomposition of hemicellulose and some of lignin constituent. Hemicellulose undergoes major decomposition reactions at torrefaction temperatures of 200 – 300 °C, resulting in producing volatile components in the forms of condensable and non-condensable volatile products. Thermal degradation of hemicellulose initiates at 150 °C, with the majority of weight loss occurring above 200 °C, depending on the chemical nature of the hemicelluloses (van der Stelt et al., 2011; Demirbas, 2009). Hemicellulose generally evolves as light volatiles, producing fewer tars and less char. Many researchers have noted that major hemicellulose decomposition reactions occur at temperature range between 220 and 280 °C. Cellulose degradation occurs at temperature range between 240 and 350 °C, resulting in anhydrous cellulose and

levoglucosan. Amorphous regions in the cellulose contain waters of hydration and hold free water within the plant. When it is heated rapidly, this water is converted to steam, which can further rupture the cellulose structure (Tumuluru et al, 2011). Thermal degradation of lignin takes place over a wide range of temperature (Saleh et al., 2013). At temperatures below 200 °C, some thermal softening has been observed resulting in a small weight loss of a few percent. Char formation and the release of volatiles result from a devolatilisation process in the temperature region of 240 – 600 °C (Tumuluru et al, 2011; van der Stelt et al., 2011).

During torrefaction, three different products are produced: (1) a brown to black solid biomass, which is often used for combustion in a boiler (bioenergy applications), (2) condensable volatile organic compounds comprising water, acetic acid, aldehydes, alcohols, and ketones, and (3) non-condensable gases like carbon dioxide (CO_2), carbon monoxide (CO), and small amounts of methane (CH_4) (Tumuluru et al, 2011). The condensable (liquid) can be further divided into four groups which are reaction water produced from thermal decomposition, freely bound water that has been released through evaporation, organics (in liquid form) which consist of organics produced during devolatilization and carbonization, and lipids which contain compounds such as waxes and fatty acids (Tumuluru et al, 2011). The emissions of condensable and non-condensable products are depending on heating rate, torrefaction temperature, residence time, and biomass composition. The release of these condensable and non-condensable products results in the changes in terms of the physical, chemical, and storage properties of biomass (Saleh et al., 2013).

2.3   Properties of torrefied biomass

In this section, the important properties of torrefied biomass are explained in terms of physical appearances, ultimate analysis, proximate analysis, higher heating value, oxygen to carbon ratio and hydrogen to carbon ratio. All of these properties are essential in determining the effectiveness of biomass undergo torrefaction process.

2.3.1 Physical appearances

By undergone torrefaction process, the colour of biomass is started to change from brown to black. The physical changes of the biomass can be seen in Figure 2.1. The physical appearances of torrefied biomass is analysed based on colour changes.

Figure 2.1 Images of oil palm frond at (a) raw, (b) torrefied at 240 °C and (c) torrefied at 300 °C

Source: Wahid et al, 2017

During the torrefaction, the colour of the sample changes from light brown to dark brown at the end of the torrefaction. However, the intensity of colour is different which is depending on the torrefaction temperature. Increment of torrefaction temperature contributes to the increment of colour intensity. Torrefied samples at higher torrefaction temperature are darker compare to lower torrefaction temperature.

2.3.2 Proximate analysis

Proximate analysis is an analysis to determine the properties of volatile matter, ash content, fixed carbon and moisture content of the biomass. It is a process that is relatively simple and in terms of cost it is not expensive. Bergman & Kiel (2005) stated that in their study, the decrease of volatile matter and increase of fixed carbon are in the range of 10 to 15% and 25 to 60% respectively when the biomass underwent torrefaction process. The torrefaction temperature used was at 280 °C. The trends for volatile matter and fixed carbon also have been studied by Matali et al. (2016), Uemura et al. (2015) and Jaafar & Ahmad (2011) where the same results were obtained. The increasing and decreasing of fixed carbon and volatile matter respectively are depending on the torrefaction temperature. Higher torrefaction temperature is known to affect the increase of fixed carbon and decrease the volatile matter composition of the biomass. The amount of fixed carbon and volatile matter contribute to the heating value

of the biomass whereas fixed carbon is important for the heat generation during the heating process. As the amount of fixed carbon indicates the heating value of biomass, a high amount of fixed carbon represents high amount of the heating value which is essential for biomass to be used as a fuel. Usually the proximate analysis was conducted by referring to the American Standard for Testing Material (ASTM) E871 for moisture content analysis, D1762 for volatile matter analysis and E1755 for ash content analysis.

2.3.3   Ultimate analysis

The main elements in ultimate analysis are consisting of carbon (C), hydrogen (H), nitrogen (N), oxygen (O) and sulphur (S). This analysis was conducted using CHNS analyser which analyse the composition of each elements in terms of percentage by mass of the biomass. The analysis is important to determine the quantity of air needed for combustion reaction as well as giving the overview on the volume and composition of combustible gases released during torrefaction. In this analysis carbon, oxygen and hydrogen are three important components for the combustion process. Although oxygen are used in combustion, higher composition of oxygen in biomass leads to lower heating value. When comparing with coal, the carbon, nitrogen and sulphur composition of the biomass are lower while the hydrogen and oxygen composition are higher than the rest of elements in biomass. When undergone torrefaction process, several studies (Asadullah, 2014; Sabil et al., 2013; Chen et al., 2016) stated that at higher torrefaction temperature, the carbon composition is increased and hydrogen and oxygen compositions are decreased.

2.3.4   Higher heating value (HHV)

Higher heating value (HHV) is an important properties to measure the energy content of a fuel. Higher HHV means that it requires less fuel to achieve high energy compare to fuel with low HHV. HHV is usually being determined by using bomb calorimeter. It can also be determined by the amount of heat released by the unit of volume or mass of fuel from combustion and the product returned to initial temperature of 25 °C.

2.3.5 Hydrogen to carbon and oxygen to carbon ratios

Generally, the oxygen to carbon ratio and hydrogen to carbon ratio for the raw biomass are in the range of 0.4 to 0.8 and 1.2 to 2.0 respectively. The moisture and light volatiles in the biomass which contains the hydrogen and oxygen are removed while the carbon is retained. This phenomena are occurring when the biomass undergone torrefaction process. Due to the torrefaction process, the hydrogen to carbon and oxygen to carbon ratio are decreased to the ranges of 0.7 – 1.6 and 0.1 – 0.7 respectively (Chen et al., 2015). The trends for decreasing both of these ratios are the same with the findings made by Uemura et al. (2015), Matali et al. (2016) and Na et al. (2013)

2.4 Torrefaction of oil palm waste

Torrefaction of oil palm waste has been a topic of interest because of its potential to upgrade the biomass properties that can be further used as a fuel for power generation. Many studies has been done previously by using the by-products of oil palm mill for example empty fruit bunch, palm kernel shell and palm mesocarp fibre.

Traditionally, empty fruit bunch is used as fertilizer or soil conditioner. This is because it contains nutrient and its quality is equivalent with the use of fertilizer properties. It is also being used to improve the nutrient levels and growth of the plants (Yusoff, 2006). Meanwhile, palm kernel shell (PKS) is buried into the ground by oil palm practitioner to turn it into black colour compost. It acts as a fertilizer but because of its hard shell, it takes long time to turn into organic fertilizer. With high calorific value, PKS is considered to be used as a source of renewable energy. On the other hand, palm mesocarp fibre (PMF), it is usually used as a fuel for the boiler (Then et al., 2014). It can also be mixed with other material that has high nitrogen content in order to transform into more compost mass that can be used as organic fertilizer (Sreekala et al., 1997). Oil palm waste has been used directly as a fuel without any pre-treatment, and some studies (Acharya, Dutta, & Minaret, 2015; Jaafar & Ahmad, 2011) reported that pre-treatment process such as torrefaction can improve the properties of oil palm waste. Before the biomass undergo pre-treatment process using torrefaction approach, the proximate analysis and ultimate analysis are carried out in order to determine the characteristic of raw biomass used. Examples of proximate analysis and ultimate

analysis of raw EFB is shown in Table 2.3. In a study carried out by Munawar & Subiyanto (2014), by measuring and comparing the moisture content of EFB and other biomass waste such as palm kernel shell (PKS), oil palm frond (OPF) and palm mesocarp fibre (PMF), it shows that the moisture content of EFB is the highest. In the torrefaction studied by Uemura et al. (2011), the composition of carbon, hydrogen and oxygen of PMF is analysed and the composition of carbon is increased as the torrefaction temperature is increased but for both hydrogen and oxygen compositions, the opposite trends are obtained. Similar results also reported by Aziz et al. (2012) with the additional analysis for the compositions of nitrogen and sulphur using two different particle sizes in the ranges of 250 – 355 µm and 355 – 500 µm. For both particle sizes the nitrogen content is below 2% and sulphur content is closing to zero. According to Uemura et al. (2011), the calorific value of raw PMF is better than raw EFB but lower than raw PKS. The calorific value are shown in Source: Idris et al. (2012)

Table 2.4.

Table 2.3 Characteristic of empty fruit bunch

Proximate analysis (wt% dry basis)	
Volatile Matter	77.10
Fixed Carbon	16.80
Ash	6.1
Ultimate analysis (wt% dry basis)	
Carbon	47.65
Hydrogen	5.20
Oxygen	44.97
Nitrogen	1.82
Sulphur	0.36
Calorific value (MJ/kg)	16.80

Source: Idris et al. (2012)

Table 2.4 Calorific value of different oil palm waste

Biomass	Calorific Value (MJ/kg)
Empty fruit bunch	17.02
Palm kernel shell	19.78
Palm mesocarp fibre	19.61

Source: Uemura et al. (2011)

Uemura et al. (2011) stated that when the torrefaction temperature is increased, the mass yield and energy yield of EFB show decreasing trends as shown in Figures 2.1 and 2.2. Based on the comparison with other oil palm waste, EFB obtained the lowest

yields for both mass and energy yields. As for mass and energy yields of PKS, the trend is the same with EFB whereas the torrefaction temperature is increased, both mass and energy yields are decreased. In the work of Uemura et al. (2011), the trend of mass yield is the same whereas the energy yield is slightly increased at torrefaction temperature of 300 °C as shown in Figure 2.2.3. While for the mass and energy yields of PMF, it is higher than EFB but lower than PKS. This is in agreement with the finding of Sabil et al. (2013).
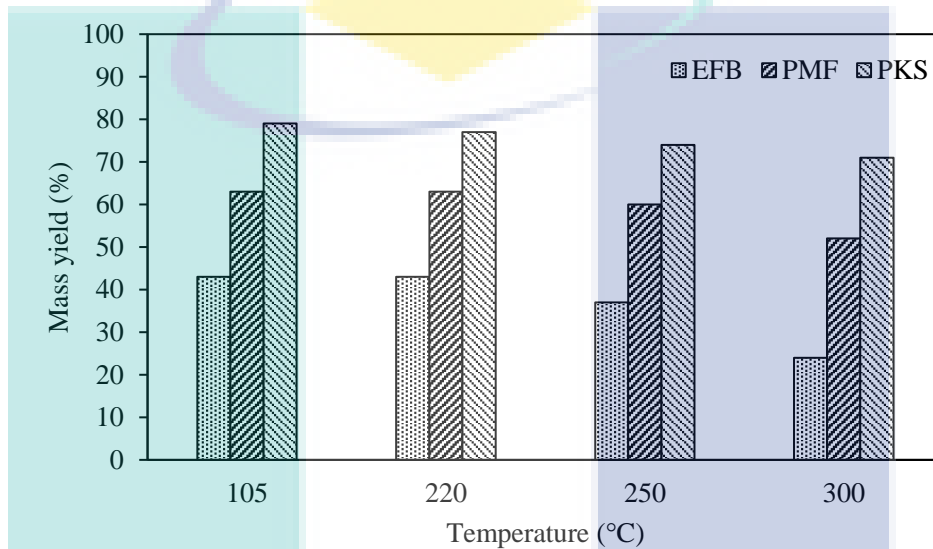

Figure 2.2.2 Effect of different torrefaction temperatures on mass yield of oil palm waste

Source: Uemura et al. (2011)
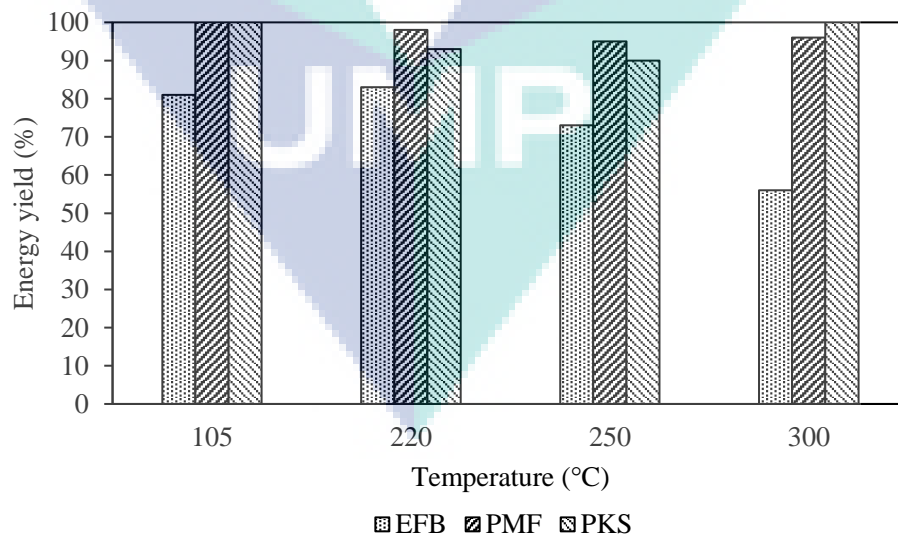
Figure 2.2.3 Effect of different torrefaction temperatures on energy yield of oil palm waste

Source: Uemura et al. (2011)

Torrefaction of palm kernel shell is also being studied by other researcher. In the work done by Saadon et al. (2014), the effect of different torrefaction gas on the torrefaction process of PKS are investigated. There were three types of torrefaction gases being used which are the nitrogen gas, mixture of nitrogen gas and oxygen at 3, 9 and 15% of oxygen concentration and lastly the mixture of nitrogen and carbon dioxide at 3, 9 and 15% of carbon dioxide concentration. The result from this study shows that in the mixture of oxygen and nitrogen gas as torrefaction gas, it did not influence the yield of products indicating the torrefaction is best performed under inert condition.

Generally, the mass and energy yields are decreased when torrefaction temperature is increased. Saadon et al. (2014) highlighted that torrefaction temperature plays more important role to affect the torrefaction process compare to residence time. Uemura et al. (2015) used two different PKS samples, grinded and not grinded samples. The effect of particles sizes are studied while varying the torrefaction gas like the study done by Saadon et al. (2014). Energy yield obtained from their study shows a higher yield is obtained when using biomass sample without grinding in any of the torrefaction gas. The oxygen and carbon dioxide mixture had a small effect early in the temperature and started to have more effect when temperature reaches 300 °C for both size of the PKS. Moreover, in inert condition, the unground biomass have higher energy yield compare to when using oxygen and carbon dioxide mixture as torrefaction gas. Their study also stated that both in mixture of oxygen and carbon dioxide gas, its effect on the solid phase conversion only at 300 °C. Matali et al. (2016) performed torrefaction of oil palm frond and compare the result obtained it with Leucaena wood. This comparison is based on the effect of torrefaction on the non-woody and woody biomass. The authors concluded that both types of biomass can be transformed into a promising bio-fuel based on the increment of HHV and decrement of hydrogen to carbon and oxygen to carbon ratios.

2.5 Torrefaction of forestry residue

In forest products industry, the residue can be divided into two parts which are the left over from harvesting logs from the forest and the waste generated from the process of manufacturing timber, plywood and particleboard. Some of the types of

residues are branches, sawdust, bark and decayed wood. Example of sawdust that are commonly found in Malaysia's forest industries are Meranti, Seraya, Kulim and Chengal (Shafie et al., 2017; Uemura et al., 2010).

Meranti and Seraya belongs to light hardwood category which purposes in light construction, pallet and expensive plywood (Malaysian Timber Council, n.d.; Malaysian Timber Council, n.d.). While Kulim belongs to medium hardwood category (Malaysian Timber Council, n.d.) and Seraya belongs to heavy hardwood category (Malaysian Timber Council, n.d.). Kulim and seraya are mainly used in boat building, flooring and structural component of cooling tower. In terms of torrefaction of these biomass, Uemura et al. (2010) conducted studies by using seraya wood whereas there is lack of studies done with the other biomass. Uemura et al. (2010) finds that when torrefied at 250 and 300 °C, the calorific value of seraya increases when increasing torrefaction temperature but lower in value compare to other biomass (acasia and golden powder) used in the study. The authors concluded that seraya may consist of lower hemicellulose coomposition compate to the other samples.

Moreover, the torrefaction of forestry residue has been studied by many authors for example spruce branches (Tran et al., 2016), wood and barks of Eucalyptus globulus and Eucalyptus nitens (Arteaga-Peréz et al., 2015a), Pinus radiata (Arteaga-Pérez et al., 2015b) and sawdust (Li et al., 2012) to represent forestry residue. In the research done by Arteaga-Perez et al. (2015a), there are two experimental conditions being studied which are the residence times (15 and 30 minutes) and temperatures (250 and 280 °C). The biomass used is the wood and bark of Eucalyptus globulus and Eucalyptus nitens. From the experiment, the authors concluded that the mass yield is decreased with increasing temperature and residence time. In their study they also found that the torrefaction temperature give a significant effects on the properties of torrefied wood compare to residence time.

In the study of using spruce branches by Tran et al. (2016), there are 4 types of torrefaction gas have been used, which were nitrogen, carbon dioxide, mixture of carbon dioxide and steam and lastly the mixture of carbon dioxide, steam and oxygen. The authors concluded that from all of the four torrefaction gaseous that are introduced in the torrefaction process, when carbon dioxide gas is used, the mass yield obtained is lower than the mass yield obtained under inert condition. By mixing steam and carbon dioxide, the mass yield is increased while the mixture of carbon dioxide, steam and

oxygen used as torrefaction gas shows a reduction in both mass and energy yields. However it is important to note that most of the studies involving wood species in Europe. There is a limited work carried out for forestry residue in Malaysia and thus there is a need to perform a study on suitability of forestry residue in Malaysia as biofuel using torrefaction as pre-treatment method.

2.6 Estimation of higher heating value (HHV)

Higher heating value (HHV) is important as it is an important properties of fuel that define the energy content of the fuel. Estimating HHV by using proximate and ultimate analysis have been established using a correlation model. Dulong's correlations is one of the first correlations introduced in the late 1800s and is based on the ultimate properties of a coal (Channiwala & Parikh, 2002). Some of the published correlations of estimating HHV are presented in Table 2.5.

Table 2.5 Summary of published correlations for estimating higher heating value (HHV)

No	Correlation	Based on	References
1	HHV = 19.914 - 0.2324Ash	Proximate analysis	Sheng & Azevedo (2005)
2	HHV = -3.0368 + 0.2218VM + 0.2601FC	Proximate analysis	Sheng & Azevedo (2005)
3	HHV = 0.1905VM + 0.2521FC	Proximate analysis	Yin (2011)
3	HHV = 19.2880 - 0.2135VM/FC - 1.9584ASH/VM + 0.0234FC/ASH	Proximate analysis	Nhuchhen & Salam, (2012)
4	HHV = 20.7999 - 0.3214(VM/FC) + 0.0051(VM/FC)^2 - 11.2277(ASH/VM)	Proximate analysis	Nhuchhen & Salam, (2012)
5	HHV = 0.3536FC + 0.1559VM - 0.0078ASH	Proximate analysis	Ahmaruzzaman, (2008)
6	HHV = 0.2949C + 0.8250H	Ultimate analysis	Yin (2011)
7	HHV = 0.3491C + 1.1783H + 0.1005S - 0.1034O - 0.0151N - 0.0211A	Ultimate analysis	Channiwala & Parikh, (2002)
8	HHV = −3.147 + 0.468C	Ultimate analysis	Callejón-Ferre et al. (2011)
9	HHV = 5.736 + 0.006C^2	Ultimate analysis	Callejón-Ferre et al. (2011)
10	HHV = -1.3675 + 0.1337C + 0.7009H + 0.03180O	Ultimate analysis	Sheng & Azevedo (2005)

Sheng & Azevedo (2005) uses wide range of biomass to estimate the HHV by using the ultimate and proximate analysis. The authors found out that HHV that is estimated by using ultimate analysis have a higher accuracy compare to the one estimated by using proximate analysis. This has been proven in the work performed by

Yin (2011), where the estimated correlations of HHV using the ultimate analysis yield the lowest error. The database used by Yin (2011) also covers a wide variety of biomass. Ahmaruzzaman (2008) developed a correlation model for estimating HHV using proximate analysis with the data from various types of coal, biomass and the mixture of coal and biomass are used. By using ultimate analysis of solid, liquid and gaseous fuels, Channiwala & Parikh (2002) estimated HHV error is lesser than 1.45%. Nhuchhen & Salam (2012) also uses a wide variety of biomass but only estimating HHV by using the proximate analysis using several proposed correlations where the best correlation is selected on the lowest error. However the estimated HHV from published correlations only consider the raw condition of biomass and not the torrefied conditions. Although the published correlations cover wide ranges of biomass from various country, it does not guarantee the accuracy of HHV for torrefied biomass. Using established correlations to estimate the HHV of torrefied biomass often yields a significance error when compare to the measured HHV. In addition, oil palm waste data are usually not included as part of the biomass database in the most correlations development and thus limiting the correlations capability.

2.7   Biomass gasification

Chemical reactions involve in biomass gasification are listed in Table 2.6. Different types of reaction occurred during gasification, therefore all of these reactions must be taken into account when considering gasification process. Other than that, when using different types of biomass, it will affect the output data such as the gas yield, cold gas efficiency, gas production and carbon conversion (Emami-Taba et al., 2013). Mainly, the gasification process will produce char, gas and condensable vapours (Esther Cascarosa, 2012).

Table 2.6 Biomass gasification processes

Process	Reactions
Partial Oxidation	$2C + O_2 \leftrightarrows 2CO$
Oxidation	$C + O_2 \leftrightarrows CO_2$
Hydro-gasification reaction	$C + 2H_2O \leftrightarrows CH_4 + O_2$
Water-gas shift reaction	$CO + H_2O \leftrightarrows CO_2 + H_2$
Steam reforming reaction	$CH_4 + H_2O \leftrightarrows CO + 3H_2$
Water gas reaction	$C + H_2O \leftrightarrows CO + H_2$
Boudouard reaction	$C + CO_2 \leftrightarrows 2CO$

Source: Vélez et al. (2009)

According to Vélez et al. (2009), depending on the type of biomass used, the increase in steam to biomass ratio is a must for producing syngas particularly hydrogen gas (H_2). Complete de-volatilization of biomass occur during pyrolysis and at the same time all the condensable vapours and tar rise with air/steam and only the char remain in the gasification zone. The vapours that rise never had a chance to come into contact with fresh air/steam and the formation of methane and ethylene does not occur in a reduction atmosphere. Pyrolysis can be confirmed to takes place when there are methane and ethylene forms as the product. Lastly, the char that remain in the gasification zone will undergone gasification process to form carbon monoxide (CO), carbon dioxide (CO_2), hydrogen (H_2) and other gases. (Brar et al., 2012).

There are several types of reactor that involved in the gasification process which are (Siedlecki et al. , 2011):

1)   Fixed beds (updraft, downdraft, crossdraft)

2)   Fluidized beds (bubbling, circulating, dual)

3)   Entrained flow reactors

Table 2.7 shows the advantages and disadvantages for each of the gasifier. For biomass gasification, the fluidized bed gasifier is suitable to be used as it can be scale up, higher conversion rate and most importantly, can be used for a wide ranges of biomass.

Table 2.7 A Comparison on different types of gasifier

Gasifier types	Advantages	Disadvantages
Fixed bed	• For small-scale size operations • Low tar • Moderate dust	• High amounts of ash • Not suitable for large scale biomass gasification • Easily produce lumps
Fluidized bed	• Uniform temperature profile • High conversion rate of feedstock • Can be used with wide range of biomass • Can be scaled-up	• Easily erode • High char content • High maintenance
Entrained flow	• Can gasify all types of coal • Large capacity	• The use of biomass is limited • Involves slagging of ash

Using Aspen Plus for simulating biomass gasification process has been done before by Nikoo & Mahinpey, (2008), Fatoni et al., (2014) and Pala et al., (2017). In studies done by Nikoo & Mahinpey and (2008), Fatoni et al., (2014), the biomass use are pine dust and wood pellets, while Pala et al., (2017) uses various types of biomass such as coffee bean husks, food wastes, pine sawdust and wood chips. The feedstock biomass for these studies are by using only the raw biomass.

In each of the gasification process there will be some parameters that will affect the output or syngas produced, for example temperature of the gasifier, the steam flow rate and the air to biomass ratio. According to Kuo et al. (2014), when the temperature of the feed is higher than the syngas yield is better and this is based on the perspective of syngas formation. ABR which is defined as the amount of oxygen supplied divided by the amount of oxygen required for complete combustion is calculated to know what its effects on the syngas formation. Kezhong et al. (2010) reported that by increasing ABR values from 0.31 to 0.47, it is not only increase the bed temperature to 1026 °C but the effectiveness of feed combustion is also increased due to the increase in oxygen as gasifying agent.

In addition the amount of carbon monoxide is decreased when ABR is increased. The most ideal value for gasification is when ABR is less than 0.25 (Kezhong, et al, 2010) and this is due to the fact that pyrolysis occur which increases the value of hydrogen and carbon dioxide concentrations in the product stream. In the work of Kuo et al. (2014), the range for appropriate ABR for biomass gasification is between the range of 0.2 – 0.4. Other than gasification temperature and ABR, steam also have its effect on the syngas formation. At a fixed ABR, when varies the steam flow rate, the syngas yield will be increased when the flow rate is increased. Kuo et al. (2014) stated that the gasification temperature also plays an important role where more syngas production is obtained when the gasifier is operated at higher temperature.

Furthermore, other factor to be considered when carrying out gasification process is the cold gas efficiency (CGE). Both the quality and quantity of the gas produced are measured to determine the gasifier performance. By considering the amount of biomass converted into gas, the efficiency of the gasifier can be known and expressed by cold gas efficiency (Basu, 2013). Studies carried out by Ruoppolo et al. (2013), Zaccariello & Mastellone, (2015) and Rodrigues et al, (2016), found that by using wood pellet, rice husk, wood waste and cane bagasse the CGE are ranging from

34% to 66 %. The large range is due to different operating condition such as the gasifier temperature and airto biomass ratio. Zaccariello & Mastellone, (2015) and Ruoppolo et al. (2013) uses gasifier temperature ranging from 750 – 850 °C, while 1000 °C for Rodrigues et al, (2016). Only raw biomass are used in these studies when calculation of CGE is made. Thus, comparison of CGE between raw and torrefied biomass can be further studied.

Besides that, in gasification, biomass plays an important role as it can affect how much syngas will be produced. Biomass has different physical and chemical properties, thus each biomass is different and the syngas formation will differ depending on the types of biomass used. Biomass is known to have low fixed carbon compare to coal and that is why hydrogen produced will be higher while carbon monoxide is lower (Kezhong, et al, 2010).

2.8 Torrefied biomass as a fuel for gasification process

Torrefied biomass can be used in other process such as gasification process. The usage of torrefied biomass as a fuel for gasification process is one of the promising area of fuel generation. Many attempts have been made by researchers using torrefied biomass as a fuel in gasification process. Most of their finding indicated that the amount of syngas yield can be increased from 15% to 37% when using torrefied biomass as an input compare to when using raw biomass. (Kuo et al., 2014; Tapasvi et al., 2015; Chen et al., 2013). Study conducted by Chen et al. (2013) shows that the gasification performance of torrefied bamboo is higher than the performance obtained when using raw bamboo as the feed.

By using sawdust as the feed, Qing et al. (2011) studied the effect of torrefied biomass on gasification technology. The findings of the study suggest that the syngas yield from the torrefied biomass is higher when comparing to the syngas yield using raw biomass. For example, previous study done by Prins et al. (2006) shows that the syngas production for biomass underwent torrefaction process is higher than raw biomass. In another study, Batidzirai et al. (2013) provides the improvement of thermal efficiency in torrefied biomass compare to raw biomass.

Furthermore, Dudynski et al. (2015) evaluated an industrial-scale gasification experiments for raw and torrefied biomass feedstock which resulting the increasing of higher calorific value of synthesis gas for torrefied biomass compare to raw biomass. In

addition, Tapasvi et al. (2015) provides a biomass gasification simulation study using Aspen Plus software for two-stage gasification model based on Gibbs free energy minimization approach in order to compare the syngas production using raw and torrefied biomass as feedstock. It was reported that the carbon conversion and syngas yield was higher for torrefied biomass than the raw biomass.

Except for these few studies, there is a considerable lack of information on the behaviour of torrefied biomass in terms of the best torrefaction temperature and residence time. In addition also often the synthesis gas produced usually depending on the types of biomass and the effects of torrefaction on the palm oil wastes and forestry residue in Malaysia as biomass is still not investigated yet which forms the basis of this work.

2.9   Summary

Biomass is known to be one of the source for renewable energy. In the year 2016, the top two renewable sources from Malaysia by its energy value are oil palm waste and forestry residue (Fazeli et al., 2016). But due to the characteristics of the biomass itself which have high moisture content, easily absorb moisture from the surrounding and low calorific value, the prospect of using biomass as a biofuel is not favourable. Thus, pre-treatment process can be carried out as an alternative to counter its drawbacks. From various process of pre-treatment, torrefaction is shown to be suitable to use as it covers a wide range of biomass.

Torrefied biomass, mainly has a darker colour compare to it raw state. Its carbon composition, fixed carbon, and higher heating value increases when higher torrefaction temperature is used. Meanwhile hydrogen composition, oxygen composition, volatile matter, hydrogen to carbon ratio and oxygen to carbon ratio decrease as torrefaction temperature increases. In terms of torrefied oil palm waste, it can be used as benchmark for the study before using forestry residue as a biofuel since some studies on oil palm waste torrefaction have been done by various researchers (Aziz et al, 2012; Jaafar & Ahmad, 2011; Uemura et al., 2011). The data for torrefied forestry residue from Malaysia is scarce thus the effect of torrefaction is not really known, making further studies must be conducted to investigate its effect.

Based on the review from literature, correlation model for predicting the HHV is widely established. The HHV for biomass can be predicted either using the ultimate

analysis or proximate analysis of the biomass. However the established correlation only applicable to predict HHV for raw biomass only. Since the torrefaction as a pre-treatment is indeed increasing the HHV for biomass, thus the HHV prediction using the existing correlation model may no longer accurate and yield significance error. Other than that, both oil palm waste and forestry residue particularly in Malaysia are usually not included in the database. Thus, new correlations must be constructed by taking account the data for raw and torrefied of oil palm waste and forestry residue.

For biomass gasification, there are three types of gasifier widely used to produce synthesis gas which are fixed bed, fluidized bed and entrained flow. From these gasifiers, fluidized bed gasifier is the best to gasify biomass as it can be used for wide ranges of biomass, can be scale-up and has high conversion rate. As for using torrefied biomass as a feedstock for gasification process, studies done by Batidzirai et al. (2013), Dudynski et al. (2015) and Tapasvi et al. (2015) showed that the carbon conversion and the syngas yield increases when using torrefied biomass. Thus, a suitability of oil palm waste or forestry residue undergo torrefaction process as feedstock for gasification needs to be further evaluated for synthesis gas production.

CHAPTER 3

METHODOLOGY

3.1   Overview

This chapter presents experimental procedure for torrefaction, estimation of higher heating value (HHV) using correlation model and simulation procedure for gasification process.

3.2   Torrefaction experimental procedure

Figure 3.1 shows the overall flow for the torrefaction experiments. There are 3 steps which are the raw materials preparation, how the experiment is carried out and lastly, the collection of experimental data. Details explanation for each steps are provided in the following subchapters.

```
                    ┌─────────────┐
                    │    Start    │
                    └──────┬──────┘
                           │
                           ▼
                    ┌─────────────┐        ┌──────────────────────┐
                    │Raw materials│        │ • Oil palm waste     │
                    │ preparation │        │ • Forestry residue   │
                    └──────┬──────┘        └──────────────────────┘
                           │
                           ▼
                    ┌──────────────────┐
                    │Torrefaction experiment│
                    └──────┬───────────┘
                           │
                           ▼
                    ┌─────────────┐
                    │Data collection│
                    └──────┬──────┘
                           │
                           ▼
                    ┌─────────────┐
                    │Data analysis│
                    └──────┬──────┘
                           │
                           ▼
                    ┌─────────────┐
                    │   Finish    │
                    └─────────────┘
```
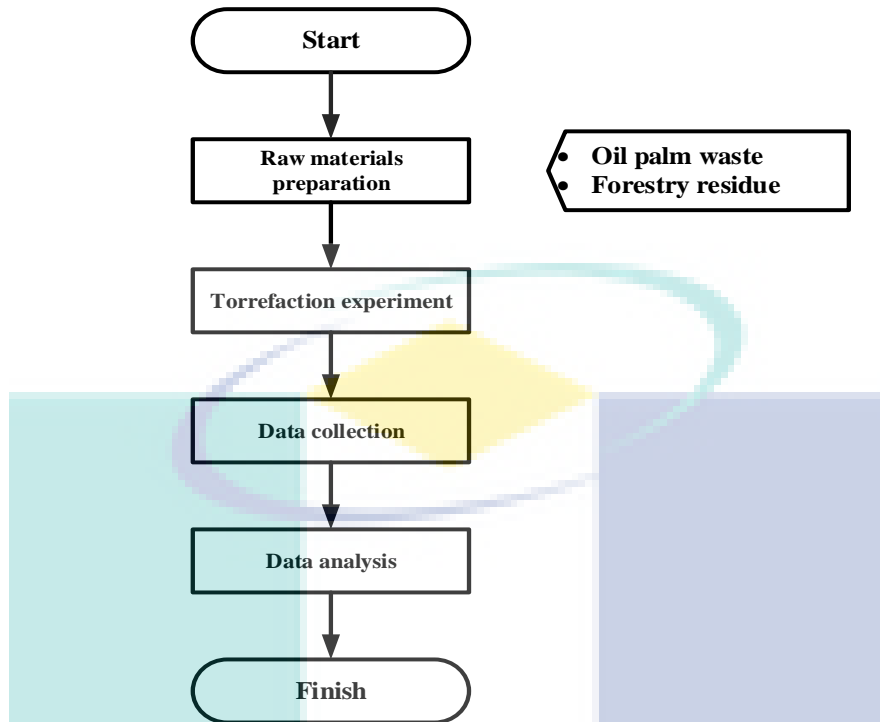
Figure 3.1 Process flow for torrefaction experiment

3.2.1 Raw materials preparation

The biomass used in this study were oil palm waste (OPW) and forestry residue (FR). For OPW, four different types of OPW were used which consists of empty fruit bunch (EFB), palm kernel shell (PKS), oil palm fronds (OPF) and palm mesocarp fibre (PMF). Meanwhile four different species of forestry residue were selected which are meranti, seraya, kulim and chengal sawdust. The biomass were collected from palm oil plantation and wood processing mill at Lepar Hilir Palm Oil Mills, Gambang, Pahang and Kilang Papan Aman Sdn Bhd, Kuantan, Pahang respectively. Two groups of biomass were taken in order to study the characteristics of different group of biomass when undergo torrefaction process. The oil palm waste and forestry residue samples were dried in the oven for 10 to 20 hours at temperature of 50 °C in order to reduce the moisture content. The targeted initial moisture content of raw biomass was approximately less than 20 wt%. Subsequently the biomass were grinded and sieved into particles size of 0.5 – 1.0 mm. This particles size were chosen as it do not have significant effects on the torrefaction process (Sabil et al., 2013; Encinar et al., 1996). The samples were kept in an air-tight container and stored in a desiccator at room

temperature before it is being used for experiment. Desiccator was used to store the sample and prevent the moisture from the air that could contaminated the sample.

3.2.2 Torrefaction experiments

Figure 3.2 shows the experimental set up for torrefaction process. First, 0.5 gram of glass wool was weighed and loaded in the tubular reactor. The dimension of tubular reactor with length of 39.7 cm and outer diameter of 1.27 cm was used in this study. About 2-3 grams of biomass was weighed, then it was loaded into the tubular reactor with the position as shown in Figure 3.2.

1. Regulator
2. Flow rate controller
3. Reactor
4. Heating element
5. Glass wool
6. Biomass sample
7. Temperature controller
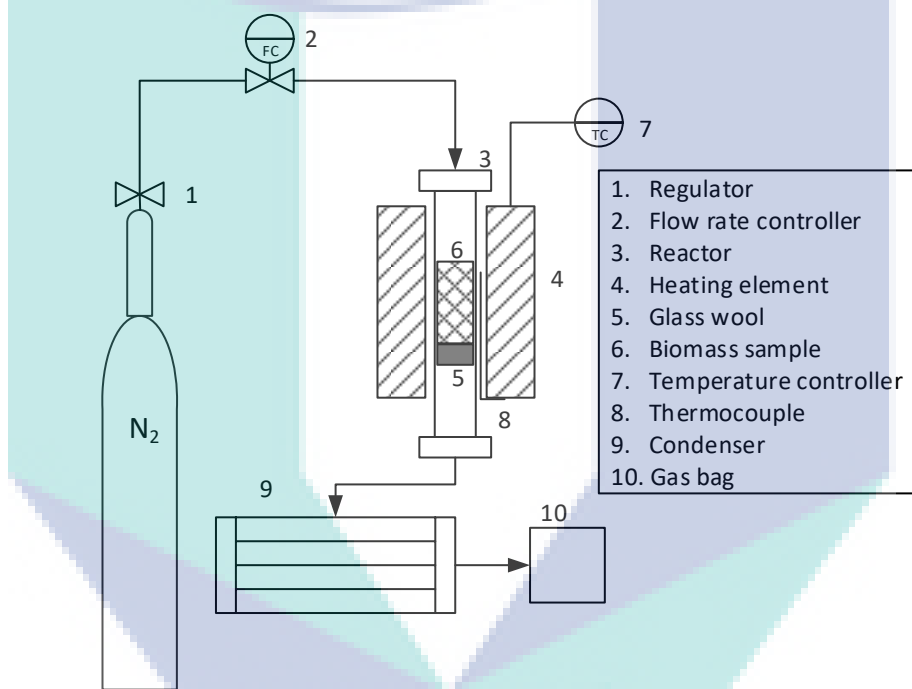8. Thermocouple
9. Condenser
10. Gas bag

Figure 3.2 Schematic diagram of torrefaction experimental setup

Before performing the torrefaction experiment, the tubular reactor was purged with 50 mL/min nitrogen for 5 minutes in order to ensure the inert condition was achieved inside of the tubular reactor. Then, the temperature of the furnace was set to desired operating condition. To ensure the targeted torrefaction temperature was reached, investigation on temperature distribution for the reactor was carried out. The temperature was measured at several points based on the distance from the top of reactor. Thermocouple was used to measure the temperature at each point of the reactor. The data shown in Table 3.1 using the setting furnace temperature of 300 °C. At distance of 25 cm from the top of the reactor, the highest temperature was obtained (270

°C) which has the difference of 30 °C from the set temperature. Several tests at different setting temperature resulted in the differences between setting and achieved temperature in the range of 28 – 30 °C. This indication shows that in order to reach the targeted torrefaction temperature, the furnace temperature need to be set 30 °C higher than the targeted temperature. For example, the furnace temperature is set to 300 °C for targeted torrefaction temperature of 270 °C, and set to 330 °C for torrefaction at 300 °C.

Table 3.1 Temperature distribution for tubular reactor

Distance from the top of reactor, cm	Temperature, °C
5.0	83
10.0	96
15.0	145
20.0	168
25.0	270
30.0	263
35.0	258
39.7	250

Another important indication from Table 3.1 was the location of biomass placed in the reactor. As can be seen, the first 20 cm from top of reactor was not heated up to the desired temperature. So, during the experiment, the biomass was placed at the distance between 25 to 35 cm from top of reactor.

After reaching the targeted temperature, torrefaction process was carried out for a set of residence time. Details on the operating condition for this experiment is shown in Table 3.2. The value shown in Table 3.2 are the operating condition of the experiment. When conducting the experiment, 30 °C was added to the set value to ensure the experiment conducted at the specified temperature.

Table 3.2 Operating condition for torrefaction experiment

Operating condition	Set value
Temperature (°C)	240, 270, 300 and 330
Residence time (min)	15, 30 and 60

After the experiment was completed at the specified temperature and residence time, the tubular reactor was cooled to the ambient temperature. The torrefied product was taken out from the reactor and the mass of torrefied biomass was recorded. The torrefaction experiments were repeated for 3 times and the average mass of torrefied biomass were taken in order to ensure the validity of the result obtained. The same

procedure with the same set of operating conditions were used for both oil palm waste and forestry residue.

3.2.3 Data collection

In this work, the data obtained from the experimental work was collected and analysed in terms of mass yield, higher heating value (HHV), energy yield, proximate analysis and ultimate analysis. For the mass yield, the mass of raw and torrefied biomass were taken before and after torrefaction. The calculation for mass yield is shown in Equation 3.1.

$$Mass\ yield(\%) = \frac{mass\ of\ torrefied\ biomass}{mass\ of\ raw\ biomass} \times 100\%$$ 3.1

$$Energy\ yield(\%) = Mass\ yield(\%) \times \frac{HHV_{torrefied\ biomass}}{HHV_{raw\ biomass}}$$ 3.2

The energy yield as shown in Equation 3.2 is obtained based on mass yield and HHV. It is defined by the energy ratio of torrefied biomass and raw biomass and multiply by the mass yield. As torrefaction aims to improve the properties of biomass, it should achieve this by not losing too much energy and volatiles. Thus both mass and energy yield are important parameters to evaluate the torrefaction process. In this work, model 1341 bomb calorimeter was used to measure the heating value of the raw and torrefied biomass. In bomb calorimeter, 0.5 gram of sample was weighed and put into the combustion capsule. 10 cm of fuse wire was cut and attached to the bomb head. The bomb head was attached to combustion bomb and oxygen gas was filled inside the bomb. 2 litres of water was filled in the oval bucket and the bomb was slowly dropped inside the bucket. Ignition lead wires were pushed inside terminal of the bomb. Then the cover with thermometer was put on and the stirrer was turned on. After 1 minute, the ignition button was pushed and the temperature was recorded at 1-minute interval until constant reading was obtained. The setup for bomb calorimeter was shown in Figure 3.3. In order to calculate the higher heating value, Equation 3.3 was used where t_{dif}, W, m and b_{fuse} are temperature different, constant value (2409.26 cal/°C), weight of sample (gram) and length of burnt fuse wire, respectively.

$$HHV = \frac{t_{dif}W - 2.3b_{fuse}}{m}$$ 3.3

Example calculation for bomb calorimeter are as follows:

A bomb calorimeter experiment were carried out with a 0.4947 g of biomass. The value obtained from the thermometer reading are 29.8 and 29 °C for the final and initial temperature respectively. The unburnt fuse was left with the measurement of 7.2 cm. The HHV is calculated based on Equation 3.3:

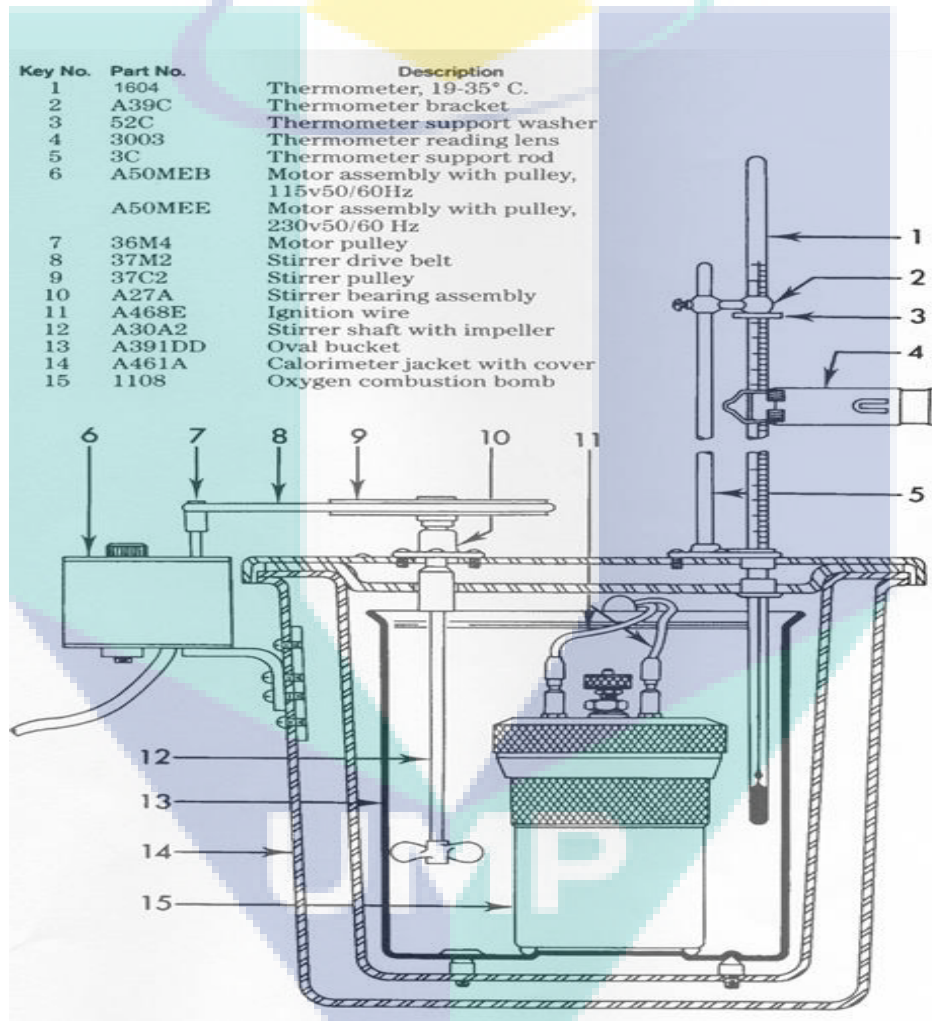$$HHV = \frac{((29.8-29)2409.26)-2.3(10-7.2)}{0.4947} = 3883.68 cal/g = 16.25 MJ/kg$$

Key No.	Part No.	Description
1	1604	Thermometer, 19-35° C.
2	A39C	Thermometer bracket
3	52C	Thermometer support washer
4	3003	Thermometer reading lens
5	3C	Thermometer support rod
6	A50MEB	Motor assembly with pulley, 115v50/60Hz
	A50MEE	Motor assembly with pulley, 230v50/60 Hz
7	36M4	Motor pulley
8	37M2	Stirrer drive belt
9	37C2	Stirrer pulley
10	A27A	Stirrer bearing assembly
11	A468E	Ignition wire
12	A30A2	Stirrer shaft with impeller
13	A391DD	Oval bucket
14	A461A	Calorimeter jacket with cover
15	1108	Oxygen combustion bomb

Figure 3.3 Bomb calorimeter setup (Parr Instrument Company, 2018)

After obtaining the heating value of the sample, the energy yield were calculated based on Equation 3.2.

3.2.4   Data analysis

In order to observe the physical changes of biomass undergone torrefaction process, the images for raw and torrefied biomass are taken and arranged based on the torrefaction temperature and residence time. The changes of its physical appearances are then observed based on the colour of solid torrefied product. In terms of chemical properties, the biomass is usually measured in the forms of proximate analysis and ultimate analysis. For proximate analysis, the analysis was carried out according to the American Standard for Testing Material (ASTM) E871, D1762 and E1755 for moisture content (MC), volatile matter (VM) and ash content, respectively. ASTM E871 moisture content analysis stated that, the sample was first dried for 30 minutes at 103 °C and left to cool at room temperature in the desiccator. The crucible was first weighed and 1 g of sample was put inside the crucible. Then the crucible was placed inside the oven for 2 hours at 103 °C. The crucible was left to cool at room temperature after 2 hours and weighed. Next, the crucible was placed inside the oven for 1 hour and weighed after it has been left to cool at room temperature. This process was repeated until the changes in weight less than 0.2%. The equation used to calculate moisture content is shown in Equation 3.4. In Equation 3.4 and 3.5, m_i, m_f, m_t and m_c is the initial mass of biomass, final mass of biomass, weight of crucible and biomass and weight of crucible. Equations 3.4 and 3.5 have the same formula but the different is based on the values of m_f. In Equation 3.4, m_f value can only be used when the different between the last weight and current weight is less than 0.2%, while for m_f in Equation 3.5, the value can be taken right after cooling.

$$Moisture\ content(\%) = \frac{m_i - m_f}{m_t - m_c} \times 100 = B \qquad\qquad 3.4$$

In order to measure the volatile matter, ASTM D1762 was referred. 1 g of sample was heated in the furnace at 950 °C. This temperature was required as volatile matter are liberated at that temperature under specific conditions (Morley et al, 2017). A crucible with its lid and biomass inside was first weighed and placed inside the furnace for 6 minutes. Then the crucible was left to cool for 1 hour before it was being weighed. Equation 3.5 was first used to calculate the mass loss and the volatile matter was calculated using Equation 3.6.

$$Mass\ loss\ (\%) = \frac{m_i - m_f}{m_t - m_c} \times 100 = A \qquad\qquad 3.5$$

$$Volatile\quad matter\ (\%) = A - B \qquad\qquad 3.6$$

In the ASTM E1755 procedure, the crucible was firstly heated in the furnace at 575 °C for 3 hours. At this temperature, ash is the only residue left after the process (Sluiter et al., 2008). The weight of crucible was taken before it is it is placed into the furnace for 1 hour at the same temperature. After 1 hour it was cooled and weighed. The process was repeated until the weight change was less than 0.3 milligram. After obtaining the weight of the crucible, 0.5 to 1 gram of sample was weighted and place inside the crucible and put into the furnace at minimum 3 hours. Then, the crucible was removed and left to cooled and weighed. The crucible was placed in the furnace for 1 hour and weighed after cooled. The process was repeated until less than 0.3 milligram of weight change was obtained. Ash content was then calculated based on Equation 3.7. Lastly, after MC, VM and ash content were obtained, the FC was calculated by using Equation 3.8.

$$Ash\ content\ (\%) = \frac{m_{ash} - m_c}{m_i - m_c} \times 100 \qquad\qquad 3.7$$

$$Fixed\ carbon\ (\%) = 100 - MC - VM - Ash \qquad\qquad 3.8$$

For ultimate analysis, all of the samples were analysed by using CHNS analyser. The composition of carbon, hydrogen, nitrogen and sulphur can be obtained while the value of oxygen was calculated by using Equation 3.9. After obtaining the composition of biomass, the hydrogen to carbon and oxygen to carbon ratios were calculated by using Equations 3.10 and 3.11 respectively. These ratios are then used to plot the Van Krevelen plot.

$$O\ (\%) = 100 - C - H - N - S \qquad\qquad 3.9$$

$$Hydrogen\ to\ carbon\ ratio = \left(\frac{\dfrac{Mass\ fraction\ of\ Hydrogen}{Atomic\ weight\ of\ Hydrogen}}{\dfrac{Mass\ fraction\ of\ Carbon}{Atomic\ weight\ of\ Carbon}} \right) \qquad\qquad 3.10$$

$$Oxygen\ to\ carbon\ ratio = \left(\frac{\dfrac{Mass\ fraction\ of\ Oxygen}{Atomic\ weight\ of\ Oxygen}}{\dfrac{Mass\ fraction\ of\ Carbon}{Atomic\ weight\ of\ Carbon}} \right) \qquad\qquad 3.11$$

To better understand the changes in HHV, the calculation of enhancement factor of HHV is needed. The enhancement factor of the HHV can be calculated as in Equation 3.12.

$$Enhamcement\ factor\ of\ HHV = \left(\frac{HHV\ of\ torrefied\ biomass}{HHV\ of\ raw\ biomass} \right) \qquad 3.12$$

3.3 Model application

In model application, it consists of two parts which were the development of HHV correlations and simulation of fluidized bed gasification using raw and torrefied biomass. HHV correlations are developed for estimating the HHV through the use of model and thus overcoming the time-consuming bomb calorimeter implementation. For fluidized bed gasification, the raw and torrefied biomass from torrefaction experiment was employed for studying the effects of torrefaction as pre-treatment method on the synthesis gas production.

In this work the model correlations were developed based on the linear relationship. The HHV was predicted based on the information of ultimate or proximate analysis obtained from the data analysis. Meanwhile the fluidized bed gasification was studied on the simulation basis where the gasification model is developed in the Aspen Plus software. The model application used in this study are listed as follows:

1. Higher heating value (HHV) linear correlation model based on ultimate analysis
2. Higher heating value linear (HHV) correlation model based on proximate analysis
3. Simulation of fluidized bed gasification using Aspen Plus software.

3.3.1 Higher heating value (HHV) correlation model

Correlations is a statistical method to demonstrate the interaction and relationship of variables. In this study the correlations between HHV with ultimate analysis and proximate analysis are being tested. The steps to determine the HHV using the proposed correlations are shown in Figure 3.4.
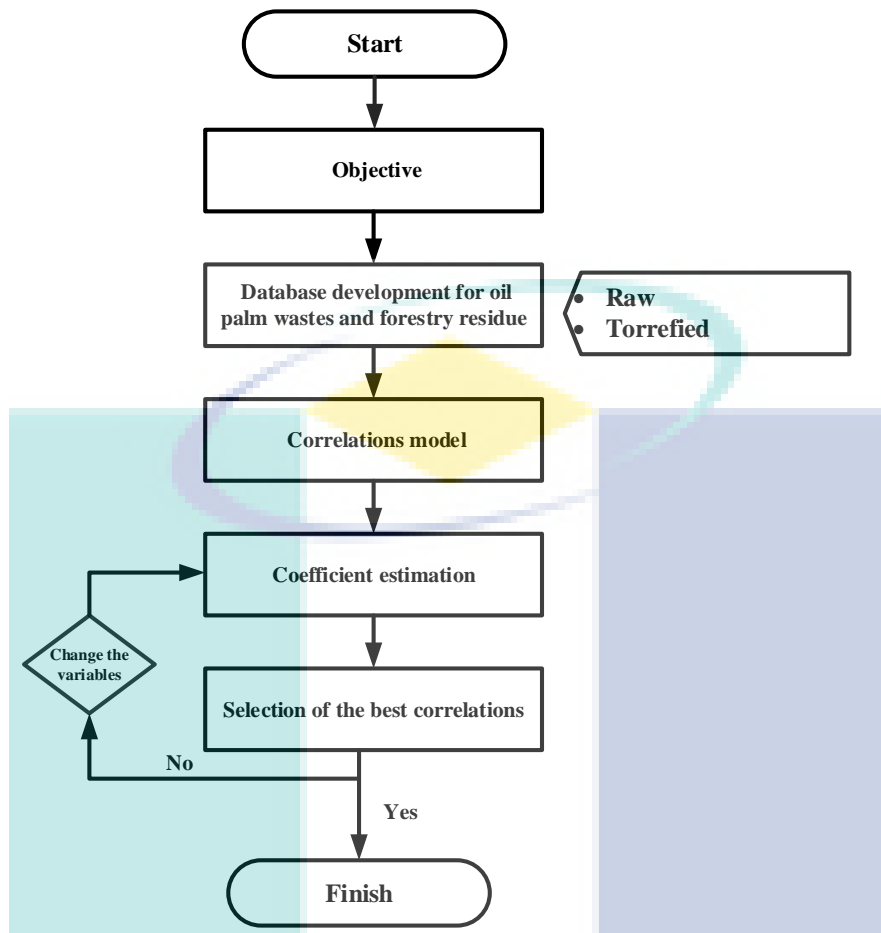
Figure 3.4 Higher heating value (HHV) correlations work flow

3.3.1.1 Objective

The objective is to develop correlation using either ultimate or proximate analysis for raw and torrefied biomass used in this study.

3.3.1.2 Database development for oil palm waste and forestry residue

The data of higher heating value, ultimate analysis and proximate analysis for raw and torrefied oil palm waste and forestry residue are collected and arranged in the database. In addition the data found in the literatures involving oil palm waste and forestry residue are also included in the database in order to increase the usefulness and reliability of the developed correlation. Figure 3.5 shows the screenshot of the developed database.

Ref			HHV	C	H	N	O	S	Ash
		300	23.79	55.724	5.959	4.318	33.779	0.22	4.76
		330	25.83	54.118	5.674	4.677	28.445	7.086	5.15
PKS		240	19.68	51.79	5.01	1.86	41.259	0.081	7.28
		270	21.91	52.35	5.334	1.63	40.614	0.072	8.13
		300	23.64	54.51	4.55	1.999	38.868	0.073	12.11
		330	25.46	59.92	3.911	2.56	33.523	0.086	13.71
PMF		240	18.05	47.7	5.599	1.35	45.243	0.108	6.08
		270	19.17	50.5	5.588	0.97	42.835	0.107	6.67
		300	21.49	53.7	5.435	1.77	38.978	0.117	7.10
		330	22.91	53.99	4.926	1.78	39.19	0.114	8.16
EFB		240	15.59	46.079	6.795	5.449	40.038	1.639	6.70
		270	17.99	47.647	6.631	6.022	39.204	0.496	7.67
		300	19.60	54.634	6.454	6.37	32.252	0.29	7.70
		330	22.07	54.06	5.626	4.071	36.035	0.208	11.88
Yoshimitsu Uemura, 2011a (EFB)		220	17.17	46.75	4.68	1.27	41.42	0.12	5.75
		250	17.67	47.07	4.95	1.35	42.24	0.11	4.28
		300	20.41	49.56	4.38	1.27	43.19	0.02	1.58
Yoshimitsu Uemura, 2011a (PMF)		220	19.03	46.93	5.50	1.83	43.40	0.10	2.34
		250	19.24	47.70	5.20	1.74	40.18	0.10	5.10
		300	22.17	48.60	4.87	2.14	40.03	0.09	4.26
Yoshimitsu Uemura, 2011a (PKS)		220.30m	18.85	45.87	6.31	0.40	43.07	0.02	4.33
		250.30m	19.07	51.89	5.71	0.47	38.50	0.01	3.42
		300.30m	21.68	54.21	5.08	0.50	36.66	0.02	3.53
Amin A Jaafar, 2011 (PKS)		240.30m	19.70	49.08	5.10	1.07	39.67	0.12	4.89
		260.30m	19.72	49.26	4.37	1.02	39.00	0.07	6.21
		280.30m	19.86	49.90	3.92	1.07	39.45	0.00	5.62
		240.60m	20.35	50.84	4.68	1.03	36.99	0.03	6.37
		260.60m	21.09	50.50	4.36	1.12	37.11	0.02	6.82
		280.60m	20.59	51.49	4.06	1.08	36.61	0.01	6.69

Figure 3.5 Biomass database example

3.3.1.3 Correlations model

There are 20 original correlations based on the proximate analysis obtained from Nhuchhen & Salam (2012). Meanwhile 10 original correlations (Channiwala & Parikh, 2002; Yin, 2011; Sheng & Azevedo, 2005; Demirbas A., 2009) based on ultimate analysis normally used for predicting the higher heating value. Both original correlations indicate that the HHV is depending on the properties of ultimate and proximate analysis. Furthermore the original correlations have been developed specifically on the raw biomass and thus it may not be accurate for predicting the HHV of torrefied biomass. In addition it is important to note that the torrefaction condition plays an important role on the higher heating value. Thus two new variables are then introduced in the original correlations which are t, residence time and T, torrefaction temperature into the correlations. Three forms of terms were being included in the 20 original correlations based on proximate analysis which are 'ct + dT', 'ct/T' and 'ct + d/T'. The new 60 correlations based on proximate analysis are shown in Table 3.3. Similarly these three terms were also included in the 10 original correlations based on ultimate analysis as shown in Table 3.4. As shown in Tables 3.3 and 3.4, the

coefficients denoted by a, b, c, d, e, f, g, h and i were the unknown variables that needs to be estimated.

Table 3.3 Proposed correlations based on proximate analysis

No	Proximate analysis
1	HHV = a + bFC/VM + ct + dT
2	HHV = a + bFC/VM + ct/T
3	HHV = a + bFC/VM + ct + d/T
4	HHV = a + bVM/FC + ct + dT
5	HHV = a + bVM/FC + ct/T
6	HHV = a + bVM/FC + ct + d/T
7	HHV = a + bFC/ASH + ct + dT
8	HHV = a + bFC/ASH + ct/T
9	HHV = a + bFC/ASH + ct + d/T
10	HHV = a + bASH/FC + ct + dT
11	HHV = a + bASH/FC + ct/T
12	HHV = a + bASH/FC + ct + d/T
13	HHV = a + bVM/ASH + ct + dT
14	HHV = a + bVM/ASH + ct/T
15	HHV = a + bVM/ASH + ct + d/T
16	HHV = a + bASH/VM + ct + dT
17	HHV = a + bASH/VM + ct/T
18	HHV = a + bASH/VM + ct + d/T
19	HHV = a + bFC/VM + cVM/FC + dt + eT
20	HHV = a + bFC/VM + cVM/FC + dt/T
21	HHV = a + bFC/VM + cVM/FC + dt + e/T
22	HHV = a + bVM/ASH + cASH/VM + dt + eT
23	HHV = a + bVM/ASH + cASH/VM + dt/T
24	HHV = a + bVM/ASH + cASH/VM + dt + e/T
25	HHV = a + bFC/ASH + cASH/FC + dt + eT
26	HHV = a + bFC/ASH + cASH/FC + dt/T
27	HHV = a + bFC/ASH + cASH/FC + dt + e/T
28	HHV = a + bFC/VM + cVM/ASH + dt + eT
29	HHV = a + bFC/VM + cVM/ASH + dt/T
30	HHV = a + bFC/VM + cVM/ASH + dt + e/T
31	HHV = a + bVM/ASH + cASH/FC + dt + eT
32	HHV = a + bVM/ASH + cASH/FC + dt/T
33	HHV = a + bVM/ASH + cASH/FC + dt + e/T
34	HHV = a + bASH/FC + cFC/VM + dt + eT
35	HHV = a + bASH/FC + cFC/VM + dt/T
36	HHV = a + bASH/FC + cFC/VM + dt + e/T
37	HHV = a + bVM/FC + cASH/VM + dt + eT
38	HHV = a + bVM/FC + cASH/VM + dt/T
39	HHV = a + bVM/FC + cASH/VM + dt + e/T
40	HHV = a + bASH/VM + cFC/ASH + dt + eT
41	HHV = a + bASH/VM + cFC/ASH + dt/T
42	HHV = a + bASH/VM + cFC/ASH + dt + e/T
43	HHV = a + bFC/ASH + cVM/FC + dt + eT
44	HHV = a + bFC/ASH + cVM/FC + dt/T
45	HHV = a + bFC/ASH + cVM/FC + dt + e/T
46	HHV = a + bFC/VM + cVM/ASH + dASH/FC + et + fT
47	HHV = a + bFC/VM + cVM/ASH + dASH/FC + et/T
48	HHV = a + bFC/VM + cVM/ASH + dASH/FC + et + f/T

Table 3.3 Continued

No	Proximate analysis
49	HHV = a + bVM/FC + cASH/VM + dFC/ASH + et + fT
50	HHV = a + bVM/FC + cASH/VM + dFC/ASH + et/T
51	HHV = a + bVM/FC + cASH/VM + dFC/ASH + et + f/T
52	HHV = a + b(FC+VM)/ASH + ct + dT
53	HHV = a + b(FC+VM)/ASH + ct/T
54	HHV = a + b(FC+VM)/ASH + ct + d/T
55	HHV = a + b(FC+ASH)/VM + ct + dT
56	HHV = a + b(FC+ASH)/VM + ct/T
57	HHV = a + b(FC+ASH)/VM + ct + d/T
58	HHV = a + b(ASH+VM)/FC + ct + dT
59	HHV = a + b(ASH+VM)/FC + ct/T
60	HHV = a + b(ASH+VM)/FC + ct + d/T

Table 3.4 Proposed correlations based on ultimate analysis

No	Ultimate analysis
1	HHV = a + bC + cH + dO + et + fT
2	HHV = a + bC + cH + dO + et/T
3	HHV = a + bC + cH + dO + et + f/T
4	HHV = a + bC + cH + dN + eO + fS + gt + hT
5	HHV = a + bC + cH + dN + eO + fS + gt/T
6	HHV = a + bC + cH + dN + eO + fS + gt + h/T
7	HHV = a + bC + cH + dN + eO + fS + gAsh + ht + iT
8	HHV = a + bC + cH + dN + eO + fS + gAsh + ht/T
9	HHV = a + bC + cH + dN + eO + fS + gAsh + ht + i/T
10	HHV = a +bC + ct + dT
11	HHV = a +bC + ct/T
12	HHV = a +bC + ct + d/T
13	HHV = aC + bH + cS + dt + eT
14	HHV = aC + bH + cS + dt/T
15	HHV = aC + bH + cS + dt + e/T
16	HHV = aC + bH + cS + d(O + N) + eA + f + gt + hT
17	HHV = aC + bH + cS + d(O + N) + eA + f + gt/T
18	HHV = aC + bH + cS + d(O + N) + eA + f + gt + h/T
19	HHV = aC + bH + cS + d(O + N) + eA + ft + gT
20	HHV = aC + bH + cS + d(O + N) + eA + ft/T
21	HHV = aC + bH + cS + d(O + N) + eA + ft + g/T
22	HHV = aC + b(H - (O/8)) + cS + dt + eT
23	HHV = aC + b(H - (O/8)) + cS + dt/T
24	HHV = aC + b(H - (O/8)) + cS + dt + e/T
25	HHV = aC + bH + cS + dO + et + fT
26	HHV = aC + bH + cS + dO + et/T
27	HHV = aC + bH + cS + dO + et + f/T
28	HHV = aC + bH + cN + dO + et + fT
29	HHV = aC + bH + cN + dO + et/T
30	HHV = aC + bH + cN + dO + et + f/T

3.3.1.4   Coefficient estimation

The estimation of coefficients in the proposed correlations as shown in Tables 3.3 and 3.4. The coefficients (a, b, c, d, e, f, g, h and i) are estimated by using the Microsoft Excel Solver Tool based on the higher heating values, proximate/ultimate analysis data.

3.3.1.5   Selection of the best correlations

The selection criteria is formed based on the absolute error (AE) and average absolute error (AAE) as shown in Equations 3.13 and 3.14. The i and N refer to specific sample of a biomass, and total number of samples respectively. While, HHV_{est} and HHV_{exp} represent the estimated HHV value and experimental HHV value respectively. AE are an error for an individual biomass while AAE are obtained based on the average error for multiple biomass. Here the predicted HHV was calculated from each proposed correlation based on the estimated coefficients obtained from previous step. The predicted and experimental values of HHV were then used for determining the absolute error AAE. In this case, lower absolute error means the correlation was able to estimate the HHV value accurately. The best correlation was selected based on the AAE values closer to zero which indicating the HHV predicted was closed to the experimental value.

$$Absolute\ error = \left| \frac{HHV_{est} - HHV_{exp}}{HHV_{exp}} \right| \times 100\% \qquad 3.13$$

$$Average\ absolute\ error = \sum_{i=1}^{N} \left| \frac{HHV_{est} - HHV_{exp}}{HHV_{exp}} \right| \times 100\% \Big/ N \qquad 3.14$$

3.3.2   Simulation of fluidized bed gasification

In second part of model application, the data from torrefaction experiment were used in the simulation of fluidized bed gasification where the usefulness of torrefaction as biomass pre-treatment was evaluated. For this simulation, the effects of raw and torrefied biomass on the synthesis gas production were studied. The process flow for simulation of gasification process is shown in Figure 3.6.
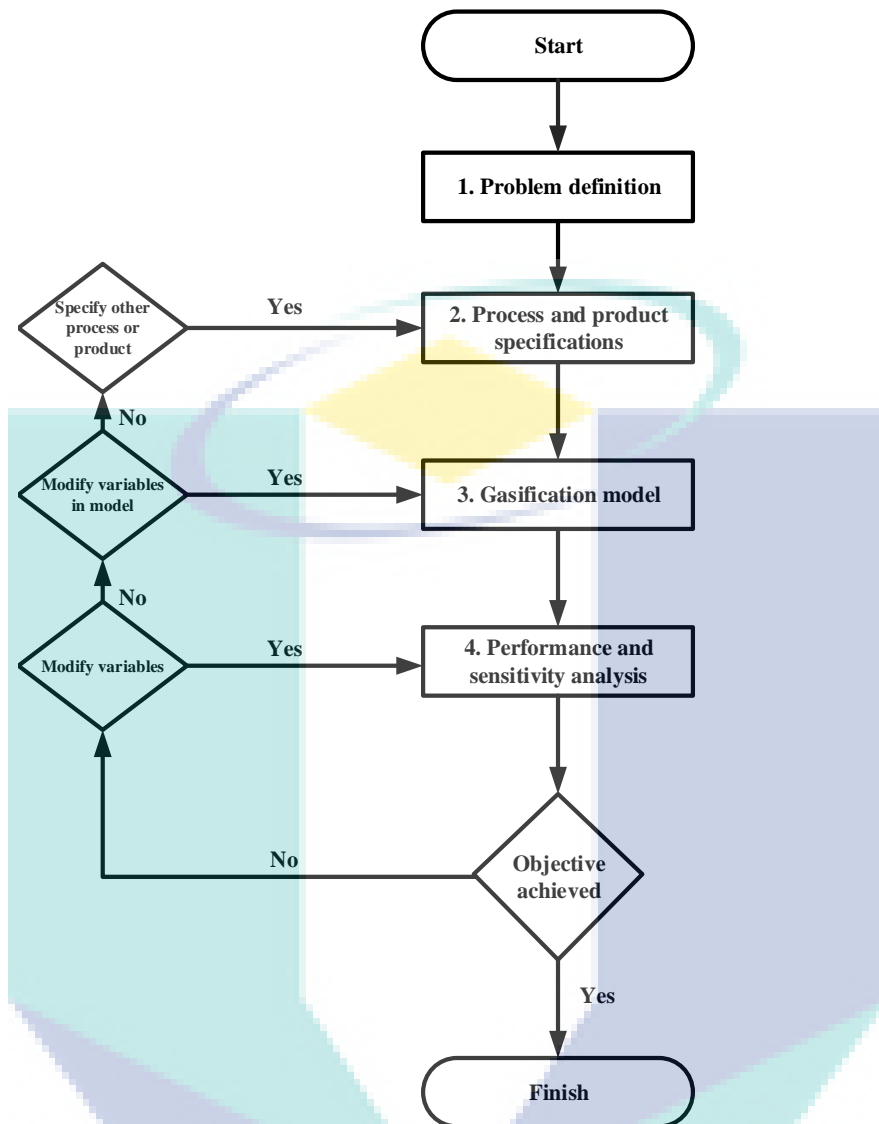
Figure 3.6 Gasification simulation process flow

3.3.2.1 Problem definition

In this step, the objective was defined in terms of gasification to be studied. For example the objective could be to simulate gasification process or to compare the synthesis gas production using raw and torrefied biomass.

3.3.2.2 Process and product specifications

Step 2 involves the specification of desired process and product. Basically in this step, all the raw materials specification and conditions that will be used in the simulation are chosen based on the objective selected in Step 1. For process

specification, basically the selections were divided into two parts which are the selection of biomass to be studied and the types of gasifier for gasification simulation. For biomass selection, a biomass database has been developed in Excel software for raw and torrefied OPW and forestry residue as shown in the model correlations step which acts as supporting tools of the framework. All the collected biomasses were arranged based on its ultimate analysis, proximate analysis and HHV. All of these properties are essential and were used in Aspen Plus for simulation process.

Once the biomass was selected, the gasifier to be used is specified which was bubbling fluidized bed gasifier. In terms of the product specification, the user needs to specify the desired gas to be produced. Usually in the gasification process, the term synthesis gas (syngas) was commonly used when describing the product of gasification process. It consists of several types of gas components for example hydrogen, carbon monoxide, carbon dioxide and traces of methane. For this part, the production of hydrogen gas was the main focus as it is used in many energy related applications such as fuel cell.

3.3.2.3   Gasification model

Step 3 was focusing on the model development of gasification system. The gasification model has been developed in the Aspen Plus software due to its capabilities of process decomposition into its constituent elements for individual study of performance (Eden, 2012). For physical property method, the Redlich-Kwong-Soave cubic equation of state with Boston-Mathias alpha function (RKS-BM) has been used to estimate all physical properties of the conventional components in the gasification process. This property method is comparable to the Peng Robinson cubic equation of state with the Boston-Mathias alpha function (PR-BM) property method. RKS-BM was mostly recommended since it is applicable for refinery, gas-processing and petrochemical applications such as gas plants, crude towers and ethylene plants (Eikeland et al., 2015). This method is generally used for non-polar or mildly polar mixtures, like hydrocarbons and light gases such as CO_2, H_2 and hydrogen sulphide. Using RKS-BM, reasonable results can be expected at all temperatures and pressures. The RKS-BM property method is consistent in the critical region.

In typical gasifier, there are three main thermochemical processes take place which are pyrolysis (>150 °C), combustion (150 °C – 170 °C) and gasification (600 °C

-1100 °C). The pyrolysis process separates the water vapour, organic liquids and non-condensable gases from the char or solid carbon of the fuel. This process involves the degradation of biomass by heat under absence of oxygen. The devolatilization or pyrolysis processes start slowly at temperature lesser than 350 °C, accelerating to an almost instantaneous rate above 700 °C. The composition of the evolved products was a function of the temperature, pressure, and gas composition during devolatilization. The feed are then decomposed in this stage to specific components such as hydrogen, oxygen, nitrogen and carbon based on the yield distribution. In addition, some product gas such as CO, H_2, CH_4, and H_2O are produced during this stage. Char (C), a solid residue from biomass mainly containing carbon element also are also produced from the pyrolysis process (Basu, 2013).

Subsequently the combustion process oxidizes fuel constituents in an exothermic reaction, while the gasification process reduces them to combustible gases in an endothermic reaction. The combustion process involves reaction with oxygen, which may be supplied as pure oxygen or from air, and forms carbon monoxide and carbon dioxide. The reactions of combustion are shown below:

$$C + O_2 \rightarrow CO_2 \qquad\qquad 3.15$$
$$C + 0.5O_2 \rightarrow CO \qquad\qquad 3.16$$

The heat of reaction for both reactions are shown in Equations (3.15) and (3.16). For gasification process, the reactions involved are shown in Equations (3.17) to (3.23):

$$H_2 + 0.5O_2 \rightarrow H_2O \qquad\qquad 3.17$$
$$C + CO_2 \leftrightarrow 2CO \qquad\qquad 3.18$$
$$C + H_2O \leftrightarrow CO + H_2 \qquad\qquad 3.19$$
$$C + 2H_2 \rightarrow CH_4 \qquad\qquad 3.20$$
$$CO + H_2O \leftrightarrow CO_2 + H_2 \qquad\qquad 3.21$$
$$CH_4 + H_2O \leftrightarrow CO + 3H_2 \qquad\qquad 3.22$$
$$CH_4 + 2H_2O \leftrightarrow CO_2 + 4H_2 \qquad\qquad 3.23$$
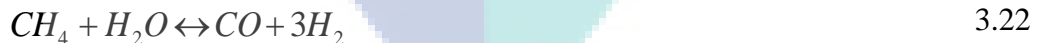
Based on the given reactions, the gasification process will produces combustible gases such as hydrogen, carbon dioxide, carbon monoxide, and methane. The main reactions of gasification process are Boudouard reaction (Equation 3.18), steam reforming reaction (Equation 3.19), methanation (Equation 3.20) and water-gas shift reaction (Equation 3.21). Boudouard reaction known as the reaction of carbon dioxide

present in the gasifier reacts with char to produce carbon monoxide gas under endothermic condition. Steam reforming reaction is the partial oxidation of carbon by steam, which could come from a host of different sources, such as water vapour associated with the incoming air, vapour produced from the evaporation of water, and pyrolysis of the solid fuel. Steam reacts with the hot carbon according to the heterogeneous water–gas reaction. Methane also produced in the gasifier from the methanation process through hydrogasification of hydrogen and char (Lee et al., 2014). For water-gas shift reaction, the carbon monoxide will be reacted with steam to produce hydrogen gas.

For the purpose of model development in Aspen Plus software, the assumptions used for both gasification models are: (i) the processes are in the isothermal and steady state conditions; (ii) the composition of char consists only carbon, void and ash; (iii) all chemical reactions occur under equilibrium state in the gasifier and there is no pressure loss; (iv) all the particles are assumed in the spherical shape, uniform size and the average diameter remains constant during the gasification meaning that no species concentration or thermal gradients exist within the particles; (v) the synthesis gas produced in the ideal gases state, including H_2, CO, CO_2, steam (H_2O) and CH_4; (vi) all hydrogen and oxygen components contain in the biomass are assumed to be released during devolatilization; (vii) The pressure drop and heat losses from the equipment and pipelines were not included; (vi) All sulphur produced will be neglected in the output product.

All the reactions shown in Equations (3.15) to (3.23) were employed using different unit operations block in Aspen Plus. For pyrolysis process, the RYIELD block was used since the specialized of this block is to convert non-conventional biomass into conventional components based on mass balance. For combustion reaction, RGIBBS block was used since this block has the capability to run several restricts chemical equilibrium or simultaneous phase of specified reactions in order to simulate the gasification. For purification, the RSTOIC was applied since this reactor used stoichiometry and extent of reaction in order to perform a simulation. Once the model has been developed, the model will undergo performance analysis.

3.3.2.4   Performance and sensitivity analysis

After the model from Step 3 has been developed, the next step was Step 4 which consists of performance and sensitivity analysis. In this step, the results from model simulation are evaluated in terms of its behaviour which in accordance with the theory. In addition the model validation can be performed in this step where the simulation results obtained are compared with experimental or literature data. For model validation purpose, the root mean square error (RMSE) are used for assessing the reliability of the model based on the following equations:

$$RMSE = \frac{\sqrt{\sum \frac{\left(y_{ie} - y_{ip}\right)^2}{y_{ie}}}}{N}$$

3.24

Second features of this step was to perform sensitivity analysis. Sensitivity analysis is a common techniques to determine how different values of an independent variable will impact output variables under a given set of assumptions. It is important to perform sensitivity analysis for investigating the effects of varying the values of key parameters on model performance in order to ascertain the validity of the approach. Several simulation trials were conducted by varying the relevant parameter while all other parameters were kept constant. In this step, the model are undergoing sensitivity analysis in specific range of operating conditions. The relevant parameters selected for sensitivity analysis in fluidized bed gasification process were gasification temperature, air to biomass ratio (ABR), and steam to biomass ratio (SBR). The air to biomass ratio is defined as the ratio of the actual air to biomass ratio divided by the stoichiometric air to biomass ratio required for complete combustion. In biomass gasification the range of air biomass ratio is varying from 0.20 to 1. Steam to biomass ratio is defined as moles of steam as a gasifying agent per mole of biomass in the feedstock. Steam to biomass ratio has a significant effect on the output synthesis gas in gasification. Basically, the ranges for investigating the steam to biomass analysis were set between 0.2 and 1.0. The ranges were selected based on the common ranges used in literature as stated by Suwatthikul et al. (2017) for SBR and Jangsawang et al. (2015) for ABR. In this work the summary of tested range for each process variables are shown in Table 3.5.

Table 3.5 Tested range for process variables.

Process Variables	Low	Mid	High
Temperature (°C)	600	800	1000
ABR	0.2	0.6	1.0
SBR	0.2	0.6	1.0

In addition, the amount of lower heating value (LHV) and cold gas efficiency (CGE) were also calculated in this work. In this work, LHV was calculated for product synthesis gas and biomass as shown in Equations (3.25) – (3.26). The LHV for product synthesis gas was accounted for the amount of heat available from a fuel after the latent heat of vaporisation. Meanwhile LHV of biomass was calculated based on the HHV value and elemental composition of biomass. Meanwhile the cold gas efficiency (CGE) as shown in Equation (3.27) was defined as the fraction of the chemically bound energy in the biomass that is converted into chemically bound energy in the product gas from the gasification process.

$$LHV_{PG} = 0.126\,\chi_{CO} + 0.358\,\chi_{CH_4} + 0.108\,\chi_{H_2} \qquad 3.25$$

$$LHV_{bio} = HHV - 0.212 \times H - 0.00245 \times M - 0.008 \times O \qquad 3.26$$

$$CGE = \frac{\overset{\bullet}{m}_{PG}\,LHV_{PG}}{\overset{\bullet}{m}_{Bio}\,LHV_{Bio}} \times 100\% \qquad 3.27$$

Where ṁPG and ṁBio is the mass flow rates of product gas and biomass in kg/h respectively. χ_{CO}, χ_{CH4} and χ_{H2} is the product composition of output carbon monoxide, methane and hydrogen (Arena, 2012). *HHV* is the higher heating value of the biomass (MJ/kg), *H*, *M*, and *O* are the weight percentages of hydrogen, moisture content and oxygen obtained from ultimate analysis. Both of LHV and CGE is the important indicator to measure an efficiency of biomass conversion in the gasifier reactor (Jayathilake & Rudra, 2017).

CHAPTER 4

TORREFACTION EXPERIMENT DATA ANALYSIS

4.1   Overview

In this chapter, the changes of characteristics and properties for oil palm waste (PMF, EFB, PKS and OPF) and forestry residue (Meranti, Seraya, Kulim and Chengal) are analysed in order to evaluate the effects of torrefaction process. Firstly, the physical appearances of raw and torrefied biomass are discussed, followed by the obtained mass and energy yields, proximate analysis, ultimate analysis, H/C and O/C ratios, and higher heating value (HHV). In addition, the HHV correlation models are developed based on the ultimate and proximate analysis and its accuracy in predicting the HHV is evaluated.

4.2   Physical appearances

In this study, the physical appearances of the raw and torrefied biomass were observed based on the images taken using digital camera. By comparing the colour changes from raw to different temperature of torrefied biomass, the severity of torrefaction process can be observed. In this research, the oil palm waste and forestry residue were undergone torrefaction process under four different temperatures and three different residence time. The physical appearances of oil palm waste and forestry residue are illustrated in Table 4.1 and Table 4.2.

Table 4.1 Physical appearances of raw and torrefied oil palm waste
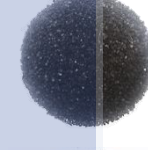
Biomass	Residence time, min	Condition				
		Raw	240 °C	270 °C	300 °C	330 °C
Oil palm frond	15					
	30					
	60					
Palm kernel shell	15					
	30					
	60					
Palm mesocarp fibre	15					
	30					
	60					
Empty fruit bunch	15					
	30					

Table 4.1 Continued

Biomass	Residence time, min	Condition				
		Raw	240 °C	270 °C	300 °C	330 °C
Empty fruit bunch	60					

Table 4.2 Physical appearances of raw and torrefied forestry residue
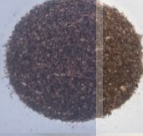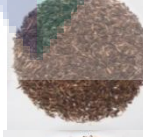
Biomass	Residence time, min	Condition				
		Raw	240 °C	270 °C	300 °C	330 °C
Meranti	15					
	30					
	60					
Seraya	15					
	30					
	60					
Kulim	15					
	30					
	60					

Table 4.2 Continued
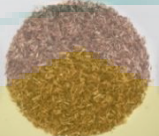
Biomass	Residence time, min	Condition				
		Raw	240 °C	270 °C	300 °C	330 °C
Chengal	15					
	30					
	60					

Table 4.1 and Table 4.2 show that the colour of the samples change from light brown to darker colour when biomass is torrefied from lower to the higher torrefaction temperature. However, the intensity of colour is different which is depending on the torrefaction temperature. Increment of torrefaction temperature contributes to the increment of colour intensity. Torrefied samples at higher torrefaction temperature are darker compare to lower torrefaction temperature. In addition, the longer the residence time, the darker are the torrefied products. This is because, when sample is heated, the hydrocarbon is broken down and carbon is left and deposited on the surface of the sample. Based on the torrefaction of oil palm waste, empty fruit bunch at torrefaction temperature of 330 °C and residence time of 60 minutes shows the darkest colour. The other oil palm waste at the same condition still have a little light colour indicate that it is not fully torrefied. For forestry residue, the darkest colour is observed for torrefied Kulim at torrefaction temperature of 330 °C and residence time of 60 minutes. Although there are some visible yellowish/brownish spot for all of Kulim sample, meaning that it is not fully torrefied, it is still lesser compare to other forestry residue. The changes in colour is in agreement with the studies done by Asadullah et al. (2014) and Nhuchhen et al. (2014).

4.3   Mass and energy yields

The mass yield was calculated by using Equation 3.1. The mass yield of oil palm waste and forestry residue are summarised in Figure 4.1. The mass yield shows a

decreasing trend when the torrefaction temperature is increased. Temperature is the dominant parameter in torrefaction. The higher the temperature, the higher the mass loss thus the lower the mass yield of the biomass is obtained. The residence time indeed affecting the mass yield. The longer the process, the mass loss is higher thus the lower the mass yield.

At 15 minutes residence time, in Figure 4.1 (a) and (d), both oil palm waste and forestry residue show a decreasing trend. For oil palm waste, the highest mass yield for every torrefaction temperature is PKS. This is due to PKS consist of less hemicellulose (PKS: 22.7 wt%, PMF: 26.1 wt%, OPF: 40.4 wt% and EFB: 35.3 wt%) and cellulose (PKS: 20.8 wt%, PMF: 33.9 wt%, OPF: 30.4 wt% and EFB: 38.3 wt%) composition compare to other oil palm waste (Kong et al., 2014). Hemicellulose and cellulose start to decompose at temperature ranges from 220 to 350 °C (van der Stelt et al., 2011) while for lignin it ranges from 200 to 800 °C (Sukiran et al., 2017).

As for forestry residue, Seraya is the highest for all torrefaction temperature. It can be said from these that Seraya have less hemicellulose and cellulose composition than the other forestry residue. The lowest mass yield for oil palm waste is EFB (53.83%) when torrefied at 330 °C while it is Kulim (76.74%) for forestry residue at the same condition. Comparing both oil palm waste and forestry residue, forestry residue biomass have a higher mass yield from lower torrefaction temperature to higher torrefaction temperature. This result shows that, the oil palm waste biomass have higher composition of hemicellulose and cellulose compare to forestry residue. Other than that, forestry residue, for example Chengal, have higher lignin composition (44.7%) (Ahmad et al., 2013), thus takes longer time to torrefy and has high mass yield.

The same mass yield trends for 15 minutes torrefaction is observed as torrefaction for 30 and 60 minute. The difference is that for oil palm waste, the highest mass yield are from PMF in Figure 4.1 (b) and (c). This may due to the difference between PMF and PKS hemicellulose and cellulose composition is not significant. Studies done by Sabil et al., (2013), found that the hemicellulose of PMF is 23.03% while for PKS it is 24.10%. This result indicated that by having more hemicellulose composition, PKS mass yield are lower than PMF. This is due to the degradation of hemicellulose and cellulose ate temperature ranging from 220 to 350 °C (van der Stelt et al., 2011).

Overall, increasing in torrefaction temperature and residence time for both biomass types shows a decrease in the range of 0.04 to 33.07% for both oil palm waste and forestry residue. From Figure 4.1, although longer residence time relatively decrease the mass yield, it effects was not as significant as compared to the temperature. This indicates that temperature is an important variable when it comes to torrefaction process. This finding is in agreement with Jaafar & Ahmad (2011), Pimchuai et al. (2010) and Chiou et al. (2015).
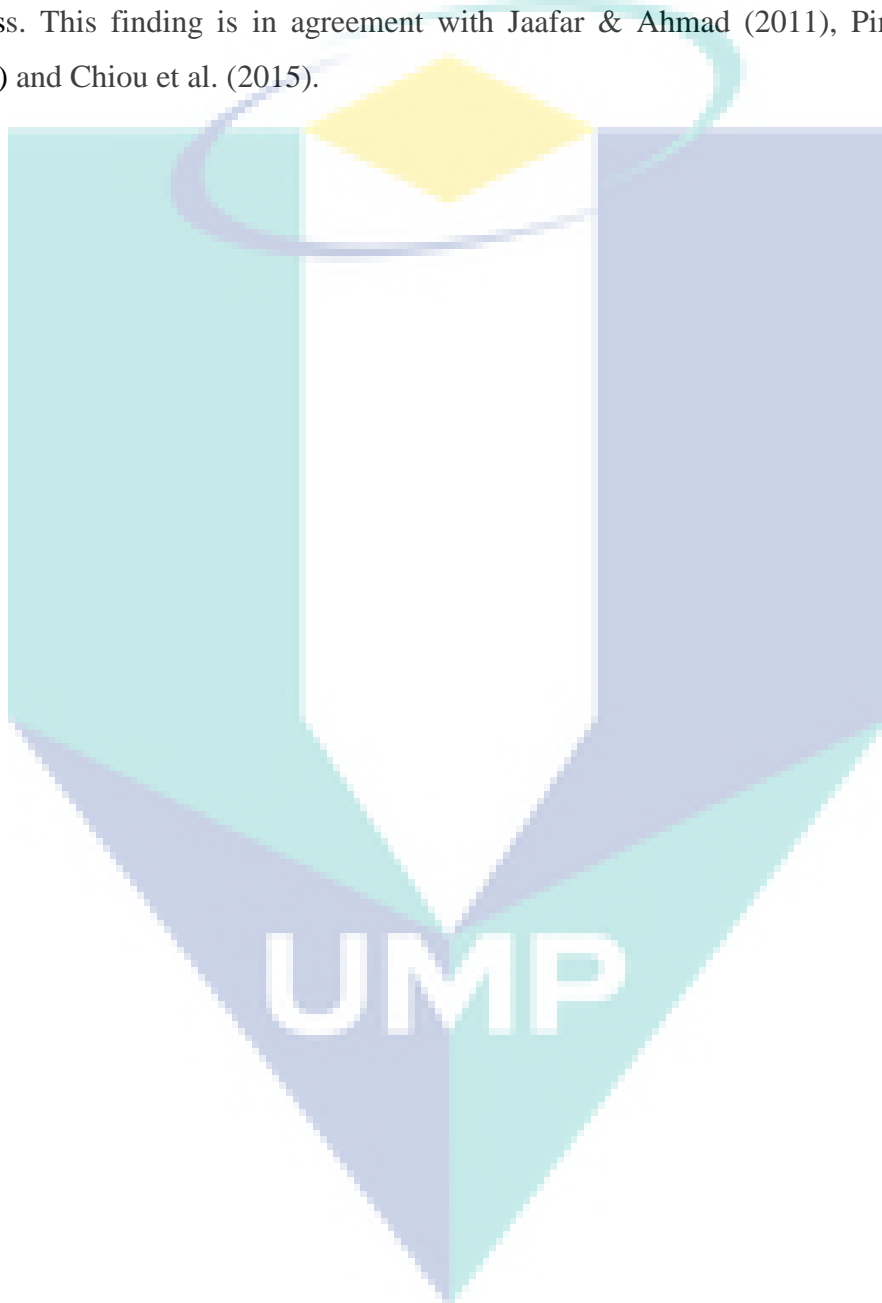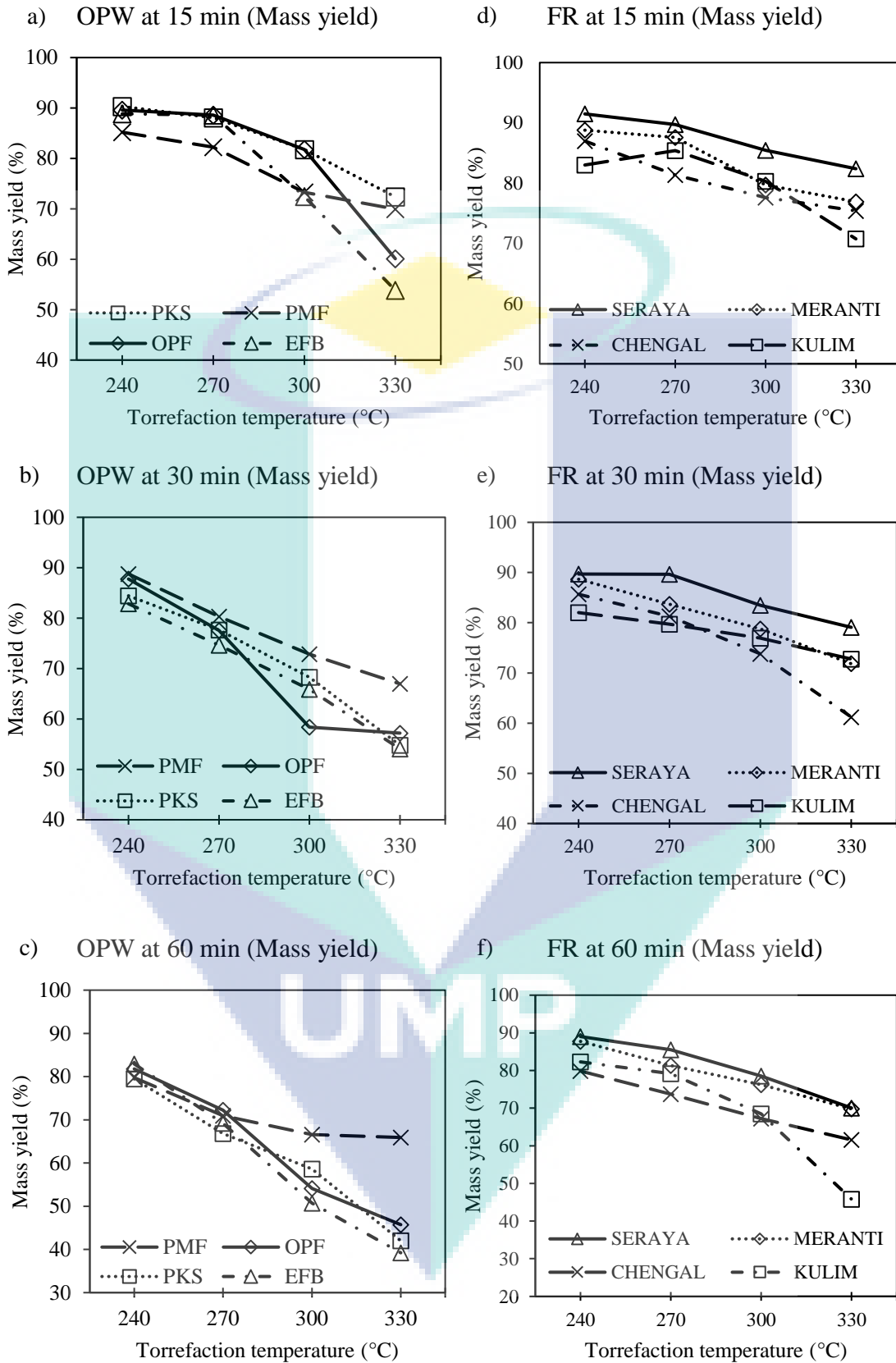
Figure 4.1 Mass yield for oil palm waste at a) 15 minutes, b) 30 minutes, c) 60 minutes and forestry residue at d) 15 minutes, e) 30 minutes, f) 60 minutes

Energy yields for both the oil palm waste and forestry residue are presented in Figure 4.2. Calculation of energy yield was determined using Equation 3.2. According to Asadullah (2014), there are two important factors in torrefaction process, which are the mass and energy yields, as well as the higher heating value of the raw and torrefied product. From Equation 3.2, the energy yield calculation includes the mass yield and higher heating value of the product. Thus, mass yield and higher heating value have a significant effect on the value of energy yield.

In Figure 4.2, the trends for both energy yield profiles cannot be described precisely as they are inconsistent. The energy yield for oil palm waste shows a decreasing trend while forestry residue shows an increasing trend. Most researchers reported that energy yield decreased linearly with the decreasing of solid yield (Chen et al., 2011; Sabil et al., 2013; Wannapeera et al., 2011). However, in this study, the trends are inconsistent as the enhancement factor in HHV and mass yield not increase or decrease gradually. However there are some studies that have inconsistent trends such as studies carried out by Uemura et al., (2013) and Uemura et al., (2015b).

In Figure 4.2 (b), in the case of torrefaction of EFB using 30 minutes residence time, initially the HHV for raw EFB is 15.49 MJ kg^{-1} and the HHV is increased to 17.99 MJ kg^{-1} for torrefied EFB at 270 °C and further increased to 19.6 MJ kg^{-1} for torrefied EFB at 300 °C. Thus, the enhancement factor in HHV ratios at torrefaction temperature of 270 °C and 300 °C are 1.16 and 1.27 respectively. When the enhancement factor in HHV for EFB at torrefaction temperature of 300 °C is multiplied with its mass yield, the energy yield obtained is much lower than EFB at 270 °C due to lower mass yield obtained at the given torrefaction temperature.

Torrefaction of OPF shows that at torrefaction temperature of 300 °C and 330 °C at 30 minutes torrefaction, the energy yield obtained for OPF is increased from 78% to 83% as shown in Figure 4.2 (b). Although the enhancement factor in HHV for 330 °C is higher which is 1.46 compared to 270 °C which is 1.34, it doesn't give a lower value for energy yield because in the case of OPF, the mass yield for torrefaction temperature of 300 °C and 330 °C are slightly different. Because of this situation, energy yield cannot be used as an indicator to evaluate the energy content in biomass thus an enhancement factor is needed to elaborate this trend. Details on the enhancement factor are further discuss in subchapter 4.7. The same trends are also observed for energy yield of forestry residue as shown in Figure 4.2 (d), (e) and (f).

Torrefaction at 15 minutes shows that for both biomass group, majority of the biomass achieved more than 70% mass yield but their energy yield lower compared to biomass torrefied at 30 and 60 minutes. At time 60 minutes, because of longer time was used, more components are definitely have a lower yield indicating more volatile components have been released during the torrefaction process. Based on the mass yields (Figure 4.1) and energy yields (Figure 4.2), the most suitable residence time for torrefaction process using oil palm waste and forestry residue is at 30 minutes.
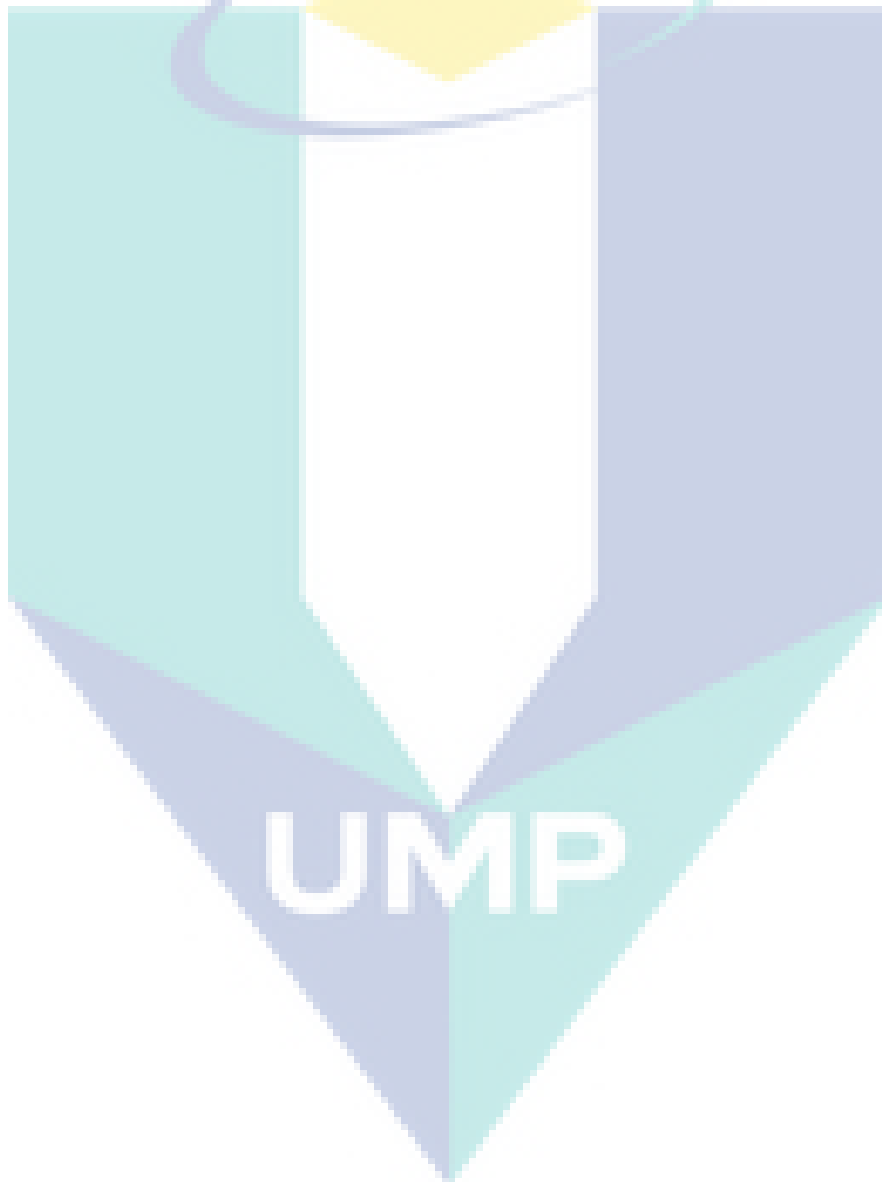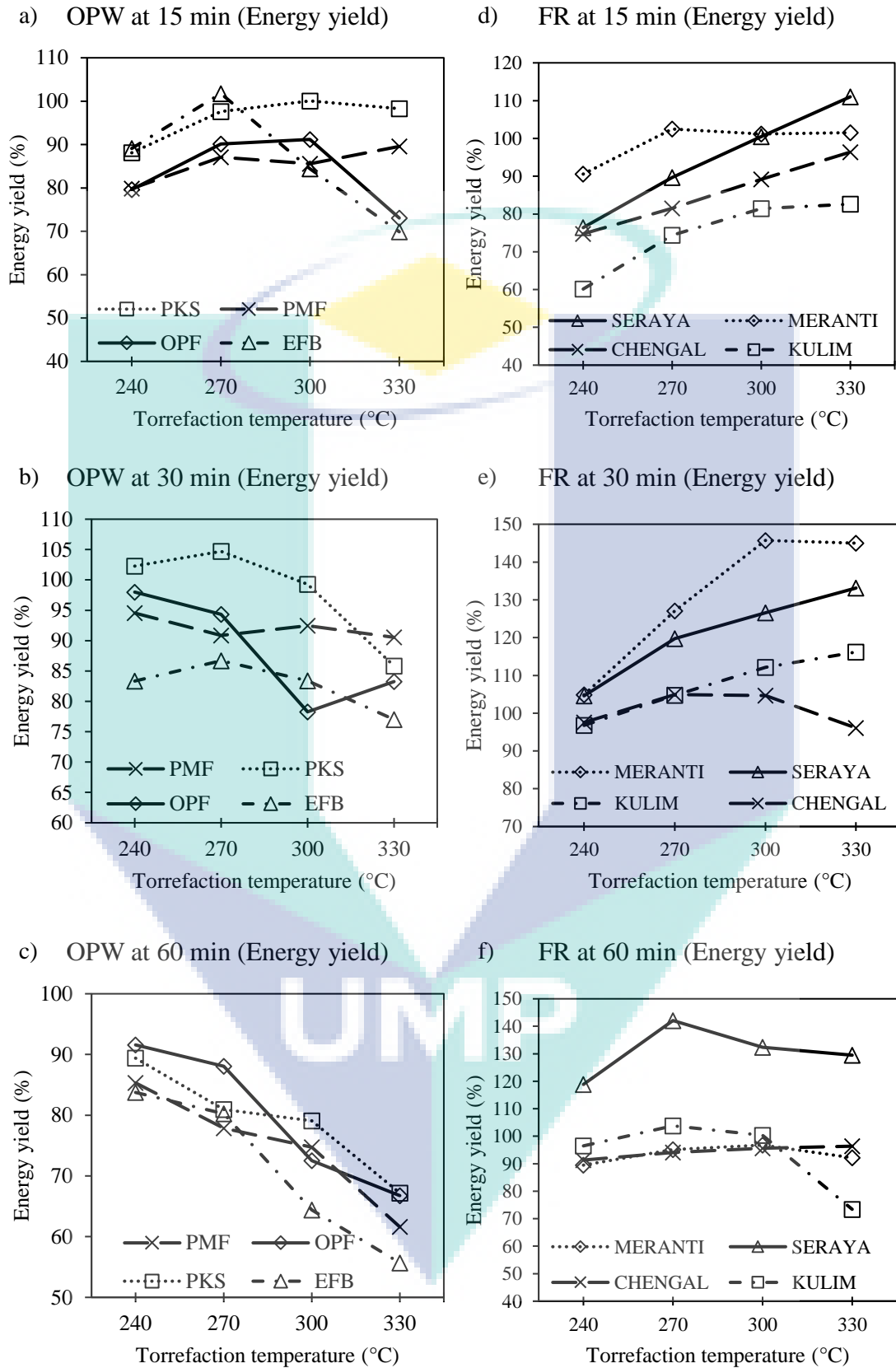
Figure 4.2 Energy yield for oil palm waste at a) 15 minutes, b) 30 minutes, c) 60 minutes and forestry residue at d) 15 minutes, e) 30 minutes, f) 60 minutes

4.4 Proximate analysis

Proximate analysis was carried out to investigate the composition of volatile matter (VM), fixed carbon (FC) and ash of the raw and torrefied biomass. For this analysis, all torrefied oil palm waste and forestry residue samples for 30 minutes residence time at different temperatures were analysed. The results are shown in Tables 4.3 and 4.4 for oil palm waste and forestry residue respectively. For both oil palm waste and forestry residue, VM shows a decrease in composition while FC and ash content are increased in composition. The range of VM for raw oil palm waste and forestry residue are 66.17 to 70.02 wt% and 72.33 to 76.48 wt% respectively. When undergone torrefaction process, the VM of torrefied oil palm waste decreases to 37.95 wt% and 64.55 wt% for forestry residue. This is because of the dehydration process occur and the light volatiles are released from the biomass. This process also affect the FC and increases its compositions. For raw biomass, FC for oil palm waste and forestry residue are in the range of 23.94 to 30.96 wt% and 22.66 to 29.30 wt% respectively. After torrefaction, FC range is increased from 26.45 to 55.89 wt% for oil palm waste and 24.88 to 46.89 wt% for forestry residue. Increment in the FC content is due to the decomposition of hemicellulose that turn into a carbon rich solid product at the temperature ranging from 235 to 275 °C as reported by Tumuluru et al (2011). Higher FC are preferred as its affect the higher heating value of the biomass. On the contrary, lower ash content is the most preferable for torrefied product because the high content of ash usually leads to lower heating value (Chen et al., 2015).

Table 4.3 Proximate analysis of raw and torrefied oil palm waste

Biomass	Proximate analysis (wt%) (dry basis)	Raw	240 °C	270 °C	300 °C	330 °C
Oil palm frond	Volatile matter	66.17	62.86	56.15	45.54	37.95
	Fixed carbon	30.96	33.93	39.23	49.70	56.89
	Ash content	2.87	3.20	4.62	4.76	5.15
Palm kernel shell	Volatile matter	70.02	66.27	65.70	58.55	49.68
	Fixed carbon	23.94	26.45	26.17	29.34	36.61
	Ash content	6.04	7.28	8.13	12.11	13.71
Palm mesocarp fibre	Volatile matter	69.04	66.07	64.60	59.58	56.43
	Fixed carbon	25.30	27.84	28.73	33.33	35.41
	Ash content	5.66	6.08	6.67	7.10	8.16
Empty fruit bunch	Volatile matter	67.01	63.51	56.50	48.44	38.63
	Fixed carbon	29.14	29.79	35.83	43.86	49.49
	Ash content	3.85	6.70	7.67	7.70	11.18

Table 4.4 Proximate analysis of raw and torrefied forestry residue

Biomass	Proximate analysis (wt%) (dry basis)	Raw	240 °C	270 °C	300 °C	330 °C
Meranti	Volatile matter	76.48	73.99	71.76	69.61	65.86
	Fixed carbon	22.66	24.88	26.24	28.24	31.43
	Ash content	0.86	1.13	2.00	2.16	2.71
Seraya	Volatile matter	74.85	73.55	73.43	71.35	66.48
	Fixed carbon	24.46	25.50	25.56	26.82	31.51
	Ash content	0.69	0.95	1.01	1.83	2.02
Kulim	Volatile matter	72.33	70.81	69.40	67.73	64.55
	Fixed carbon	26.76	28.16	29.43	30.98	33.99
	Ash content	0.91	1.03	1.17	1.29	1.46
Chengal	Volatile matter	73.17	71.59	69.82	68.02	65.29
	Fixed carbon	26.30	27.86	29.46	31.26	33.89
	Ash content	0.53	0.55	0.72	0.78	0.82

4.5 Ultimate analysis

Ultimate analysis was conducted to determine the carbon, hydrogen, nitrogen, oxygen and sulphur compositions of the raw and torrefied biomass. For this analysis, samples torrefied for 30 minutes at different temperatures were analysed. The results of ultimate analysis for both oil palm waste and forestry residue are shown in Tables 4.5 and 4.6 respectively. The significant changes for ultimate analysis can be seen from its carbon, hydrogen and oxygen compositions. The changes for this compositions explain how the torrefaction affect the biomass. For both oil palm waste and forestry residue, the sulphur and nitrogen compositions are low and thus it can be negligible (Deng et al., 2009). For oil palm waste, the carbon composition increment are in the range of 5.24% to 23.06% and the decrement of hydrogen and oxygen compositions are ranging from 5.57% to 34.26% and 5.02% to 43.30% respectively. While for forestry residue, carbon composition is increased in the range of 2.11% to 16.29% and hydrogen and oxygen compositions are decreased from 1.38% to 24.85% and 2% to 25.68% respectively.

When torrefaction occur, dehydration process takes place and produce carbon dioxide, carbon monoxide, methane and hydrogen (Chen & Kuo, 2010). This process subsequently decrease the compositions of hydrogen and oxygen. Hydrogen is used in combustion and oxygen is important in fuel burning. This lead to decrease in both of these components composition. Biomass which has higher hydrogen content normally has lower carbon content. Higher oxygen content will reduce the higher heating value of the biomass. This is seen from all the biomass used in this study and the findings are

the same with Chen et al. (2015). This also affect the hydrogen to carbon ratio and oxygen to carbon ratio which are further discussed in subchapter 4.6. By upgrading the biomass via torrefaction, the carbon composition can be increased while lowering the hydrogen and oxygen compositions. Thus, it contributes for the increment of higher heating value for oil palm waste and forestry residue due to the torrefaction process.

Table 4.5 Ultimate analysis of raw and torrefied oil palm waste

Biomass	Ultimate analysis (wt%)	Raw	240 °C	270 °C	300 °C	330 °C
Oil palm frond	C	43.94	48.33	51.11	55.72	57.12
	H	6.94	6.50	6.20	5.96	5.67
	N	3.52	4.14	4.22	4.32	4.68
	O	44.88	40.78	37.05	33.78	25.45
	S	0.72	0.26	1.43	0.22	7.09
Palm kernel shell	C	47.79	51.79	52.35	54.51	59.92
	H	5.95	5.01	4.83	4.55	3.91
	N	1.77	1.86	1.93	2.00	2.56
	O	44.43	41.26	40.81	38.87	33.52
	S	0.06	0.08	0.072	0.07	0.086
Palm mesocarp fibre	C	45.20	47.70	50.50	53.70	54.59
	H	5.94	5.60	5.59	5.44	4.93
	N	1.12	1.35	1.67	1.77	1.78
	O	47.63	45.24	42.14	38.98	38.59
	S	0.11	0.11	0.11	0.12	0.11
Empty fruit bunch	C	43.53	46.08	47.65	54.63	54.86
	H	7.20	6.80	6.63	6.10	5.93
	N	1.73	5.45	5.62	5.90	6.07
	O	47.09	41.17	39.60	32.82	32.61
	S	0.46	0.51	0.50	0.55	0.53

Table 4.6 Ultimate analysis of raw and torrefied forestry residue

Biomass	Ultimate analysis (wt%)	Raw	240 °C	270 °C	300 °C	330 °C
Meranti	C	46.40	47.40	49.61	51.54	56.09
	H	6.69	6.58	6.39	5.60	5.03
	N	0.20	0.24	0.25	0.26	0.32
	O	46.64	45.71	43.70	42.44	38.41
	S	0.07	0.07	0.06	0.16	0.15
Seraya	C	46.80	48.45	49.81	51.10	52.64
	H	6.91	6.81	6.65	6.30	5.85
	N	0.20	0.26	0.28	0.29	0.31
	O	45.89	44.30	43.10	42.16	41.05
	S	0.20	0.18	0.16	0.15	0.15
Kulim	C	46.64	49.10	50.37	52.24	53.88
	H	6.96	6.59	6.41	6.14	6.11
	N	3.14	4.63	6.35	6.73	7.37
	O	43.21	39.64	36.84	34.89	32.63
	S	0.05	0.03	0.03	0.01	0.02

Table 4.6 Continued

Biomass	Ultimate analysis (wt%)	Raw	240 °C	270 °C	300 °C	330 °C
	C	46.82	49.57	51.62	53.97	55.93
	H	6.78	6.67	6.52	6.17	6.09
Chengal	N	3.12	3.97	4.29	5.26	5.89
	O	43.11	39.66	37.44	34.53	32.04
	S	0.16	0.13	0.14	0.08	0.05

Figure 4.3 illustrates the changes of carbon, hydrogen and oxygen for the oil palm waste and forestry residue after torrefaction process. These changes were calculated by subtracting the torrefied biomass value with the raw biomass value. Positive value shows that the composition is increasing in value while negative value shows decreasing in composition value. Apart from carbon changes in biomass that shows positive value, hydrogen and oxygen compositions show negative values from start until the end. The carbon composition changes are from 2.50 – 13.17 wt% and 1.00 – 9.69 wt% for oil palm waste and forestry residue respectively. For hydrogen and oxygen composition, oil palm waste changes are from -0.34 – -2.04 wt% and -2.39 – -19.43 wt% while for forestry residue, the changes are from -0.10 – -1.66 wt% and -0.94 – -11.07 wt% respectively. These changes are in accordance as the torrefaction temperature is increased.

The composition changes for forestry residue are lower than the changes for oil palm waste in carbon, hydrogen and oxygen compositions because it may require longer time to be torrefied. Because of more volatile have not been released due to the structural of forestry residue (mainly consist more lignin compare to oil palm waste), this causes less changes for carbon, hydrogen and oxygen composition. For the purpose of upgrading biomass properties, the torrefied biomass can achieve this feat as it increases the carbon composition and lower its hydrogen and oxygen compositions. In coal, the carbon composition are high while the hydrogen and oxygen compositions are low. Although it seem like the difference of the composition of coal and the biomass is huge, but from raw to torrefied biomass, the composition of carbon, hydrogen and oxygen is improved. This shows that by performing torrefaction process, the elemental composition of biomass have been upgraded closer to the composition of a coal (C: 82.6 %, H: 3.02 %, O: 3.06 %) (Ahmad & Subawi, 2013).
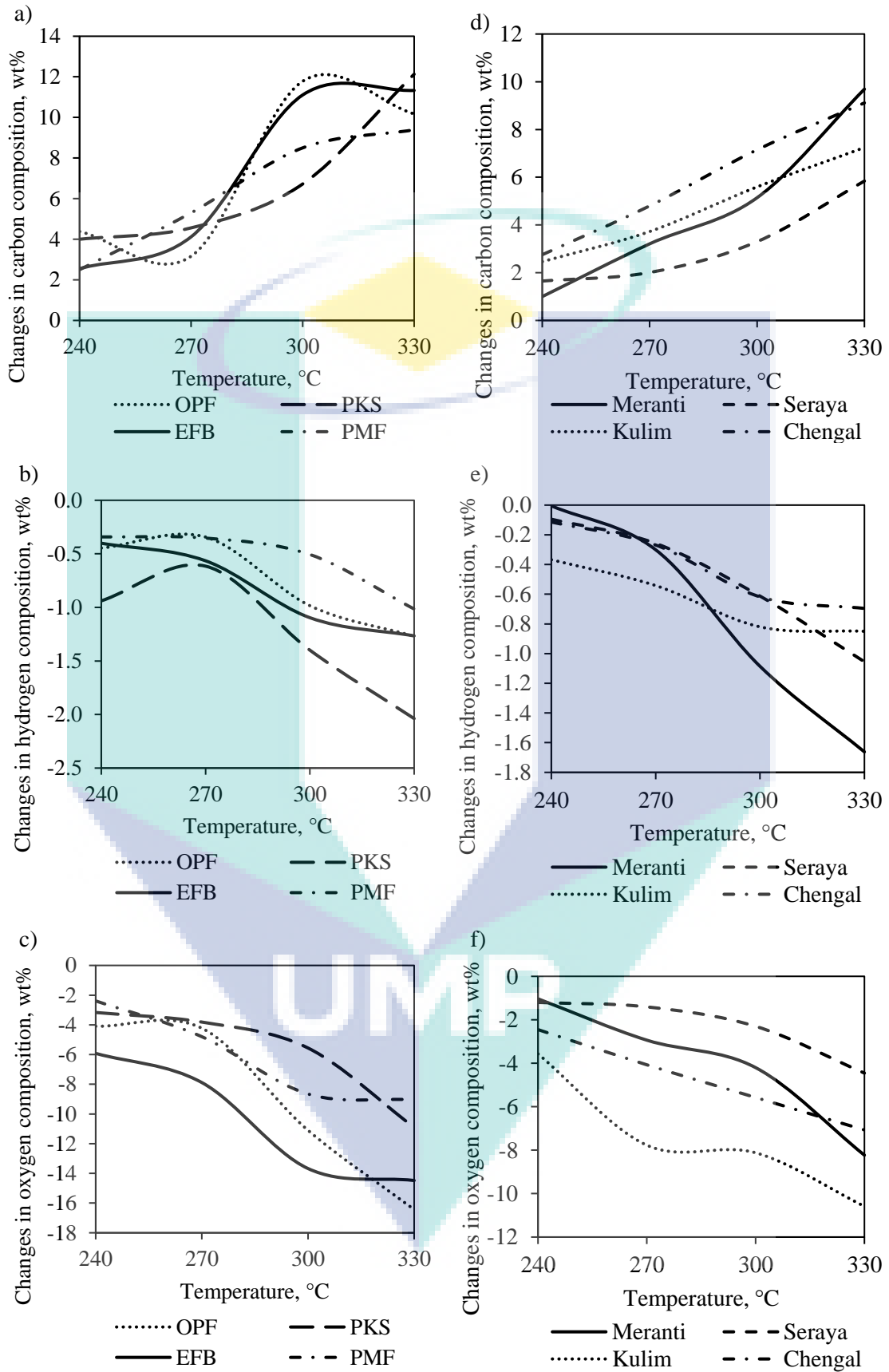
Figure 4.3 Changes in carbon, hydrogen and oxygen composition of the oil palm waste (a, b and c) and forestry residue (d, e and f) respectively

4.6   O/C and H/C ratios

Figures 4.4 and 4.5 show the Van Krevelen plot for oil palm waste and forestry residue respectively. When the torrefaction temperature is increased from 240 °C to 330 °C, both the ratios of hydrogen-to-carbon (H/C) and oxygen-to-carbon (O/C) are decreased. In general, the ratios for all oil palm waste and forestry residue show the same trends where H/C and O/C ratios for typical raw biomass are in the range of 1.2 to 2.0 and 0.4 to 0.8 respectively (Chen et al., 2015). After undergone torrefaction process, the hydrogen and oxygen are released while more carbon are retained in the biomass. This leads to carbonization of the biomass and makes the appearance of the biomass darker.

In Figures 4.4 and 4.5, the marker in a circle represents the data of raw biomass. These ratio are plotted to know the properties of the biomass. Different types of organic chemical compound categories can be known when plotting these ratio. The categories specified in Figures 4.4 and 4.5 consists of biomass, peat, lignite, coal and anthracite. For torrefaction process the main objective is to convert biomass to a more coal-like properties and from both Figures 4.4 and 4.5, the biomass used in this study approaching the properties of coal when torrefied at higher temperature. Consequently, biomass with higher HHV have lower H/C and O/C ratios (Ahmad & Subawi, 2013). Increasing the torrefaction temperature is definitely decreasing the hydrogen and oxygen compositions thus explains the increment of carbon composition that leads to higher HHV. The H/C and O/C ratios of the coal are 0.44 and 0.03 respectively. For torrefied PKS, the H/C and O/C ratios obtained are 0.78 and 0.42 respectively. Comparing with raw PKS, which has 1.49 (H/C) and 0.70 (O/C), it showed that, the H/C and O/C ratio of the torrefied PKS are moving towards to the coal.
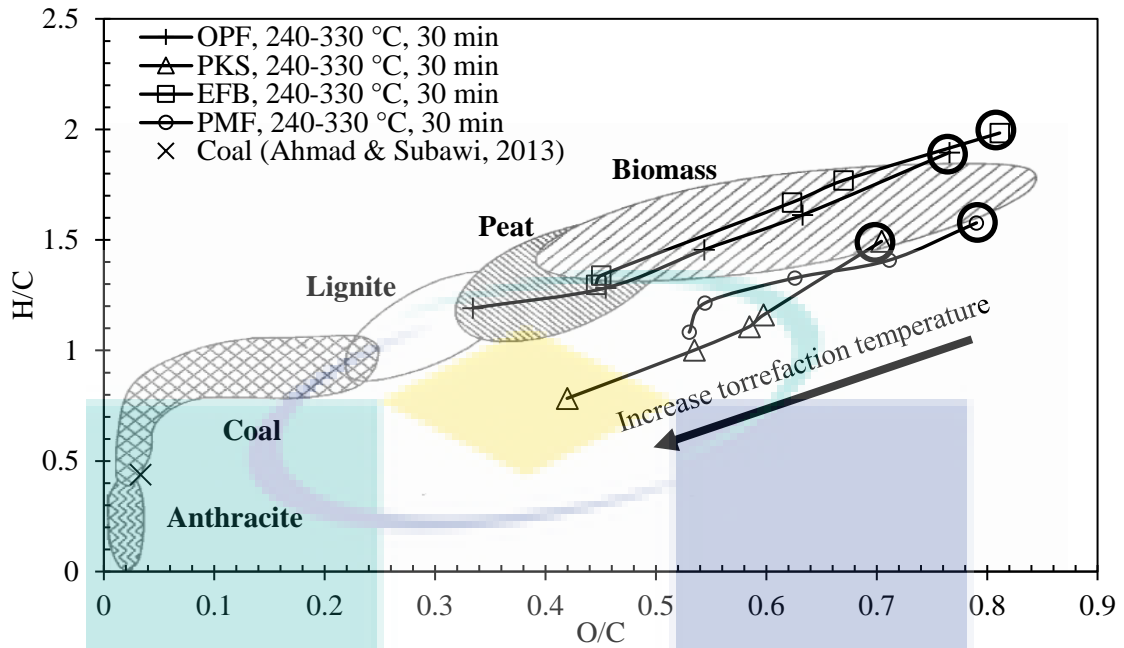
Figure 4.4 Van Krevelen plot of torrefied oil palm waste
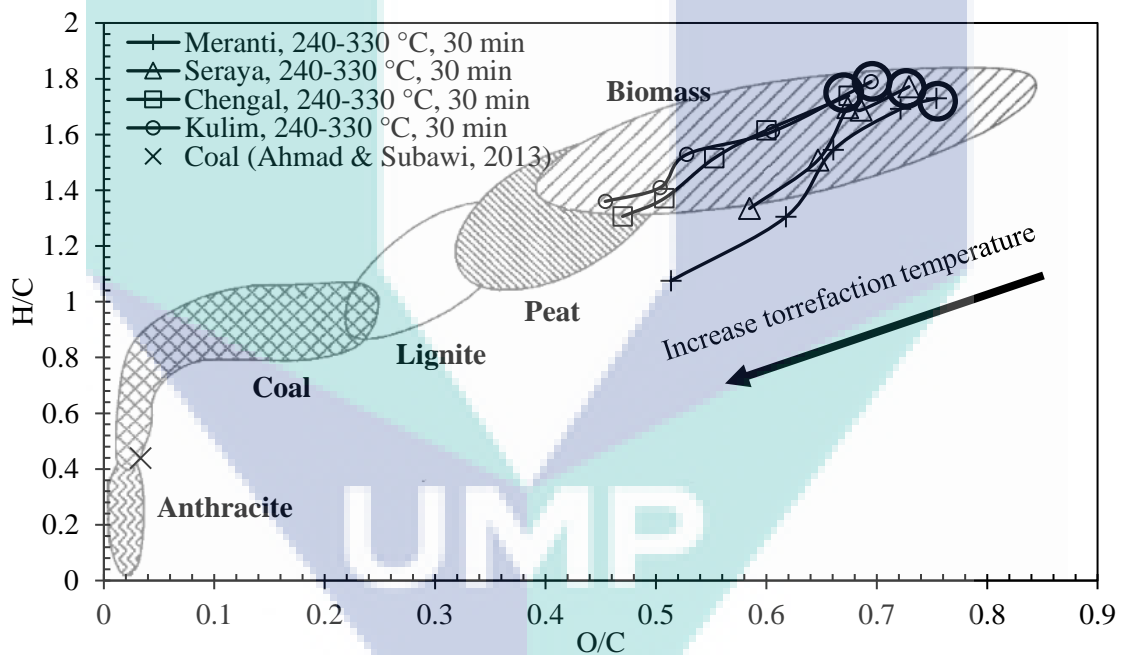
Figure 4.5 Van Krevelen plot of raw and torrefied forest residue

4.7 Higher heating value (HHV)

Tables 4.7 and 4.8 summarize the HHV of the oil palm waste and forestry residue respectively. The enhancement factor for each of the biomass is also listed. This enhancement factor are calculated by dividing the HHV of torrefied biomass with the HHV of raw biomass. By calculating this factor, the degree of HHV increment can be obtained. For HHV, the increase in torrefaction temperature leads to increase in its

value. Increment in carbon composition is also contributing to the increment of HHV. The highest value of HHV for both oil palm waste and forestry residue are 25.83 MJ/kg (oil palm frond torrefied at 330 °C) and 24.93 MJ/kg (Meranti torrefied at 330 °C) respectively. Torrefied OPF has higher heating value compared to Meranti because its oxygen composition are lower. As stated before, higher carbon composition leads to higher HHV but in the case of Meranti, it has the highest carbon composition (56.09%) when undergone torrefaction process at 330 °C. In oil palm case, the carbon and oxygen compositions of OPF are lower than PKS. According to Chen et al. (2015), the biomass with higher oxygen composition and ash content tend to have lower HHV. This contribute to a high HHV for OPF.

Table 4.7 Higher heating value for raw and torrefied oil palm waste

Biomass	Temperature (°C)	Higher Heating Value (MJ/kg)	Enhancement Factor in HHV
Palm kernel shell			
Raw		16.15	1.00
Torrefied	240	19.68	1.22
	270	21.91	1.36
	300	23.64	1.46
	330	25.46	1.58
Empty fruit bunch			
Raw		15.49	1.00
Torrefied	240	15.59	1.01
	270	17.99	1.16
	300	19.60	1.27
	330	22.07	1.42
Oil palm frond			
Raw		17.75	1.00
Torrefied	240	19.82	1.12
	270	21.60	1.22
	300	23.79	1.34
	330	25.83	1.46
Palm mesocarp fibre			
Raw		16.94	1.00
Torrefied	240	18.05	1.07
	270	19.17	1.13
	300	21.49	1.27
	330	23.91	1.41

In terms of enhancement factor, the highest value obtained is 1.58 for oil palm waste (PKS) and 1.41 for forestry residue (Seraya). This is due to both of these biomass have lower moisture content compared to other biomass in their group. Higher

enhancement factor does not mean it has the highest HHV as the factor is used to quantify how much HHV is increased from its raw biomass. As a conclusion, enhancement factor for all biomass is increased with increasing torrefaction temperature. This result indicates that the purpose of torrefaction which is to improve biomass properties is achieved where HHV of torrefied biomass is increased. With higher HHV, a higher amount of energy is expected which enabling for torrefied biomass to be used as a fuel. The highest HHV of torrefied biomass in this study is closer to the HHV of a coal which normally have HHV in the range from 25 to 35 MJ/kg (Chen et al., 2013).

Table 4.8 Higher heating value for raw and torrefied forestry residue

Biomass	Temperature (°C)	Higher Heating Value (MJ/kg)	Enhancement Factor in HHV
Meranti			
Raw		18.86	1.00
Torrefied	240	19.32	1.02
	270	22.00	1.17
	300	23.94	1.27
	330	24.93	1.32
Seraya			
Raw		17.17	1.00
Torrefied	240	18.84	1.10
	270	20.85	1.21
	300	22.40	1.30
	330	24.19	1.41
Kulim			
Raw		17.81	1.00
Torrefied	240	19.06	1.07
	270	20.88	1.17
	300	22.83	1.28
	330	24.34	1.37
Chengal			
Raw		18.03	1.00
Torrefied	240	19.56	1.08
	270	21.99	1.22
	300	23.66	1.31
	330	24.87	1.38

4.8 Estimating higher heating value (HHV) based on the properties of biomass

The model correlations based on the properties of ultimate and proximate analysis of biomass are developed in order to estimate the HHV for oil palm waste and forestry residue. The biomass database used in this study are shown in Tables 4.9 and

4.10 for raw and torrefied oil palm waste and forestry residue respectively. In general there are 56 kinds of data are collected for oil palm waste and 41 kinds of data are assembled for forestry residue. Various sources of biomass are needed to generate a reliable correlation with lowest possible error for each group of biomass. The correlations are developed separately based on the proximate and ultimate analysis of the biomass in databases. This is done to determine which of these analysis can accurately estimate the HHV.
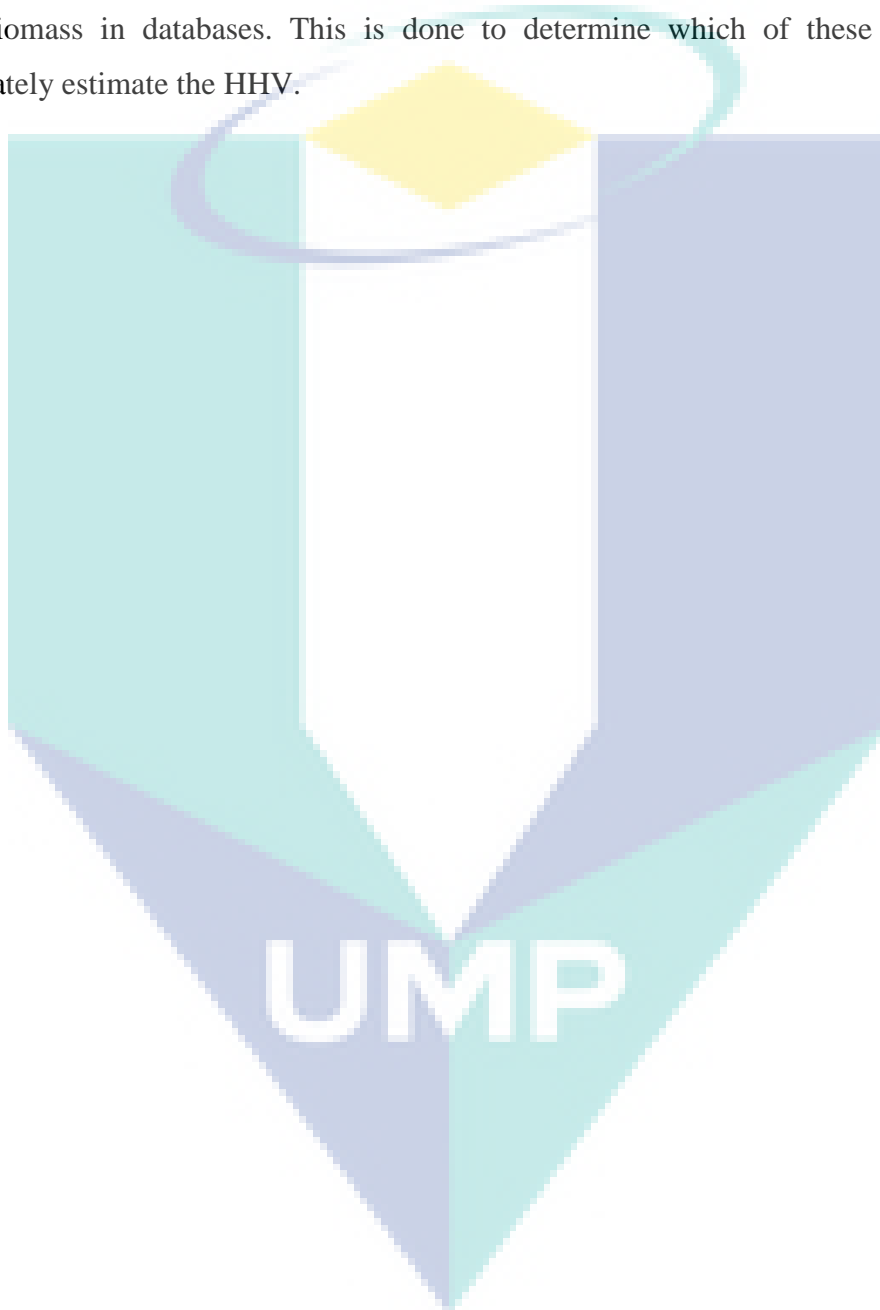
Table 4.9 Composition of different types of raw biomass used in this study

No	Biomass	Proximate analysis (wt.%)			Ultimate analysis (wt.%)					HHV (MJ/kg)	Ref.
		FC	VM	Ash	C	H	N	O	S		
Oil palm waste											
1	Oil palm frond	12.01	69.17	2.87	43.94	6.94	3.52	44.88	0.72	17.75	This study
2	Oil palm frond	79.37	20.63	25.60	41.75	5.51	1.39	51.36	0.00	17.67	Matali et al. (2016)
3	Palm kernel shell	12.07	70.02	6.04	47.79	5.95	1.77	44.43	0.06	16.15	This study
4	Palm kernel shell	15.15	73.77	11.08	-	-	-	-	-	16.30	Idris et al. (2012)
5	Palm kernel shell	-	-	-	46.68	5.86	1.01	42.01	0.06	18.49	Uemura et al. (2011)
6	Palm kernel shell	-	-	-	44.50	6.21	0.42	48.19	0.18	18.91	Sabil et al. (2013)
7	Palm kernel shell	-	-	-	38.17	4.56	0.84	44.29	0.05	18.62	Poudel et al. (2016)
8	Palm kernel shell	18.70	70.50	0.84	50.62	6.02	0.37	42.15	0.00	20.10	Uemura et al. (2015)
9	Palm kernel shell	23.00	74.00	3.00	45.10	5.10	0.56	49.20	0.04	17.58	Asadullah (2014)
10	Palm kernel shell	19.70	67.20	2.10	49.74	5.32	0.08	44.86	0.16	16.41	Abnisa et al. (2011)
11	Palm kernel shell	10.85	84.86	4.29	46.53	5.85	0.89	42.32	0.00	18.81	Jaafar & Ahmad (2011)
12	Empty fruit bunch	15.37	65.01	3.85	43.53	7.20	1.73	47.09	0.46	15.49	This study
13	Empty fruit bunch	16.80	77.10	6.10	-	-	-	-	-	16.80	Idris et al. (2012)
14	Empty fruit bunch	-	-	-	45.53	5.46	0.45	43.40	0.04	15.82	Uemura et al. (2011)
15	Empty fruit bunch	-	-	-	44.60	5.48	0.37	49.37	0.18	18.04	Sabil et al. (2013)
16	Empty fruit bunch	-	-	-	44.93	5.53	0.46	43.76	0.07	19.15	Poudel et al. (2016)
17	Palm mesocarp fibre	16.42	67.04	5.66	45.20	9.04	3.12	42.53	0.11	16.94	This study
18	Palm mesocarp fibre	-	-	-	46.92	5.89	1.12	42.66	0.09	18.31	Uemura et al. (2011)
19	Palm mesocarp fibre	19.72	9.57	9.57	49.10	1.91	1.32	38.10	0.00	16.63	Chen et al. (2016)
20	Palm mesocarp fibre	20.51	72.46	7.03	51.94	4.75	2.43	40.88	0.00	17.13	Chen et al. (2014)
Forestry residue											
1	Meranti	12.35	76.48	0.86	46.40	3.69	0.20	49.64	0.07	18.86	This study
2	Meranti	22.70	69.90	1.20	41.70	5.70	0.10	52.60	0.00	19.60	Mazlan et al. (2015)
3	Meranti	14.04	76.23	1.49	42.38	5.27	0.14	42.41	0.00	18.23	Miskam et al. (2009)
4	Chengal	17.91	70.17	0.53	46.40	3.69	0.20	49.64	0.07	18.03	This study
5	Kulim	15.23	72.33	0.91	46.82	6.78	4.12	42.11	0.16	17.81	This study
6	Seraya	15.13	74.85	0.69	46.64	6.96	3.14	43.21	0.05	17.17	This study
7	Forestry residue	20.00	79.80	0.20	53.16	6.25	0.30	40.00	0.09	19.50	Vamvuka et al. (2003)

Table 4.9 continued

No	Biomass	Proximate analysis (wt.%)			Ultimate analysis (wt.%)					HHV (MJ/kg)	Ref.
		FC	VM	Ash	C	H	N	O	S		
Forestry residue											
8	Alfafa stem	15.81	78.92	5.27	47.17	5.99	2.68	38.19	0.20	15.09	Jenkins et al. (1998)
9	Willow wood	16.07	82.22	1.71	49.90	5.90	0.61	41.80	0.07	19.59	Jenkins et al. 1998)
10	Oak wood (small branch)	18.50	77.45	4.05	48.76	6.35	2.81	42.08	0.00	19.20	Miranda et al. (2009)
11	Oak wood (medium branch)	16.18	80.82	3.00	48.62	6.52	2.58	42.48	0.00	19.24	Miranda et al. (2009)
12	Oak wood (big branch)	16.18	81.75	2.07	48.57	6.81	2.39	42.23	0.00	19.17	Miranda et al. (2009)
13	Pine chip	21.65	72.40	5.95	49.66	5.67	0.51	38.07	0.08	19.79	Masiá et al. (2007)

Table 4.10 Composition of different types of torrefied biomass used in this study

No	Biomass	Residence time (min)	Torrefaction temperature (°C)	Proximate analysis (wt.%)			Ultimate analysis (wt.%)					HHV (MJ/kg)	Ref.
				FC	VM	Ash	C	H	N	O	S		
Oil palm waste													
1	Oil palm frond	30	240	22.18	64.86	3.20	48.33	6.50	4.14	40.78	0.26	19.82	This study
2	Oil palm frond	30	270	32.44	56.15	4.62	47.11	6.60	4.22	40.65	1.43	21.60	This study
3	Oil palm frond	30	300	44.88	45.54	4.76	55.72	5.96	4.32	33.78	0.22	23.79	This study
4	Oil palm frond	30	330	52.05	38.95	5.15	54.12	5.67	4.68	28.45	7.09	25.83	This study
5	Palm kernel shell	30	240	21.85	66.27	7.28	51.79	5.01	1.86	41.26	0.08	19.68	This study
6	Palm kernel shell	30	270	23.85	65.70	8.13	52.35	5.33	1.63	40.61	0.07	21.91	This study
7	Palm kernel shell	30	300	28.29	58.55	12.11	54.51	4.55	2.00	38.87	0.07	23.64	This study
8	Palm kernel shell	30	330	35.83	49.68	13.71	59.92	3.91	2.56	33.52	0.09	25.46	This study
9	Palm kernel shell	30	240	19.77	74.56	4.89	49.08	5.10	1.07	39.67	0.12	19.70	Jaafar & Ahmad (2011)
10	Palm kernel shell	30	260	22.04	73.77	6.21	49.26	4.37	1.02	39.00	0.07	19.72	Jaafar & Ahmad (2011)

Table 4.10 Continued

No	Biomass	Residence time (min)	Torrefaction temperature (°C)	Proximate analysis (wt.%)			Ultimate analysis (wt.%)					HHV (MJ/kg)	Ref.
				FC	VM	Ash	C	H	N	O	S		
Oil palm waste													
11	Palm kernel shell	30	280	21.25	75.15	5.62	49.90	3.92	1.07	39.45	0.00	19.86	Jaafar & Ahmad (2011)
12	Palm kernel shell	60	240	21.06	73.66	6.37	50.84	4.68	1.03	36.99	0.03	20.35	Jaafar & Ahmad (2011)
13	Palm kernel shell	60	260	22.83	70.84	6.82	50.50	4.36	1.12	37.11	0.02	21.09	Jaafar & Ahmad (2011)
14	Palm kernel shell	60	280	20.51	73.63	6.69	51.49	4.06	1.08	36.61	0.01	20.59	Jaafar & Ahmad (2011)
15	Palm kernel shell	30	220	-	-	4.33	45.87	6.31	0.40	43.07	0.02	18.85	Uemura et al. (2011)
16	Palm kernel shell	30	250	-	-	3.42	51.89	5.71	0.47	38.50	0.01	19.07	Uemura et al. (2011)
17	Palm kernel shell	30	300	-	-	3.53	54.21	5.08	0.50	36.66	0.02	21.68	Uemura et al. (2011)
18	Palm mesocarp fibre	30	240	19.05	66.07	6.08	47.70	5.60	1.35	45.24	0.11	18.05	This study
19	Palm mesocarp fibre	30	270	23.02	64.60	6.67	50.50	5.59	0.97	42.84	0.11	19.17	This study
20	Palm mesocarp fibre	30	300	29.69	59.58	7.10	53.70	5.44	1.77	38.98	0.12	21.49	This study
21	Palm mesocarp fibre	30	330	33.86	56.43	8.16	53.99	4.93	1.78	39.19	0.11	22.91	This study
22	Palm mesocarp fibre	30	220	-	-	2.34	46.93	5.50	1.83	43.40	0.10	19.03	Uemura et al. (2011)
23	Palm mesocarp fibre	30	250	-	-	5.10	47.70	5.20	1.74	40.18	0.10	19.24	Uemura et al. (2011)
24	Palm mesocarp fibre	30	300	-	-	4.26	48.60	4.87	2.14	40.03	0.09	22.17	Uemura et al. (2011)

Table 4.10 Continued

No	Biomass	Residence time (min)	Torrefaction temperature (°C)	Proximate analysis (wt.%)			Ultimate analysis (wt.%)					HHV (MJ/kg)	Ref.
				FC	VM	Ash	C	H	N	O	S		
Oil palm waste													
25	Palm mesocarp fibre	60	250	27.30	63.90	8.90	-	-	-	-	-	20.10	Lu et al. (2012)
26	Palm mesocarp fibre	60	275	32.40	56.60	11.00	-	-	-	-	-	21.40	Lu et al. (2012)
27	Palm mesocarp fibre	60	300	44.40	41.30	14.30	-	-	-	-	-	23.40	Lu et al. (2012)
28	Palm mesocarp fibre	60	325	52.40	32.80	14.80	-	-	-	-	-	23.70	Lu et al. (2012)
29	Palm mesocarp fibre	60	350	55.30	29.10	15.50	-	-	-	-	-	23.90	Lu et al. (2012)
30	Empty fruit bunch	30	240	22.06	62.51	6.70	46.08	6.80	5.45	40.04	1.64	15.59	This study
31	Empty fruit bunch	30	270	30.16	54.50	7.67	47.65	6.63	6.02	39.20	0.50	17.99	This study
32	Empty fruit bunch	30	300	39.23	48.44	7.70	54.63	6.45	6.37	32.25	0.29	19.60	This study
33	Empty fruit bunch	30	330	48.91	36.63	11.88	54.06	5.63	4.07	36.04	0.21	22.07	This study
34	Empty fruit bunch	30	220	-	-	5.75	46.75	4.68	1.27	41.42	0.12	17.17	Uemura et al. (2011)
35	Empty fruit bunch	30	250	-	-	4.28	47.07	4.95	1.35	42.24	0.11	17.67	Uemura et al. (2011)
36	Empty fruit bunch	30	300	-	-	1.58	49.56	4.38	1.27	43.19	0.02	20.41	Uemura et al. (2011)
Forestry residue													
1	Meranti	30	240	16.80	73.99	1.13	47.40	3.68	0.24	48.61	0.07	19.32	This study
2	Meranti	30	270	22.37	71.76	2.00	49.61	3.39	0.24	46.71	0.06	22.00	This study
3	Meranti	30	300	26.59	69.61	2.16	51.54	2.60	0.26	45.44	0.16	23.94	This study

Table 4.10 Continued

No	Biomass	Residence time (min)	Torrefaction temperature (°C)	Proximate analysis (wt.%)			Ultimate analysis (wt.%)					HHV (MJ/kg)	Ref.
				FC	VM	Ash	C	H	N	O	S		
Forestry residue													
4	Meranti	30	330	31.01	65.86	2.71	56.09	2.03	0.32	41.41	0.15	24.93	This study
5	Chengal	30	240	25.10	68.59	0.55	49.57	6.78	3.97	39.55	0.13	19.56	This study
6	Chengal	30	270	29.32	66.82	0.72	51.62	6.52	3.69	38.04	0.14	21.99	This study
7	Chengal	30	300	38.75	59.02	0.72	53.97	6.17	3.26	36.53	0.08	23.66	This study
8	Chengal	30	330	46.00	52.29	0.82	55.93	6.09	2.89	35.04	0.05	24.87	This study
9	Seraya	30	240	17.43	73.55	0.95	48.45	2.81	0.26	48.30	0.18	18.84	This study
10	Seraya	30	270	20.74	73.43	1.01	48.81	2.90	0.28	47.85	0.16	20.85	This study
11	Seraya	30	300	23.26	71.35	1.83	50.10	3.30	0.25	46.20	0.15	22.40	This study
12	Seraya	30	330	30.21	66.48	2.02	52.64	2.85	0.31	44.05	0.15	24.19	This study
13	Kulim	30	240	18.17	70.81	1.03	49.10	6.59	4.63	39.64	0.03	19.06	This study
14	Kulim	30	270	23.99	69.40	1.17	50.37	6.41	7.75	35.44	0.03	20.88	This study
15	Kulim	30	300	28.08	67.73	1.29	52.24	6.14	0.31	41.31	0.01	22.83	This study
16	Kulim	30	330	32.63	64.55	1.46	53.88	6.11	0.37	39.63	0.02	24.34	This study
17	Willow	30	230	16.10	82.10	1.80	50.70	6.20	0.20	39.50	0.00	20.20	Bridgeman et al. (2008)
18	Willow	30	250	18.40	79.80	1.90	51.70	6.10	0.20	38.70	0.00	20.60	Bridgeman et al. (2008)
19	Willow	30	270	18.60	79.30	2.10	53.40	6.10	0.20	37.20	0.00	21.40	Bridgeman et al. (2008)
20	Willow	30	290	20.50	77.20	2.30	54.70	6.00	0.10	36.40	0.00	21.90	Bridgeman et al. (2008)
21	Pine chip	30	225	14.95	84.78	0.27	49.47	6.07	0.15	44.03	0.00	19.48	Phanphanich & Mani (2011)
22	Pine chip	30	250	17.24	82.52	0.25	51.46	5.86	0.14	42.02	0.00	20.08	Phanphanich & Mani (2011)
23	Pine chip	30	275	23.26	76.40	0.35	54.91	6.20	0.20	38.17	0.00	21.82	Phanphanich & Mani (2011)

Table 4.10 Continued

No	Biomass	Residence time (min)	Torrefaction temperature (°C)	Proximate analysis (wt.%)			Ultimate analysis (wt.%)					HHV (MJ/kg)	Ref.
				FC	VM	Ash	C	H	N	O	S		
Forestry residue													
24	Pine chip	30	300	40.85	58.72	0.43	63.67	5.58	0.20	29.99	0.00	25.38	Phanphanich & Mani (2011)
25	Pine log	30	225	17.9	80.75	1.37	50.15	6.1	0.3	42.74	0.00	19.79	Phanphanich & Mani (2011)
26	Pine log	30	250	20.37	78.16	1.49	54.91	5.87	0.31	40.96	0.00	21.21	Phanphanich & Mani (2011)
27	Pine log	30	275	26.69	71.44	1.88	53.24	5.39	0.3	40.12	0.00	22.03	Phanphanich & Mani (2011)
28	Pine log	30	300	44.76	52.92	2.32	66.07	4.92	0.48	27.24	0.00	26.41	Phanphanich & Mani (2011)
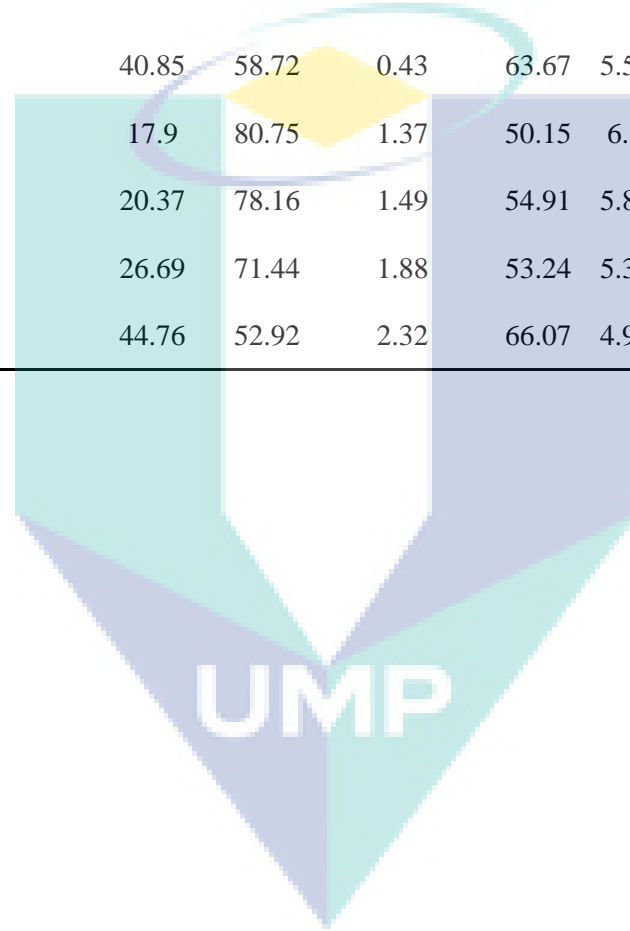
4.8.1 Estimation of HHV based on proximate analysis

In this subsection, the correlations for estimating the HHV are based on the proximate analysis. The step for estimating HHV are shown in Figure 3.5. The objective is to estimate the HHV of raw and torrefied of oil palm waste and forestry residue by using correlations based on proximate analysis. Next the data is obtained by using the proximate analysis and higher heating value data from biomass database as shown in Tables 4.9 and Table 4.10. Sixty (60) correlations are used for predicting the HHV for oil palm waste and forestry residue where the coefficients of *a, b, c, d* and *e* are estimated using Microsoft Excel Solver. In steps 4 and 5, the HHV is predicted using the estimated coefficients in order to calculate average absolute error (AAE). The top 15 correlations based on lowest values of AAE is shown in Table 4.11 for oil palm waste and forestry residue. As shown in Table 4.11, the best correlation for predicting the HHV using proximate analysis is correlation no.12 for oil palm waste and correlation no. 15 for forestry residue.

For these correlations, oil palm waste shows a positive effects for both torrefaction temperature and residence time variables while for forestry residue only torrefaction temperature variable has positive effects. This shows that for forestry residue, residence time is inversely proportional as compared to torrefaction temperature in terms of increasing HHV. This is due to the coefficient for the residence time variable are in negative value. The FC/VM ratio for oil palm waste correlations have bigger impact on HHV compared to VM/ASH and ASH/FC ratio. This indication shows that the amount of FC in the oil palm waste has more significant effect compared to VM. While it is different for forestry residue, where the most significant ratio is ASH/VM. This shows that the dominant effect of the ash over the effect of VM.

Table 4.11 Linear correlations used in this study based on proximate analysis

No	Correlations	AAE (%)
Oil palm waste		
1	HHV = 17.0706 + 2.8114FC/VM – 0.0389VM/FC + 13.9831t/T	6.46
2	HHV = 18.3388 + 2.4520FC/VM – 0.0489VM/FC + 0.0308t – 30.1360/T	6.07
3	HHV = 16.6574 + 1.9543FC/VM – 0.0131VM/FC + 0.0350t + 0.0056T	5.76
4	HHV = 15.7390 + 3.5006FC/VM + 0.0409VM/ASH + 16.4264t/T	6.14
5	HHV = 18.1825 + 2.8670FC/VM – 0.0008VM/ASH + 0.0293t – 50.0520/T	5.91
6	HHV = 15.8104 + 2.4104FC/VM + 0.0413VM/ASH + 0.0300t + 0.0066T	5.42
7	HHV = 17.2686 – 0.2497ASH/FC + 2.7501FC/VM + 13.0299t/T	6.48
8	HHV = 18.3740 – 0.2930ASH/FC + 2.2093FC/VM + 0.0298t – 25.3865/T	6.17
9	HHV = 16.3218 + 0.0364ASH/FC + 2.0316FC/VM + 0.0248t + 0.0081T	5.62

Table 4.11 Continued

No	Correlations	AAE (%)
Oil palm waste		
10	HHV = 15.5247 + 3.7767FC/VM + 0.0424VM/ASH + 0.2845ASH/FC + 16.2336t/T	6.06
11	HHV = 18.2442 + 3.3482FC/VM + 0.0421VM/ASH + 0.2477ASH/FC + 0.0053t – 69.7405/T	5.69
12	**HHV = 15.8514 + 1.9293FC/VM + 0.0418VM/ASH + 0.1398ASH/FC + 0.0234t + 0.0082T**	**5.37**
13	HHV = 16.1455 – 0.0632VM/FC + 6.3680ASH/VM + 0.1850FC/ASH + 16.4289t/T	6.62
14	HHV = 17.6915 – 0.0664VM/FC + 6.7218ASH/VM + 0.1870FC/ASH + 0.0415t – 42.8253/T	5.68
15	HHV = 15.7306 – 0.0579VM/FC + 6.4294ASH/VM + 0.1877FC/ASH – 0.0037t + 0.0124T	5.53
Forestry residue		
1	HHV = 12.2179 + 17.9152FC/VM + 0.5404VM/FC – 17.1728t/T	13.25
2	HHV = 68.4050 + 20.4351FC/VM + 1.1934VM/FC – 1.8422t – 1638.1792/T	13.10
3	HHV = 15.0150 + 2.4925FC/VM + 0.2196VM/FC – 0.5017t + 0.0608T	12.83
4	HHV = 15.3340 + 14.1250FC/VM + 0.0027VM/ASH – 20.4207t/T	13.34
5	HHV = 205.6894 – 1.8409FC/VM + 0.0109VM/ASH – 5.6162t – 5140.6200/T	12.82
6	HHV = 13.0018 + 0.9106FC/VM + 0.0122VM/ASH – 0.4448t + 0.0639T	12.58
7	HHV = 16.6552 – 0.7421ASH/FC + 11.1717FC/VM – 18.6909t/T	13.40
8	HHV = 150.1008 + 3.5955ASH/FC + 3.0437FC/VM – 4.0051t – 3569.3093/T	12.82
9	HHV = 16.4524 + 3.0244ASH/FC + 2.2585FC/VM – 0.4956t + 0.0572T	12.68
10	HHV = 6.1544 + 18.8772FC/VM + 0.0208VM/ASH + 30.8303ASH/FC + 22.1908t/T	11.59
11	HHV = 146.6117 + 6.2800FC/VM + 0.0239VM/ASH + 40.2690ASH/FC – 4.0388t – 3742.8699/T	10.66
12	HHV = 8.1584 + 1.0873FC/VM + 0.0237VM/ASH + 36.1708ASH/FC – 0.4212t + 0.0697T	10.68
13	HHV = 12.1998 – 0.4065VM/FC + 152.0368ASH/VM + 0.0854FC/ASH + 17.2125t/T	12.64
14	HHV = 222.4647 + 1.7586VM/FC + 126.8296ASH/VM + 0.0729FC/ASH – 6.3764t – 5874.9402/T	11.61
15	**HHV = 14.5782 + 0.1925VM/FC + 24.0162ASH/VM + 0.0161FC/ASH – 0.6277t + 0.0922T**	**10.37**

4.8.2 Estimation of HHV based on ultimate analysis

The same procedure is also applied for development of model correlations using ultimate analysis for oil palm waste and forestry residue. In this work, 30 correlations are used as shown in Table 3.4 for oil palm waste and forestry residue respectively. Top 15 correlations based on the lowest AAE are shown in Table 4.12. In this case the best correlation using ultimate analysis is correlation no. 3 for oil palm waste and correlation

no. 9 for forestry residue by basing on the AAE calculated. Based on this analysis, it can be seen that both correlations show torrefaction temperature and residence time are directly proportional to HHV for both types of oil palm waste and forestry residue. From oil palm waste correlations, it shows that sulphur have positive significant effect in estimating HHV while in forestry residue, it is carbon.

Table 4.12 Linear correlations used in this study based on ultimate analysis

No	Correlations	AAE (%)
Oil palm waste		
1	$HHV = 3.1162 + 0.3502C + 0.1590H - 0.2218N - 0.0409O + 0.6677S + 3.6990t/T$	6.12
2	$HHV = 0.8357 + 0.3743C + 0.1555H - 0.2143N - 0.0018O + 0.6864S + 0.0035t - 20.2723/T$	5.98
3	**$HHV = -0.2630 + 0.3072C + 0.4048H - 0.5194N + 0.0406O + 0.8409S + 0.0079t + 0.0068T$**	**5.79**
4	$HHV = 0.7875 + 0.3949C + 0.1837H - 0.3637N - 0.0409O + 0.7054S + 0.0776Ash + 1.0729t/T$	6.04
5	$HHV = 3.2287 + 0.3535C + 0.1788H - 0.3670N - 0.0409O + 0.7203S + 0.0507Ash + 0.0004t - 12.5421/T$	5.97
6	$HHV = -2.0623 + 0.3439C + 0.2735H - 0.4066N + 0.0578O + 0.8155S - 0.0279Ash + 0.0097t + 0.0062T$	5.80
7	$HHV = 0.3493C + 0.0649H + 0.5433S - 0.0682(O + N) + 0.0645A + 4.6768 - 0.7597t/T$	6.09
8	$HHV = 0.3472C + 0.1499H + 0.5749S - 0.0221(O + N) - 0.0005A + 2.8264 + 0.0030t - 20.0437/T$	6.03
9	$HHV = 0.3020C + 0.2125H + 0.5427S - 0.0355(O + N) - 0.0286A + 4.2844 + 0.0042t + 0.0041T$	5.89
10	$HHV = 0.4010C + 0.1195H + 0.5623S - 0.0257(O + N) + 0.0463A + 0.8507t/T$	6.13
11	$HHV = 0.3767C + 0.1143H + 0.6032S + 0.0129(O + N) - 0.0005A + 0.0050t - 17.7793/T$	6.03
12	$HHV = 0.3531 + 0.1655H + 0.5734S + 0.0111(O + N) - 0.0241A + 0.0063t + 0.0039T$	5.92
13	$HHV = 0.4030C + 0.0720H + 0.5655S - 0.0200O + 1.9410t/T$	6.16
14	$HHV = 0.3764C + 0.1211H + 0.6056S + 0.0131O + 0.0049t - 18.2715/T$	6.02
15	$HHV = 0.3280C + 0.1503H + 0.6331S + 0.0382O + 0.0083t + 0.0043T$	5.91
Forestry residue		
1	$HHV = 19.5867 + 0.2033C - 0.6789H - 0.1509N - 0.1391O - 0.7018S - 8.3107t/T$	13.13
2	$HHV = 12.5738 + 0.3263C - 0.6715H - 0.5000N - 0.1261O - 0.6352S + 0.0021t + 0.8268/T$	13.25
3	$HHV = 6.3713 + 0.3034C - 0.1900H - 0.0178N - 0.0410O - 0.5470S - 0.2354t + 0.0272T$	12.47
4	$HHV = 10.0077 + 0.3032C - 1.1685H + 0.6740N + 0.0257O - 0.7871S - 0.1777Ash - 8.9274t/T$	12.64
5	$HHV = 0.1668 + 0.3701C - 1.2733H + 0.6225N + 0.1750O - 0.5707S - 0.1768Ash + 0.0052t - 0.0062/T$	12.85
6	$HHV = 0.2307 + 0.3807C - 0.9942H + 0.3180N + 0.1147O - 0.3559S - 0.1574Ash - 0.3086t + 0.0363T$	11.80

Table 4.12 Continued

No	Correlations	AAE (%)
7	HHV = 0.3853C – 1.1715H – 0.4878S + 0.0719(O + N) – 0.1397A + 4.2154 – 4.5039t/T	12.95
8	HHV = 0.3776C – 0.9931H – 0.5916S + 0.0728(O + N) – 0.1437A + 3.4776 + 0.0094t – 0.0212/T	12.97
9	**HHV = 0.2269C – 0.8308H – 0.2014S + 0.0011(O + N) – 0.1572A + 11.6230 – 0.4396t + 0.0511T**	**11.75**
10	HHV = 0.4214C – 1.1079H – 0.5319S + 0.1139(O + N) – 0.1393A + 2.0509t/T	13.02
11	HHV = 0.4184C – 1.1695H – 0.4828S + 0.1248(O + N) – 0.1436A + 0.0028t + 0.1581/T	12.98
12	HHV = 0.3423C – 0.9255H – 0.1391S + 0.1431(O + N) – 0.1555A – 0.3522t + 0.0433T	11.82
13	HHV = 0.3421C – 0.2231H – 0.4533S + 0.0857O – 3.3199t/T	13.49
14	HHV = 0.3642C – 0.8219H – 0.4245S + 0.1240O + 0.0164t + 0.0812/T	13.51
15	HHV = 0.3673C – 0.0474H – 0.4598S + 0.0117O – 0.2543t + 0.0292T	12.60

4.8.3 Validation of the correlations

Validation was carried out to ensure that the correlations developed in this study capable to estimate the HHV of the biomass used in this study mainly the torrefied biomass. The validated results are presented in Tables 4.13 and 4.14 for oil palm waste and forestry residue respectively. The correlations used for this validation using proximate analysis for both oil palm waste and forestry residue. The absolute error (AE) are included to know how close the correlations developed estimate the HHV value of the biomass. In both Tables 4.13 and 4.14, both correlations estimate the HHV with AE less than 17%.

Table 4.13 Validation of develop correlations for oil palm waste

Biomass	Temperature (°C)	Experimental HHV (MJ/kg)	Estimated HHV (MJ/kg)	AE (%)
PKS				
Raw		16.15	17.54	8.65
Torrefied	240	19.68	18.15	7.79
	270	21.91	19.88	9.29
	300	23.64	21.20	10.30
	330	25.46	22.37	12.14
EFB				
Raw		15.49	17.79	14.88
Torrefied	240	15.59	18.45	2.22
	270	17.99	20.04	4.58
	300	19.60	21.35	0.69
	330	22.07	22.49	1.85
OPF				
Raw		17.75	19.00	7.06
Torrefied	240	19.82	19.75	0.36

Table 4.13 Continued

Biomass	Temperature (°C)	Experimental HHV (MJ/kg)	Estimated HHV (MJ/kg)	AE (%)
OPF				
Torrefied	270	21.60	20.27	6.13
	300	23.79	21.56	9.38
	330	25.83	22.64	12.35
PMF				
Raw		16.94	17.11	1.00
Torrefied	240	18.05	18.11	16.21
	270	19.17	19.53	8.55
	300	21.49	21.00	7.14
	330	23.91	22.13	0.29

Table 4.14 Validation of develop correlations for oil palm waste

Biomass	Temperature (°C)	Experimental HHV (MJ/kg)	Estimated HHV (MJ/kg)	AE (%)
Meranti				
Raw		18.86	18.29	3.20
Torrefied	240	19.32	19.32	0.01
	270	22.00	22.10	0.45
	300	23.94	24.85	3.78
	330	24.93	27.75	11.29
Seraya				
Raw		17.17	18.49	7.68
Torrefied	240	18.84	19.29	2.37
	270	20.85	21.98	5.40
	300	22.40	24.81	10.75
	330	24.19	27.56	13.91
Kulim				
Raw		17.81	18.83	4.04
Torrefied	240	19.06	19.25	1.00
	270	20.88	21.92	5.00
	300	22.83	24.67	8.06
	330	24.34	27.45	12.77
Chengal				
Raw		18.03	18.75	4.01
Torrefied	240	19.56	19.32	1.21
	270	21.99	21.99	0.01
	300	23.66	24.85	5.03
	330	24.87	27.66	11.22

4.8.4 Comparison with published correlations

The developed correlations using ultimate and proximate analysis are compared with the established correlations found in the literature. Tables 4.15 and 4.16 show the comparison with published correlations based on the proximate analysis and ultimate analysis respectively. Overall, all the correlations proposed in this study are better than

the published correlations based on lowest AAE. This shows that by introducing the torrefaction temperature and residence time variables are definitely improve the accuracy of correlations.

Table 4.15 Comparison with established correlations (Proximate analysis)

Correlations	AAE (%)	Sources
Oil palm waste		
HHV = 15.8514 + 1.9293FC/VM + 0.0418VM/ASH + 0.1398ASH/FC + 0.0234t + 0.0082T	5.37	This study
HHV = 0.3536FC + 0.1559VM - 0.0078ASH	7.82	Parikh et al. (2005)
HHV = 0.1905VM + 0.2521FC	9.46	Yin, (2011)
HHV = 0.3536FC + 0.1559VM - 0.0078ASH	7.82	Ahmaruzzaman (2008)
HHV = 19.2880 - 0.2135VM/FC - 1.9584ASH/VM + 0.0234FC/ASH	11.09	Nhuchhen & Salam (2012)
Forestry residue		
HHV = 14.5782 + 0.1925VM/FC + 24.0162ASH/VM + 0.0161FC/ASH – 0.6277t + 0.0922T	10.37	This study
HHV = 0.3536FC + 0.1559VM - 0.0078ASH	11.35	Parikh et al. (2005)
HHV = 0.1905VM + 0.2521FC	12.21	Yin, (2011)
HHV = 0.3536FC + 0.1559VM - 0.0078ASH	11.35	Ahmaruzzaman (2008)
HHV = 19.2880 - 0.2135VM/FC - 1.9584ASH/VM + 0.0234FC/ASH	14.73	Nhuchhen & Salam (2012)

Table 4.16 Comparison with established correlations (Ultimate analysis)

Correlations	AAE (%)	Sources
Oil palm waste		
HHV = -0.2630 + 0.3072C + 0.4048H – 0.5194N + 0.0406O + 0.8409S + 0.0079t + 0.0068T	5.79	This study
HHV = 0.3491C + 1.1783H + 0.1005S - 0.1034O - 0.0151N - 0.0211A	8.17	Channiwala & Parikh (2002)
HHV = 0.2949C + 0.8250H	8.07	Yin (2011)
HHV = -1.3675 + 0.1337C + 0.7009H + 0.03180O	46.57	Sheng & Azevedo (2005)
HHV = 0.335C + 1.423H - 0.154O - 0.145N	12.19	Demirbas (1993)
Forestry residue		
HHV = 0.2269C – 0.8308H – 0.2014S + 0.0011(O + N) – 0.1572A + 11.6230 – 0.4396t + 0.0511T	11.75	This study
HHV = 0.3491C + 1.1783H + 0.1005S - 0.1034O - 0.0151N - 0.0211A	15.88	Channiwala & Parikh (2002)
HHV = 0.2949C + 0.8250H	14.87	Yin (2011)
HHV = -1.3675 + 0.1337C + 0.7009H + 0.03180O	42.93	Sheng & Azevedo (2005)
HHV = 0.335C + 1.423H - 0.154O - 0.145N	16.69	Demirbas (1993)

4.9   Summary

Based on physical appearances, all the biomass used in this study shows a change from light colour to a more darker colour. This is mainly because the carbon composition in the biomass is increased when torrefaction temperature is increased. In terms of mass and energy yields, for both oil palm waste and forestry residue, the most suitable residence time to perform torrefaction process is 30 minutes due to majority of the oil palm waste and forestry residue have more than 70% mass yields which is preferable yield for torrefaction process. While for ultimate analysis, both oil palm waste and forestry residue show an increase in carbon composition and a decrease in hydrogen and oxygen compositions. In proximate analysis, the fixed carbon and ash content show increasing trends while volatile matter shows a decreasing trend. By plotting H/C to O/C ratios, it can be said that by using torrefaction process, the properties of torrefied biomass are closed the properties of coal. The HHV also increases when increasing torrefaction temperature and almost similar to the HHV of a coal. This indicates that by pre-treating the biomass using torrefaction, the properties of biomass are upgraded. For HHV correlations, the best correlation to estimate oil palm waste is by using linear correlations based on the proximate analysis with an AAE and ABE of 5.37 and -1.00% respectively. While for forestry residue, the most suitable correlation is by using linear correlations based on proximate analysis with an AAE of 10.37% and ABE of -1.48%.

CHAPTER 5

SIMULATION OF FLUIDIZED BED GASIFICATION USING RAW AND TORREFIED OIL PALM WASTE AND FORESTRY RESIDUE

5.1 Introduction

This chapter describes the simulation study of fluidized bed gasification process using raw and torrefied oil palm waste and forestry residue. The gasification process is developed and simulated using Aspen Plus software. The effects of changing the gasification temperature, air to biomass ratio (ABR) and steam to biomass ratio (SBR) on the synthesis gas production were carried out in the fluidized bed gasification. In addition, the cold gas efficiency (CGE) and lower heating value (LHV) are performed for raw and torrefied biomass in order to evaluate the gasifier efficiency.

5.2 Application of fluidized bed gasification: Simulation study

In this work, the gasification based on the simulation work is performed in order to evaluate the effects of torrefaction as pre-treatment method on the synthesis gas production using gasification process. For this purpose, the gasification simulation process flow as shown in Figure 3.6 is used. Based on Figure 3.6, the first step is problem definition where the objective is defined. For this study, the objective is to evaluate the synthesis gas production using gasification model by employing raw and torrefied oil palm waste and forestry residue as a fuel.

Step 2 is the process and product specifications. The process specification involves the fluidized bed gasification. Initially 4 types of raw oil palm waste (OPF, PMF, EFB and PKS) and 4 types of raw forestry residue (Meranti, Seraya, Kulim and Chengal) are employed as a fuel. The product specification is syngas production which

consists of hydrogen, carbon monoxide, carbon dioxide and methane. However the hydrogen gas is the main target for this case study.

Step 3 is the fluidized bed gasification model development. Figure 5.1 shows the fluidized bed gasification process flowsheet developed in Aspen Plus software. Since Aspen Plus do not have the properties of oil palm waste and forestry residue, non-conventional solid are being defined for both biomass. The feed stream needs to be defined based on proximate analysis and ultimate analysis. This information is obtained from the developed oil palm waste and forestry residues database in the Chapter 4.
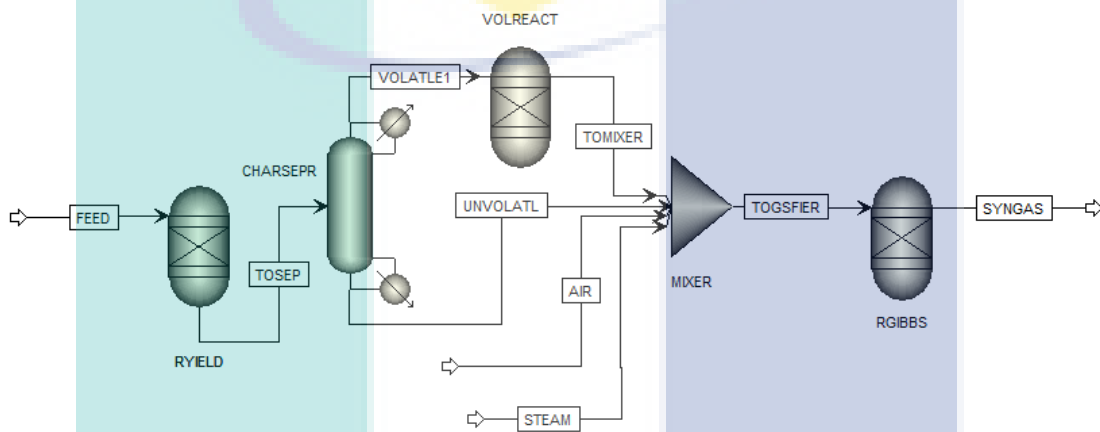
Figure 5.1 Fluidized bed gasification process flowsheet

Based on Figure 5.1, the decomposition of feed is represented by RYIELD which uses the yield reactor. The feed are fed into RYIELD at the rate of 10 kg/hr. RYIELD are used to decompose the feed into its constituent elements mainly consists of the carbon, hydrogen, nitrogen, oxygen and sulphur. A separator (CHARSEPR) and Gibbs reactor (VOLREACT) are used to represent the volatile reactions. In CHARSEPR, the products from RYIELD are separated into solids and volatile matter. Solid product is mainly the carbon and ash of the biomass. The separated volatile matter is then fed into the Gibbs reactor. The reactions from Equations 3.15 to 3.16 take places by assuming it follows Gibbs equilibrium. Lastly, the char gasification stages are represented by RGIBBS which uses Gibbs reactor. RGIBBS are used because in this study, different gasification temperatures are tested for studying its effect on the synthesis gas production. Different reactions takes places and by using RGIBBS reactor, the reactions involved in this reactor are from Equations 3.17 to 3.23. For the gasifying agents of air and steam, it is fed to the mixer at flow rate of 0.9065 and 1.8 kg/hr respectively.

Step 4 concerns with performance and sensitivity analysis. In this step the developed model underwent model validation before it is used for simulation of oil palm waste and forestry residue. The fluidized bed gasification model is simulated in Aspen Plus. For the purpose of model validation, the data from Nikoo & Mahinpey (2008) is employed. Here the same operating condition and the same biomass which is pine sawdust are used. The operating condition for the validation process can be seen in Table 5.1.

Table 5.1 Operating condition for validation process

Operating condition	Value
Fluidized bed	
Temperature, °C	700 – 900
Pressure, bar	1.05
Air	
Temperature, °C	65
Flow rate, N m^3/h	0.5 – 0.7
Steam	
Temperature, °C	145
Flow rate, kg/h	0 – 1.8

The simulation results obtained is shown in Table 5.2 where the RMSE obtained is lower than 0.3 indicating a reliable model has been obtained (Veerasamy, et al., 2011).

Table 5.2 Validation process for fluidized bed gasification process

Composition	Root Mean Square Error
H_2	0.01767
CO_2	0.22646
CO	0.31684
CH_4	0.72581

After the model validation, the gasification model is simulated using oil palm waste and forestry residue. The simulation results for both oil palm waste and forestry residue are shown in Figures 5.2 and 5.3.
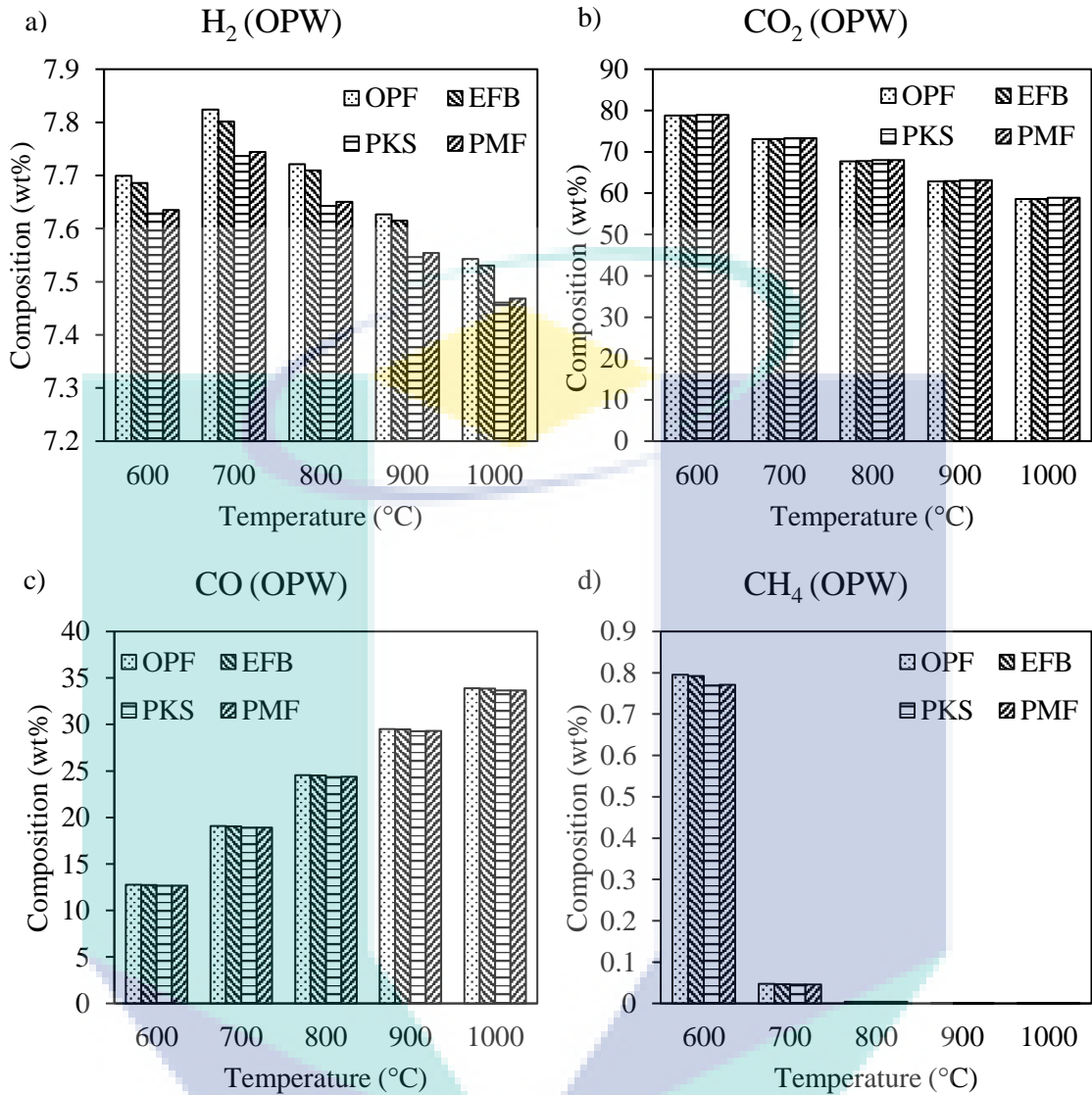
Figure 5.2 Composition of a) hydrogen, b) carbon dioxide, c) carbon monoxide and d) methane produce using raw oil palm waste

For oil palm waste, according to Figure 5.2, hydrogen composition for each biomass are increasing (OPF: 7.70% to 7.82%, PKS: 7.63% to 7.74%, PMF: 7.63% to 7.74%, EFB: 7.69% to 7.80%) when it is operated from temperature of 600 to 700 °C and then, the hydrogen composition shows a decreasing trends when it is operated from temperature of 700 to 1000 °C (OPF: 7.82% to 7.54%, PKS: 7.74% to 7.46%, PMF: 7.74% to 7.47%, EFB: 7.80% to 7.53%). The decrease in hydrogen composition after 700 °C is mainly due the hydrogen are being consumed in partial combustion in Equation 3.17. In overall, OPF shows the highest composition production for hydrogen (7.82 %), carbon monoxide (19.07 %) and methane production (0.05 %) at gasification temperature of 700 °C. While for carbon dioxide gas, PKS shows the highest production

at 73.31 % at the same gasification temperature. According to the Le Châtelier's principle, if a dynamic equilibrium is disturbed by changing the operating condition, the equilibrium will be shifted in order to counteract the changes made. The increasing of the temperature in the system will disturb the equilibrium state of the chemical reaction. The equilibrium chemical reactions then experiences a sudden change as the temperature is increased which cause the equilibrium shifts in the opposite direction to offset the changes. The increasing temperature will shifts the equilibrium of endothermic reactions (3.18) and (3.19) in the direction of the product formation (CO and H_2), while the equilibrium of exothermic reactions (3.17) and (3.20) is moved in the direction of the reactants (mainly H_2). However the increment temperature of the gasification process is not beneficial to the generation of methane since more hydrogen is produced which explains the decrement trends of methane production (Zogała, 2014). Based on the objective specified, the hydrogen gas production are the main target gas when deciding the most suitable biomass for gasification. In this case hydrogen composition produced from OPF shows the highest composition compare to the other biomass. This is due to the fact that OPF has a highest fixed carbon composition (30.96 wt%). For raw oil palm waste, the suitable biomass to be gasified is OPF as at each of the gasifier temperature, it shows the highest composition of hydrogen gas.

In forestry residue group, the hydrogen composition produced have the same patterns as gasification of OPW where after 700 °C the composition starts to drop. The hydrogen composition for forestry residue are as follows: 1) Meranti is initially increased from 7.53% to 7.63% when it is gasified from 600 to 700 °C and start to decrease up to 7.34% at final gasification temperature of 1000 °C, 2) Seraya is increased from 7.54% to 7.65% and is decreased to 7.36%, 3) Kulim is increased from 7.70% to 7.82% and is decreased to 7.55% and 4) Chengal is increased from 7.70% to 7.81% and is decreased to 7.54%. Kulim produces the highest hydrogen gas production of 7.82%, carbon monoxide gas of 19.10% and methane gas of 0.05% while for highest carbon dioxide gas of 73.53% is produced from Seraya at gasification temperature of 700 °C. The same trends are obtained as oil palm waste group where the highest composition is at the same gasifier temperature of 700 °C for hydrogen composition. Similarly to OPF, Kulim have a higher fixed carbon composition of 26.76 wt% compare to Meranti (22.66 wt%), Seraya (24.46 wt%) and Chengal (26.20 wt%). Usually the high value of fixed carbon contributes to more reactivity of gasification process which

ultimately producing more hydrogen gas. Based on the hydrogen gas production, it can be concluded that Kulim is the best forestry residue as a fuel for gasification process.

Based on simulation results obtained, OPF and Kulim are chosen as the most suitable oil palm waste and forestry residue for gasification fuel. In the next step, the effects of raw and torrefied OPF and Kulim are further investigated as a fuel in gasification process during sensitivity analysis. For sensitivity analysis, there are three parameters that have been taken into consideration which are the gasifier temperature, air to biomass ratio and steam to biomass ratio. In this analysis, 5 different inputs of OPF and Kulim are employed which consists of raw, torrefied at 240 °C, 270 °C, 300 °C and 330 °C respectively. The result obtained from the simulation are discussed in the next subchapter.
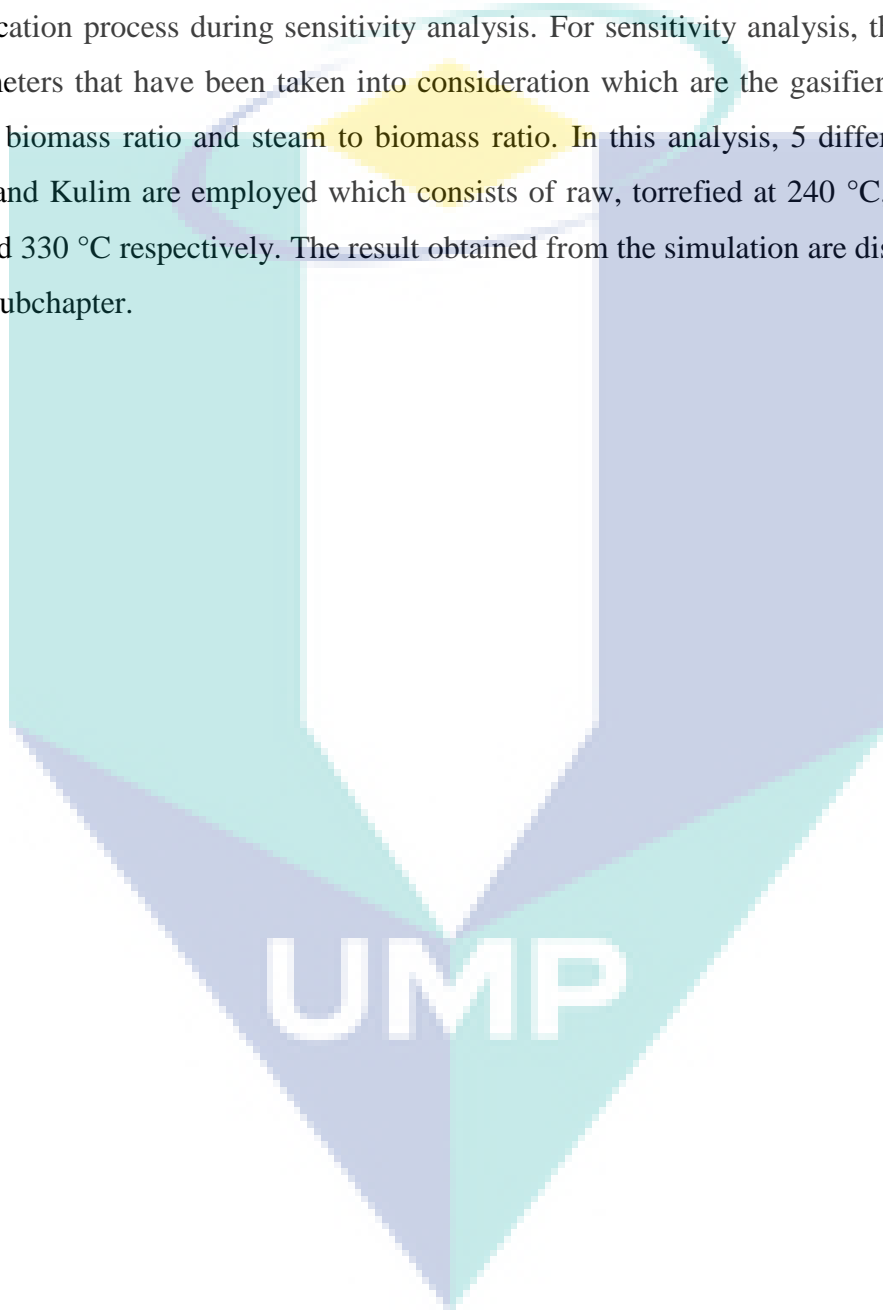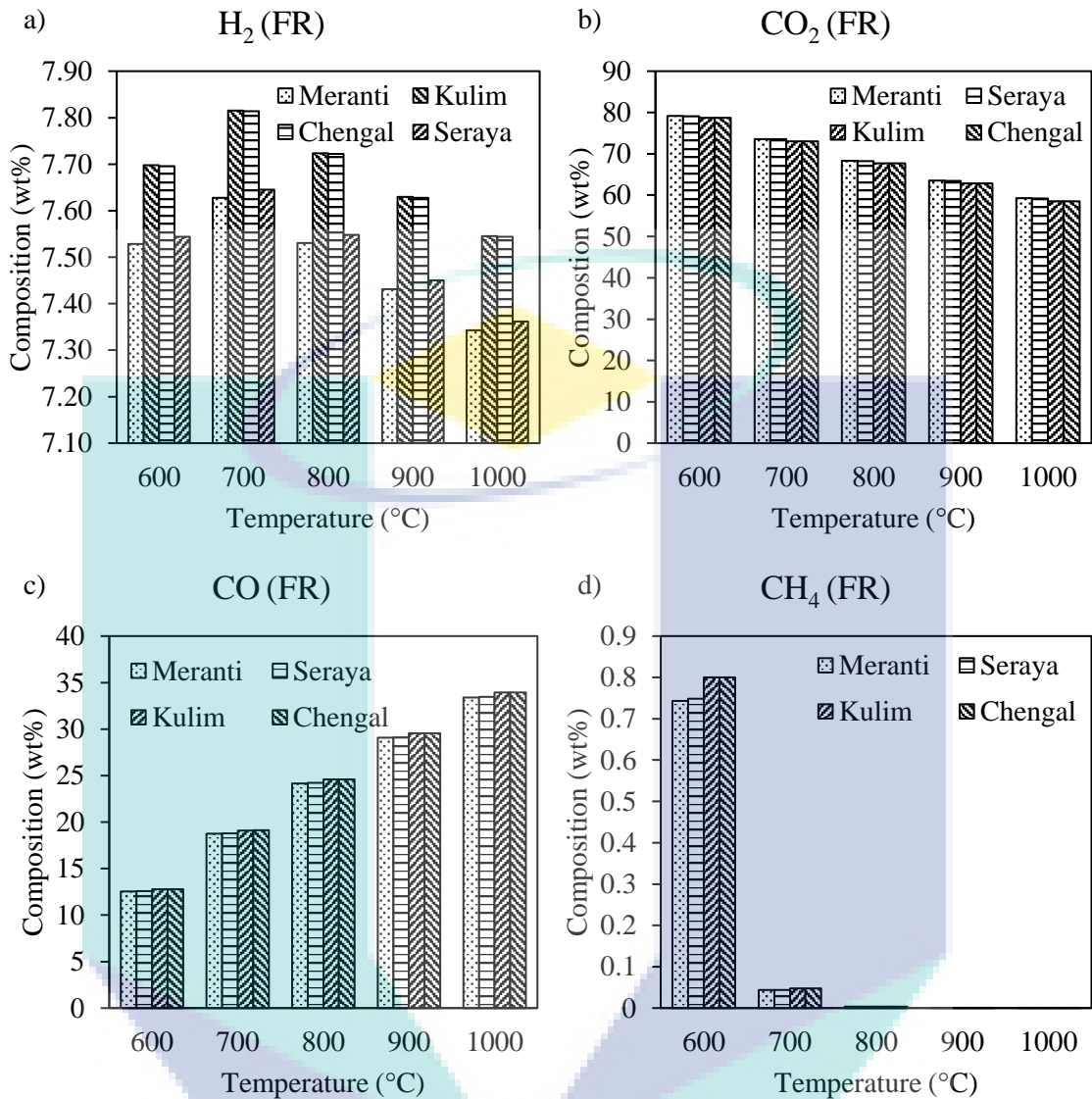
Figure 5.3 Composition of a) hydrogen, b) carbon dioxide, c) carbon monoxide and d) methane produce using raw forestry residue

5.2.1 Effect of gasification temperature on syngas production

Different gasification temperatures in the ranges of 600 to 1000 °C were simulated in this analysis for torrefied OPF and Kulim. The purpose of this simulation is to evaluate the effect of gasification temperature on the syngas production. Figures 5.4 and 5.5 show the syngas composition for OPF and Kulim. In both cases, by increasing the gasifier temperature from 600 to 700 °C, it certainly increases the hydrogen composition but it start to decrease afterwards. Meanwhile as the gasification temperature is increased, the carbon dioxide and methane show a decrement trends and

the carbon monoxide shows an increment trends. This result is in good agreement with study conducted by Schuster et al. (2001) and Atnaw et al. (2013).

Figure 5.4 Composition of a) hydrogen, b) carbon dioxide, c) carbon monoxide and d) methane produce using raw and torrefied oil palm frond under different gasification temperature

At higher gasifier temperature, Le Châtelier's principle is applied in which when the dynamic equilibrium is disturbed, the equilibrium is shifted to counteract the changes and reestablished the equilibrium (Petrucci et al., 1993). That is why the concentration of carbon monoxide is increased but the concentrations of carbon dioxide and methane are decreased. More carbon dioxide, methane and hydrogen compositions are used to produce carbon monoxide. Different syngas compositions are obtained

because the ultimate and proximate analysis used in the simulation are affecting the gas composition.

Figure 5.5 Composition of a) hydrogen, b) carbon dioxide, c) carbon monoxide and d) methane produce using raw and torrefied Kulim under different gasification temperature

Higher carbon composition increases the syngas production. This is due to the fact that gasification reaction mainly consist of carbon reacting with other components (water and oxygen) to produce syngas. Figure 5.6 shows the carbon composition from the ultimate analysis and hydrogen composition for raw and torrefied OPF and Kulim at gasification temperature of 700 °C. From Figure 5.6, it shows that when increasing carbon composition the amount of hydrogen produced are increased. This result can be observed for both OPF and Kulim. In terms of hydrogen production, the suitable

gasifier temperature to be used for raw and torrefied oil palm waste and forestry residue is at 700 °C.

Figure 5.6 Carbon and hydrogen compositions of raw and torrefied a) OPF and b) Kulim at 700 °C

5.2.2 Effect of air to biomass (ABR) ratio on syngas production

In this study, the effect of ABR used for simulation is in the range from 0.2 to 1.0, and the trends of the syngas production are observed. The gasifier temperature used is at 700 °C as it is the suitable temperature for raw and torrefied OPF and Kulim based on the sensitivity analysis of gasification temperature. The influences of air in ABR affect the products as it supplies oxygen for combustion. The data simulated for ABR are shown in Figures 5.7 and 5.8 for OPF and Kulim respectively.

Generally from Figures 5.7 and 5.8, compositions of hydrogen, carbon monoxide and methane are decreasing and carbon dioxide is increasing when ABR is increased. The production of carbon dioxide increases due to the endothermic reactions of combustion as shown in Equation 3.15. While for the decreasing of carbon monoxide is due to the homogenous reactions of carbon monoxide combustion ($CO + 0.5\ O_2 \rightarrow CO_2$) and contributes to the increase of carbon dioxide. The oxidation of hydrogen occur as in Equation 3.17 decrease the hydrogen by becoming water. This lead to the steam reforming methanisation as in Equation 3.23 which consume methane. In terms of hydrogen gas production for OPF, the production is increased in the range of 9.5% to 12.13% for raw OPF, 8.69% to 12.14% for torrefied OPF at 240 °C, 8.68% to 12.18% for torrefied OPF at 270 °C, 8.62% to 12.19% for torrefied OPF at 300 °C and 8.64% to 12.1% for torrefied OPF at 330 °C. As for Kulim, the range of increment are in the range of 8.01% to 10.44%, 7.97% to 10.42%, 7.98% to 10.39%, 8.01% to 10.37% and 8.05% to 10.42% for raw Kulim, torrefied Kulim at 240 °C, torrefied Kulim at 270 °C, torrefied Kulim at 300 °C and torrefied Kulim at 330 °C respectively. The most suitable ABR to perform gasification process are at 0.2. This findings are similar for both OPF and Kulim. At ABR of 0.2, the increment of hydrogen produced for OPF can reach up to 0.24%, while it is 0.19% for Kulim. This indicates that the gasification should be performed at lower value of ABR for both OPF and Kulim.
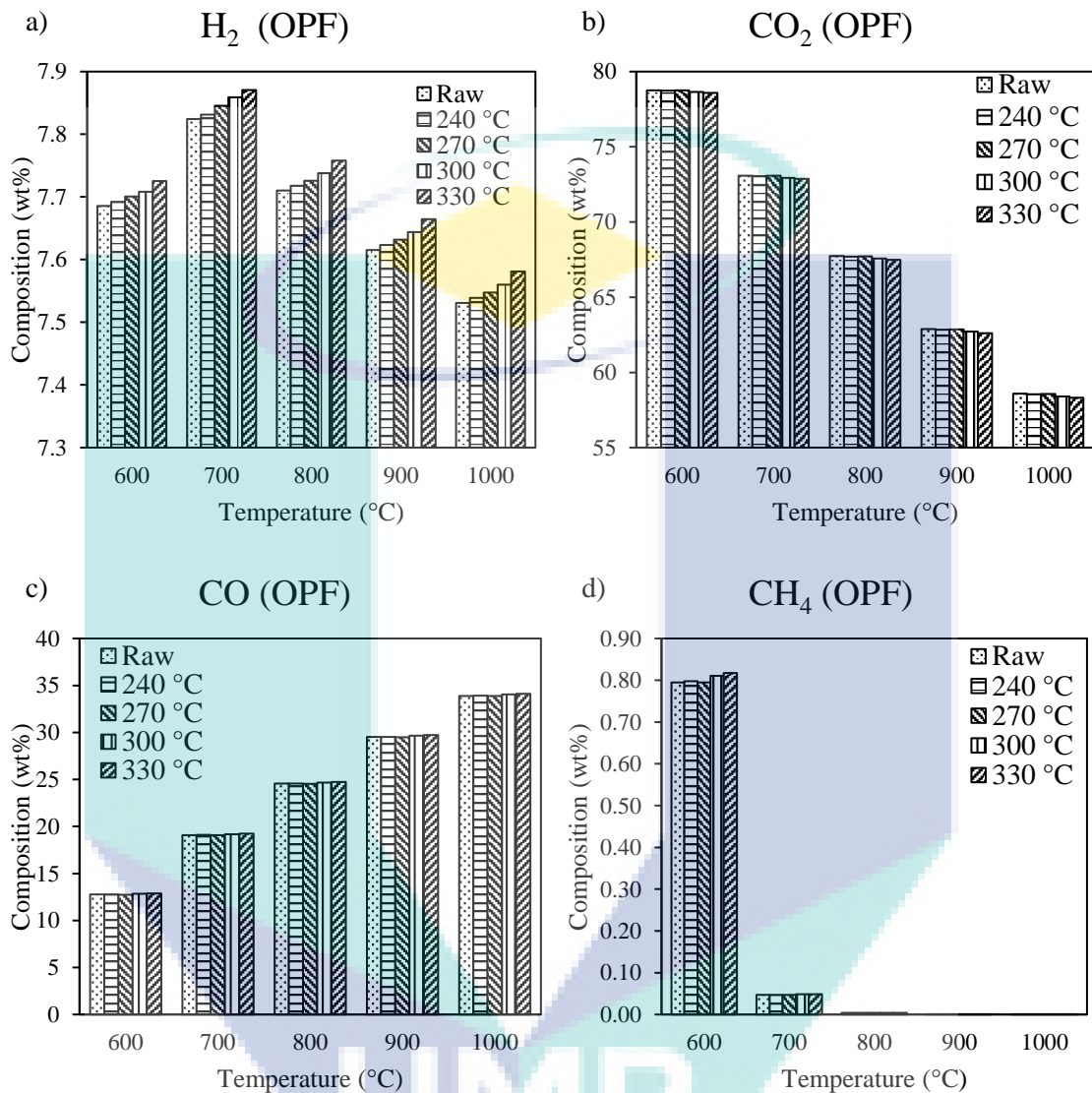
Figure 5.7 Compositions of a) hydrogen, b) carbon dioxide, c) carbon monoxide and d) methane produced using raw and torrefied oil palm frond under different air to biomass ratio
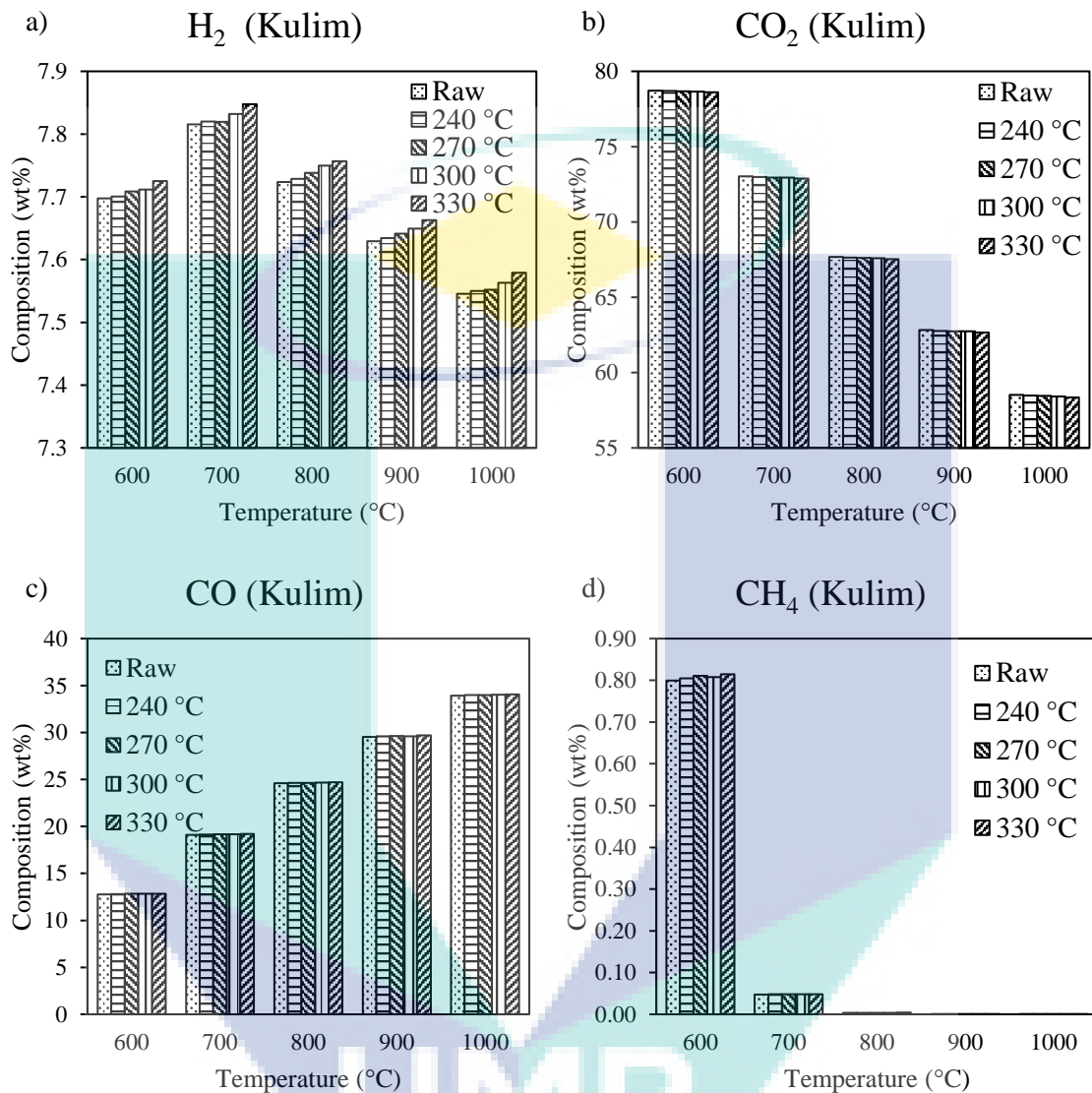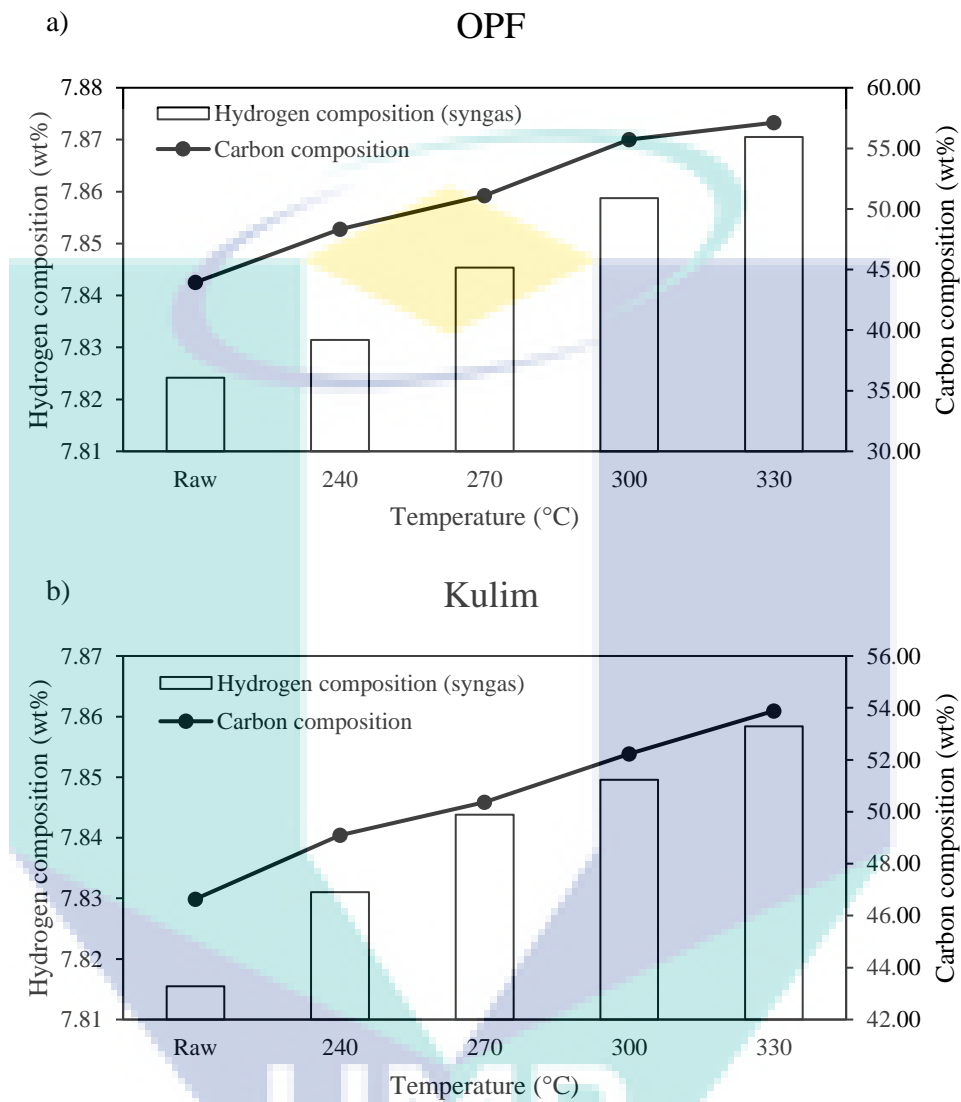
Figure 5.8 Compositions of a) hydrogen, b) carbon dioxide, c) carbon monoxide and d) methane produced using raw and torrefied Kulim under different air to biomass ratio

5.2.3 Effect of steam to biomass ratio on syngas production

The effect of steam to biomass ratio (SBR) is then performed where the SBR is varied between 0.2 to 1. The simulation results are shown in Figures 5.9 and 5.10 for OPF and Kulim respectively. The gasifier temperature used is 700 °C while the ABR is set at 0.2 based on the previous findings.

Figure 5.9 Compositions of a) hydrogen, b) carbon dioxide, c) carbon monoxide and d) methane produce using raw and torrefied oil palm frond under different steam to biomass ratio

Using steam as a gasifying agent increases the partial pressure of water (H_2O) inside the gasification reactor and favour the water gas shift and methane reforming and this leads to an increase in hydrogen, carbon dioxide and methane compositions. Although both of those reactions are favourable, it needs higher temperature from the

range of 750 to 800 °C (Kumar et al., 2009). For gasification temperature fixed at 700 °C, the reactions tends to favour both of methane reforming (Equations 3.22 and 3.23) and water gas shift (Equation 3.21). That is why higher SBR yields more hydrogen composition compare to lower SBR. At raw condition, OPF shows an increase of 0.95% to 4.37% while it is 0.94% to 4.35% for Kulim. When undergone torrefaction, OPF (torrefied at 240 °C: 0.94% – 4.37%, torrefied at 270 °C: 0.94% – 4.35%, torrefied at 300 °C: 0.94% – 4.39% and torrefied at 330 °C: 0.94% – 4.40%) and Kulim (torrefied at 240 °C: 0.94% – 4.37%, torrefied at 270 °C: 0.94% – 4.36%, torrefied at 300 °C: 1.00% – 4.91% and torrefied at 330 °C: 1.02% – 4.90%) shows an increase in its hydrogen production when SBR is increased. The highest hydrogen composition for OPF and Kulim are obtained when it was torrefied at temperature of 330 °C using SBR value of 1.0. The highest hydrogen compositions obtained for both biomass are 7.85% (OPF) and 7.92% (Kulim) when the biomass are torrefied at temperature of 330 °C. At SBR value 1.0, the hydrogen produced for OPF and Kulim shows an increase in value from raw until it is torrefied at 330 °C. The value increases up to 0.25% for OPF and 0.27% for Kulim.
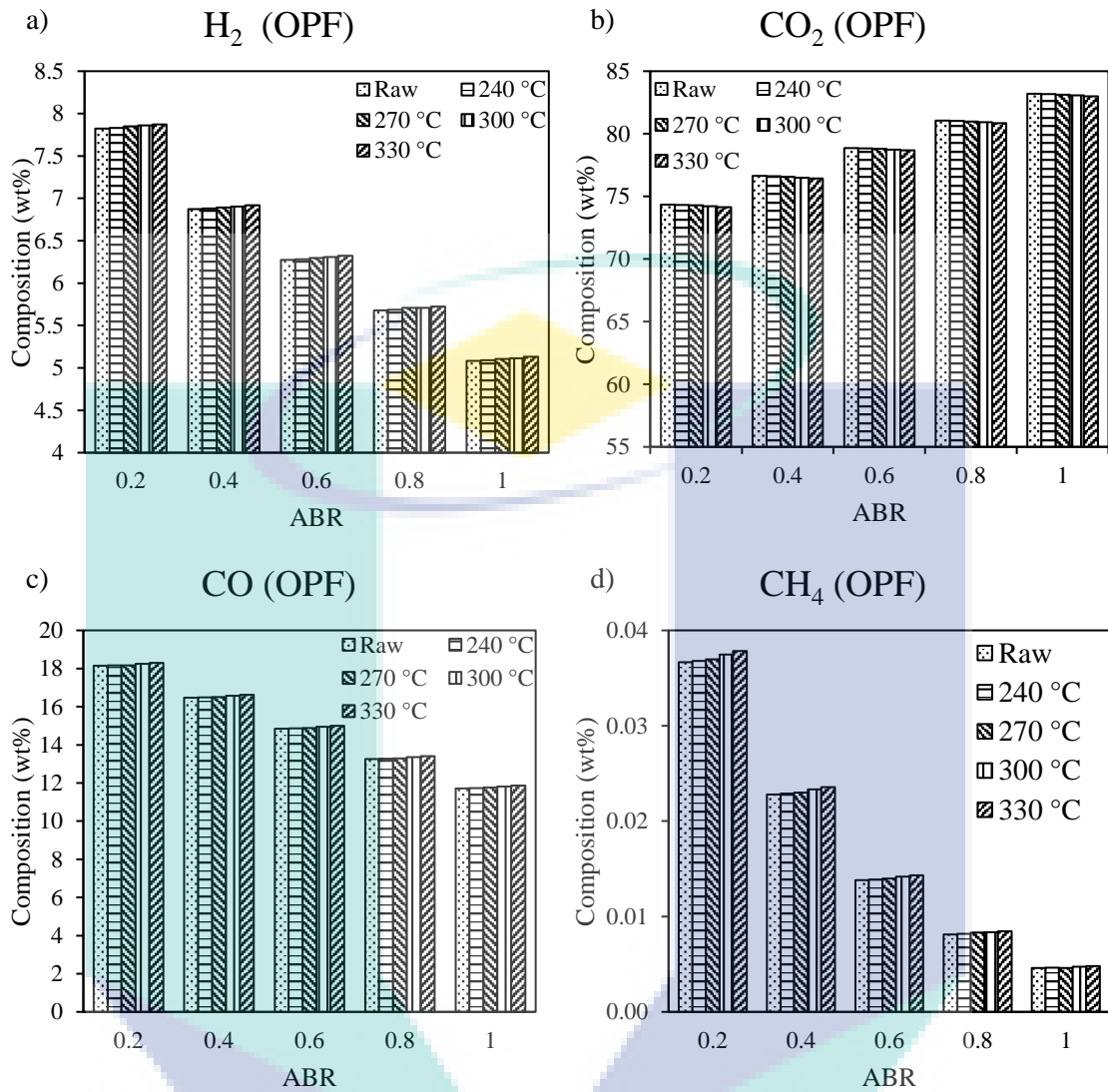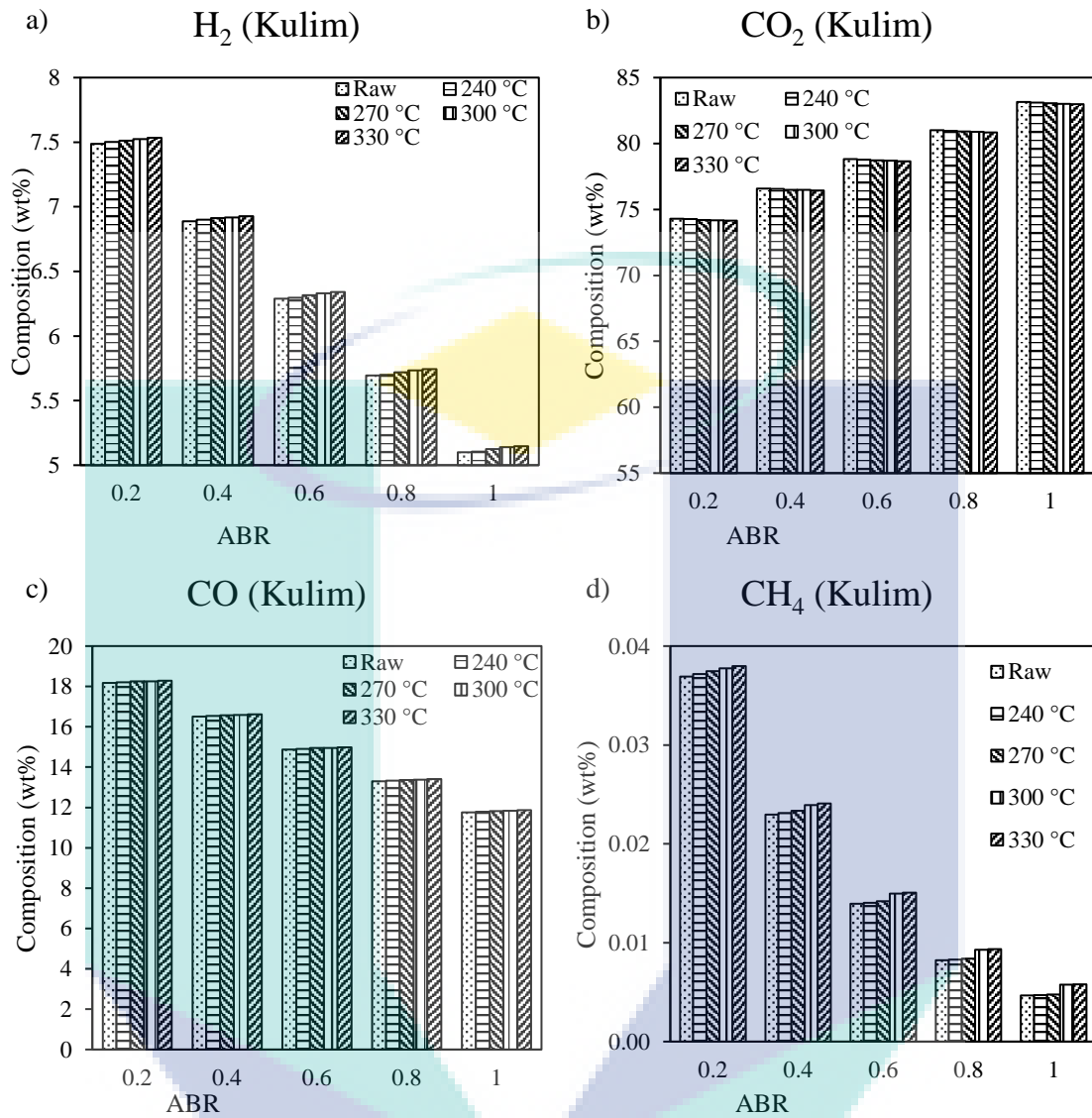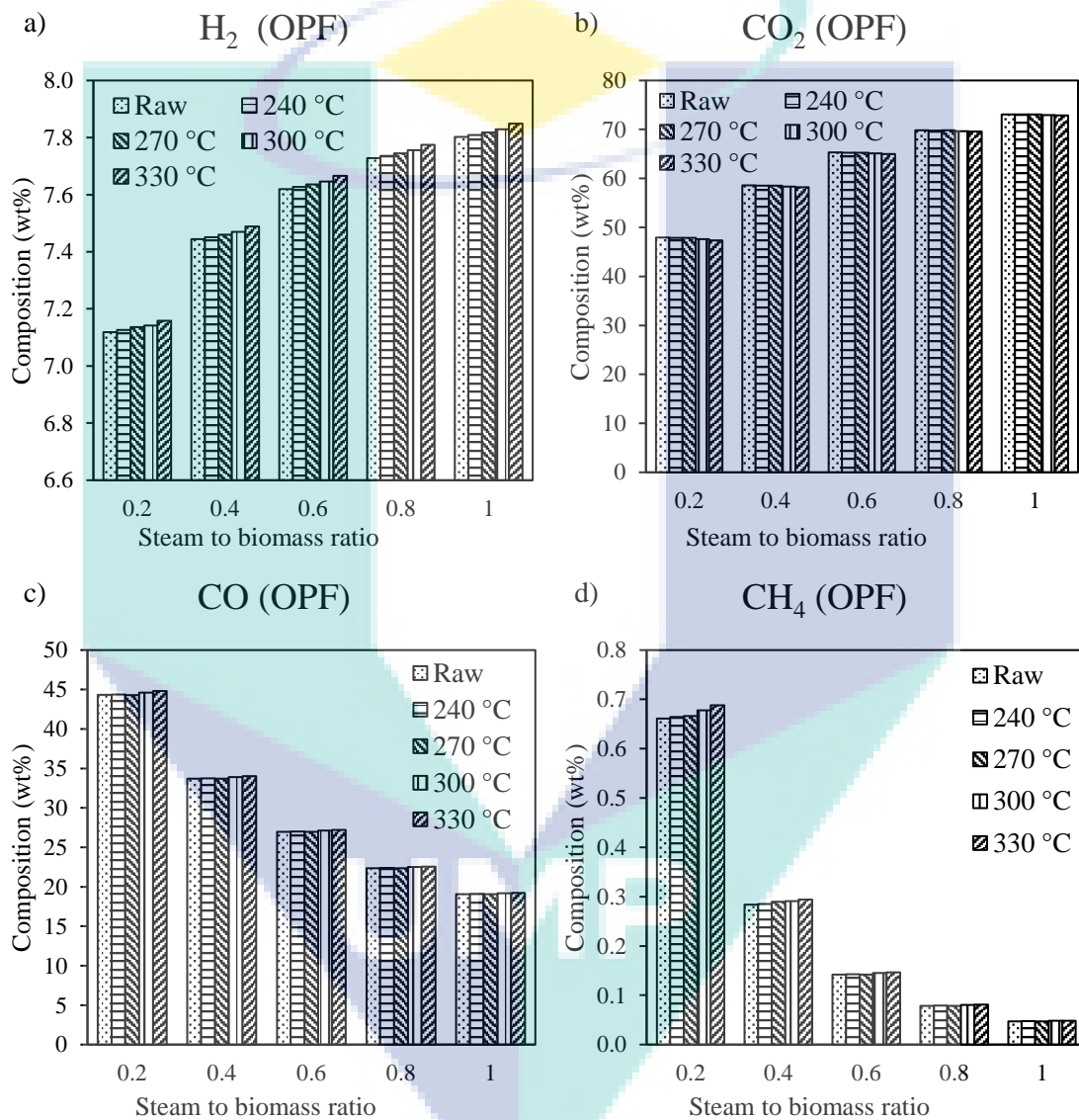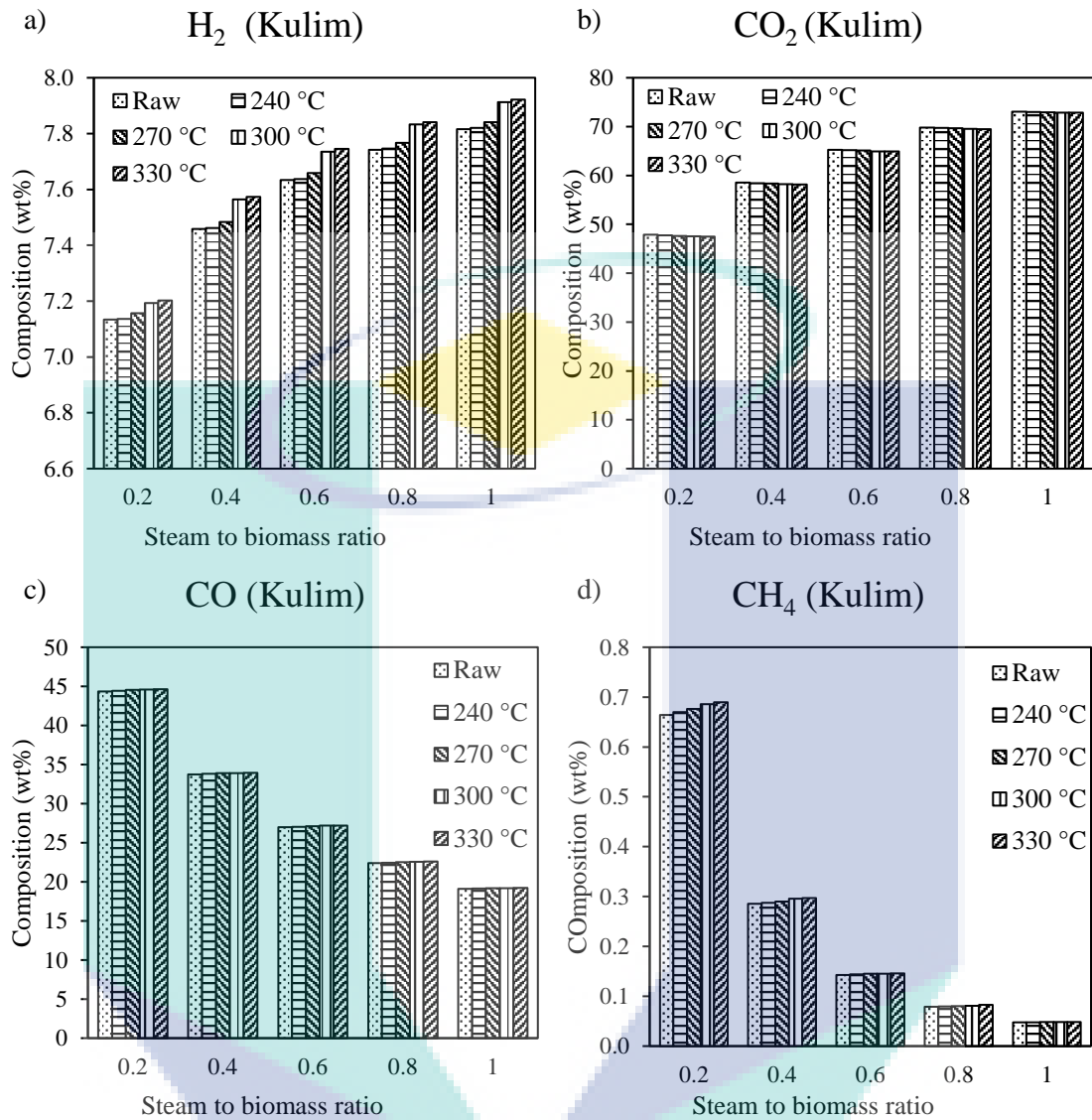
Figure 5.10 Composition of a) hydrogen, b) carbon dioxide, c) carbon monoxide and d) methane produce using raw and torrefied Kulim under different steam to biomass ratio

5.2.4 Cold gas efficiency and lower heating value

The gasifier efficiency can be determined based on the cold gas efficiency (CGE). CGE can be expressed as the energy content of gaseous products to energy content of the feed. The lower heating value (LHV) is calculated based on the HHV and taking into accounts the moisture, latent heat of vaporisation and the products of hydrogen combustion from the water obtained (Zaccariello & Mastellone, 2015). By simulating the gasification process at gasifier temperature 700 °C, ABR at 2.0 and SBR at 1.0, CGE and LHV are calculated as illustrated in Figure 5.10 (a) and Figure 5.10 (b) for raw and torrefied OPF and Kulim respectively.
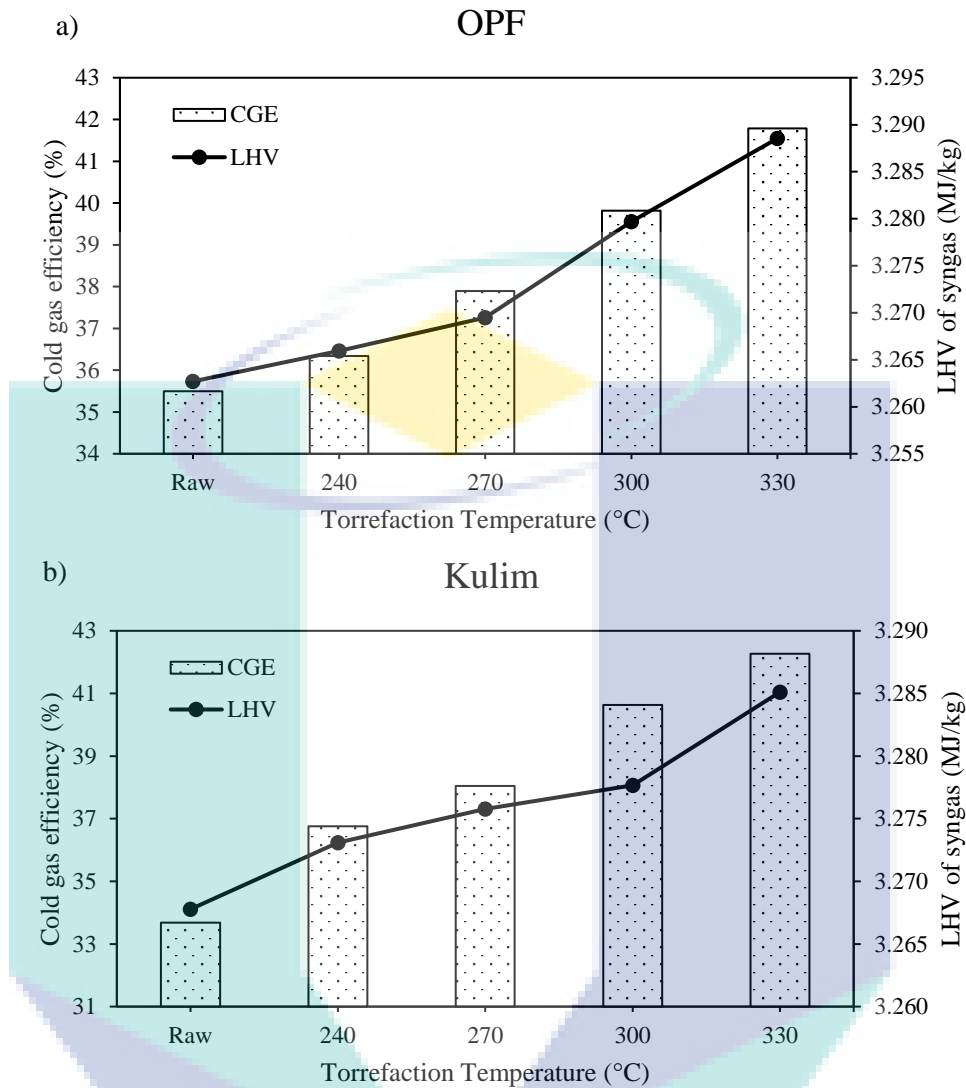
Figure 5.11 Cold gas efficiency and lower heating value of syngas for (a) OPF and (b) Kulim

Figure 5.11 (a) shows that for OPF, the CGE is increased in the range of 0.85% to 6.29% as the biomass undergone torrefaction process at higher temperature. The changes are calculated by subtracting the CGE for torrefied with CGE for raw OPF. While in Figure 5.11 (b), Kulim shows the same increasing trend but the increment are from 3.08% to 8.59%. For LHV of the syngas, both biomass have almost similar LHV except for at raw condition, torrefied at 240 °C and torrefied at 270 °C. At this point, Kulim shows higher LHV compared to OPF with the different of 0.01 MJ/kg. This finding are in accordance to Zaccariello & Mastellone (2015) and Ruoppolo et al. (2013). This shows that in terms of efficiency and LHV of the syngas, Kulim are better to be gasified than OPF.

In term of raw and torrefied biomass, the chosen biomass used in this study shows that the highest composition of hydrogen produced comes from torrefied biomass. This is due to the higher carbon content of the torrefied biomass. With more sources of carbon, char partial combustion, water-gas reactions and Boudouard reactions most likely to occur in the gasifier. This in turn produce more carbon monoxide and hydrogen. Higher carbon content and this reactions also affect the higher heating value of the biomass. Based on the syngas formation, syngas yield are higher when using biomass undergo at higher torrefaction temperature. This finding is in accordance with the findings of Kuo et al. (2014).

5.3   Summary

By simulating the gasification process, the performance of raw and torrefied biomass can be observed. The flowsheet used in this study is firstly undergo validation process in order to ensure that it can be used to simulate gasification process. The validated simulation was then applied for all eight (8) biomass used in this study. Only the raw biomass is used to evaluate the performance of biomass and the best biomass for the oil palm waste and forestry residue are chosen. OPF and Kulim are selected to represent oil palm waste and forestry residue respectively based on the highest hydrogen gas production. Sensitivity analysis is then carried out by varying the gasifier temperature, air to biomass ratio and steam to biomass ratio. It was found that the most suitable operating conditions to gasify both OPF and Kulim are; gasifier temperature at 700 °C, air to biomass ratio is 0.2 and steam to biomass ratio is 1.0. This conditions are applicable for both raw and torrefied biomass. Using this operating condition, the highest hydrogen composition of 7.85% and 7.92% are obtained when using torrefied OPF and Kulim at torrefaction temperature of 330 °C. Then, the CGE and LHV for gasification of both OPF and Kulim in raw and torrefied are calculated. Both OPF and Kulim shows a higher CGE and LHV when it is torrefied at 330 °C. The highest value for CGE calculated for OPF and Kulim are 41.78% and 42.26% respectively. While for LHV, OPF and Kulim have the same value which is 3.29 MJ/kg. From the value calculated, Kulim shows the best result with higher CGE and LHV compare to OPF in raw and torrefied condition.

CHAPTER 6

CONCLUSIONS

6.1   Conclusions

The torrefaction of oil palm waste and forestry residue have been successfully carried out. The effect of difference torrefaction temperatures (240, 270, 300 and 330 °C) and residence times (15, 30 and 60 minutes) were investigated and the results show that torrefaction temperature plays a significant role compared to residence time. The physical appearance of the biomass changes to a more darker colour. This is caused by the increasing of the carbon content in the biomass. Based on the mass and energy yields, 30 minutes residence time has been chosen as the best residence time to be used for torrefaction of both biomass group. It is found that the carbon composition increases while hydrogen and oxygen compositions decreases for both of the biomass group. For proximate analysis, the ash content and fixed carbon are increased in composition while volatile matter is decreased for both oil palm waste and forestry residue.

By undergone torrefaction process, the H/C and O/C ratios of the biomass are decreased and getting closer to the properties of coal. In addition, the higher heating value of these biomass are also increased as the higher torrefaction temperature is used. The enhancement factor for HHV can reach up to 1.58 and 1.41 for oil palm waste and forestry residue respectively. Using HHV, ultimate analysis, proximate analysis, torrefaction temperature and residence time, HHV correlations are developed in order to estimate HHV for raw and torrefied oil palm waste and forestry residue. The best correlation for both biomass are summarised in Table 6.1 along with its type of correlations, AAE.

95

Table 6.1 Summary of HHV correlations for both oil palm waste and forestry residue

Correlations	Type of correlation	AAE (%)
Oil palm waste		
HHV = 15.8514 + 1.9293FC/VM + 0.0418VM/ASH + 0.1398ASH/FC + 0.0234t + 0.0082T	Linear correlation based on proximate analysis	5.37
Forestry residue		
HHV = 14.5782 + 0.1925VM/FC + 24.0162ASH/VM + 0.0161FC/ASH − 0.6277t + 0.0922T	Linear correlation based on proximate analysis	10.37

The simulation for the performance evaluation of raw and torrefied biomass using the gasification model are successfully accomplished. The flowsheet used was validated by using the experimental data. After that, performance evaluation for both group of biomass are carried out to find the best biomass. Oil palm frond are chosen for oil palm waste and Kulim sawdust was selected from forestry residue group. Optimum condition obtained are 700 °C (gasifier temperature), 0.2 (ABR) and 1.0 (SBR). Based on this operating condition, the CGE and LHV of the syngas are calculated to investigate which of the biomass (OPF and Kulim) are suitable to be gasified. In terms of raw and torrefied biomass, it is better to use torrefied biomass as it increases the CGE. Both OPF and Kulim show the same trends where by using from raw biomass to the biomass with higher torrefaction temperature are successfully increasing the CGE and LHV of the syngas. The CGE changes for OPF is in the range of 0.85% to 6.29%. While for Kulim the increment are from 3.08% to 8.59%. For LHV of the syngas, both the biomass have almost similar LHV except for at raw condition, torrefied at 240 °C and torrefied at 270 °C. At this point, Kulim shows higher LHV compare to OPF with the different of 0.01 MJ/kg. By comparing both types of biomass (OPF and Kulim), Kulim are chosen to be the best biomass to be gasified under torrefied condition.

6.2   Recommendations

For future work, the current work can be further investigated for better understanding and improvement. Some of the suggestions for the future work are divided into two process as follows:

1. Torrefaction:
   a. The use of other types of biomass from industrial and municipal solid wastes, animal waste and agricultural residue for torrefaction process can be studied.
   b. The composition of the condensable and non-condensable products from torrefaction process can be analysed.
   c. The studies on hemicellulose, cellulose and lignin composition of raw and torrefied biomass can be studied to understand its effects on torrefaction process.

2. Gasification:
   a. Experimental work for the gasification process can be carried out for both oil palm waste and forestry residue (raw and torrefied biomass).
   b. Simulation of simultaneous torrefaction and gasification can be proposed.
   c. Using different types of reactor other than fluidized bed to studies its behaviour when using raw and torrefied biomass as its feedstock.

REFERENCES

Acharya, B., Dutta, A., & Minaret, J. (2015). Review on comparative study of dry and wet torrefaction. *Sustainable Energy Technologies and Assessments , 12* , 26–37.

Agbor, V. B., Cicek, N., Sparling, R., Berlin, A., & Levin, D. B. (2011). Biomass pretreatment: Fundamentals toward application. *Biotechnology Advances*, 675-685.

Ahmad, M., & Subawi, H. (2013). New Van Krevelen diagram and its correlation with the heating value of biomass. *Research Journal of Agriculture and Environmental Management*, 295-301.

Ahmad, M., Hale, M., Khalil, H. A., & Suryani, S. (2013). Changes in Extractive Content on Wood Surfaces of Chengal (Neobalanocarpus Heimii) and Effects on Performance. *Journal of Tropical Forest Science*, 278-288.

Ahmaruzzaman, M. (2008). Proximate analyses and predicting HHV of chars obtained from cocracking of petroleum vacuum residue with coal, plastics and biomass. *Bioresource Technology* , 5043–5050.

Almeida, G., Brito, J., & Perre, P. (2010). Alterations in energy properties of eucalyptus wood and bark subjected to torrefaction: The potential of mass loss as a synthetic indicator. *Bioresource Technology*, 9778-9784.

Arena, U. (2012). Process and technological aspects of municipal solid waste gasification. A review. *Waste Management*, 625-639.

Arias, B., Pevida, C., Fermoso, J., Plaza, M., Rubiera, F., & Pis, J. (2008). Influence of torrefaction on the grindability and reactivity of woody biomass. *Fuel Processing Technology*, 169-175.

Arteaga-Peréz, L. E., Segura, C., Bustamante-García, V., Capiro, O. G., & Jimenez, R. (2015a). Torrefaction of wood and bark from Eucalyptus globulus and Eucalyptus nitens: Focus on volatile evolution vs feasible temperatures. *Energy*, 1731-1741.

Arteaga-Pérez, L. E., Segura, C., Espinoza, D., Radovic, L. R., & Jiménez, R. (2015b). Torrefaction of Pinus radiata and Eucalyptus globulus: A combined experimental and modeling approach to process synthesis. *Energy for Sustainable Development*, 13-23.

Asadullah, M. (2014). Barriers of Commercial Power Generation Using Biomass Gasification. *Renewable and Sustainable Energy Reviews*, 201-215.

Asadullah, M., Adi, A. M., Suhada, N., Malek, N. H., Saringat, M. I., & Azdarpour, A. (2014). Optimization of palm kernel shell torrefaction to produce energy densified bio-coal. *Energy Conversion and Management*, 1086-1093.

Atnaw, S. M., Sulaiman, S. A., & Yusup, S. (2013). Syngas production from downdraft gasification of oil palm fronds. *Energy*, 491-501.

Aziz, M. A., Sabil, K. M., Uemura, Y., & Ismail, L. (2012). A Study on Torrefaction of Oil Palm Biomass. *Journal or Applied Sciences*, 1130-1135.

Basu, P. (2013). *Biomass Gasification, Pyrolysis, and Torrefaction Practical Design and Theory* (2nd ed.). Elsevier Inc.

Batidzirai, B., Mignot, A. P., Schakel, W. B., Junginger, H. M., & Faaij, A. P. (2013). Biomass torrefaction technology: Techno-economic status and future prospects. *Energy*, 196-214.

Ben, H., & Ragauskas, A. J. (2012). Torrefaction of Loblolly pine. *Green Chemistry*, 72-76.

Bergman, P., & Kiel, J. (2005). Torrefaction for biomass upgrading. *14th European Biomass Conference & Exhibition*. Paris, France.

Brar, J. S., Singh, K., J.Wang, & Kumar, S. (2012). Cogasification of Coal and Biomass: A Review. *International Journal of Forestry Research*, 1-10.

Bridgeman, T., Jones, J., Shield, I., & Williams, P. (2008). Torrefaction of reed canary grass, wheat straw and willow to enhance solid fuel qualities and combustion properties. *Fuel*, 844-856.

Callejón-Ferre, A., Velázquez-Martí, B., López-Martínez, J., & Manzano-Agugliaro, F. (2011). Greenhouse crop residues: Energy potential and models for the prediction of their higher heating value. *Renewable and Sustainable Energy Reviews* , 948–955.

Channiwala, S., & Parikh, P. (2002). A unified correlation for estimating HHV of solid, liquid and gaseous fuels. *Fuel*, 1051-1063.

Chen, W. H., & Kuo, P. C. (2010). A study on torrefaction of various biomass materials and its impact on lignocellulosic structure simulated by a thermogravimetry. *Energy*, 2580-2586.

Chen, W. H., Cheng, W. Y., Lu, K. M., & Huang, Y. P. (2011). An evaluation on improvement of pulverized biomass property for solid fuel through torrefaction. *Applied Energy*, 3636-3644.

Chen, W.-H., Chen, C.-J., Hung, C.-I., Shen, C.-H., & Hsu, H.-W. (2013). A comparison of gasification phenomena among raw biomass, torrefied biomass and coal in an entrained-flow reactor. *Applied Energy*, 421-430.

Chen, W.-H., Du, S.-W., Tsai, C.-H., & Wang, Z.-Y. (2012). Torrefied biomasses in a drop tube furnace to evaluate their utility in blast furnace. *Bioresource Technology*, 433-438.

Chen, W.-H., Peng, J., & Bi, X. T. (2015). A state-of-the-art review of biomass torrefaction, densification and applications. *Renewable and Sustainable Energy Reviews*, 847-866.

Chen, W.-H., Zhuang, Y.-Q., Liu, S.-H., Juang, T.-T., & Tsai, C.-M. (2016). Product characteristics from the torrefaction of oil palm fiber pellets in inert and oxidative atmospheres. *Bioresource Technology*, 367-374.

Chiou, B.-S., Valenzuela-Medina, D., Bilbao-Sainz, C., Klamczynski, A. K., Avena-Bustillos, R. J., Milczarek, R. R., . . . Orts, W. J. (2015). Torrefaction of pomaces and nut shellsTorrefaction of pomaces and nut shells. *Bioresource Technology*, 58-65.

Demirbas, A. (1993). Calculation of higher heating values of biomass fuels. *Fuel*, 431-434.

Demirbas, A. (2009). Pyrolysis Mechanisms of Biomass Materials. *Energy Sources, Part A: Recovery, Utilization, and Environmental Effects* , 1189-1193.

Deng, J., Wang, G.-j., Kuang, J.-h., Zhang, Y.-l., & Luo, Y.-h. (2009). Pretreatment of agricultural residues for co-gasification via torrefaction. *Journal of Analytical and Applied Pyrolysis*, 331-337.

Dudynski, M., Van Dyk, J. C., Kwiatkowski, K., & Sosnowska, M. (2015). Biomass gasification: Influence of torrefaction on syngas production and tar formation. *Fuel Processing Technology*, 203-212.

Eden, M. R. (2012). *Inroduction to Aspen Plus Simulation.*

Eikeland, M. S., Thapa, R. K., & Halvorsen, B. M. (2015). Aspen Plus Simulation of Biomass Gasfication with known Reaction Kinetic. *Electronic Conference Proceedings*, (pp. 149-155).

Emami-Taba, L., Irfan, M. F., Daud, W. M., & Chakrabarti, M. H. (2013). Fuel blending effects on the co-gasification of coal and biomass.

Encinar, J., Beltran, F., Bernalte, A., Ramiro, A., & Gonzalez, J. (1996). Pyrolysis of two agricultural residues: Olive and grape bagasse. Influence of particle size and temperature. *Biomass and Bioenergy*, 397-409.

Esther Cascarosa, L. G. (2012). Meat and bone meal and coal co-gasification: Environmental advantages. In *Resources, Conservation and Recycling* (Vol. 59, pp. 32-37).

Fatoni, R., Gajjar, S., Gupta, S., Handa, S., & Elkamel, A. (2014). Modeling Biomass Gasification in a Fluidized Bed Reactor. *Proceedings of the 2014 International Conference on Industrial Engineering and Operations Management*, (pp. 7-9). Bali, Indonesia.

Fazeli, A., Bakhtvar, F., Jahanshaloo, L., Sidik, N. A., & EsfandyariBayat, A. (2016). Malaysia's stand on municipal solid waste conversion to energy: A review. *Renewable and Sustainable Energy Reviews*, 1007-1016.

Jaafar, A. A., & Ahmad, M. M. (2011). Torrefaction of Malaysian Palm Kernel Shell into Value-Added Solid Fuels. *International Journal of Chemical, Biomolecular, Metallurgical, Materials Science and Engineering*, 62-65.

Jangsawang, W., Laohalidanond, K., & Kerdsuwan, S. (2015). Optimum Equivalence Ratio of Biomass Gasification Process Based on Thermodynamic Equilibrium Model. *Energy Procedia*, 520 – 527.

Jayathilake, R., & Rudra, S. (2017). Numerical and Experimental Investigation of Equivalence Ratio (ER) and Feedstock Particle Size on Birchwood Gasification. *energies*, 1-19.

Jenkins, B., Baxter, L., Jr., T. M., & Miles, T. (1998). Combustion properties of biomass. *Fuel Processing Technology*, 17-46.

Kezhong, L., Rong, Z., & Jicheng, B. (2010). Experimental study on syngas production by co-gasification of coal and biomass in a fluidized bed. *35*(7), 2722-2726.

Kong, S.-H., Loh, S.-K., Bachmann, R. T., Rahim, S. A., & Salimon, J. (2014). Biochar from oil palm biomass: A review of its potential and challenges. *Renewable and Sustainable Energy Reviews*, 729-739.

Kumar, A., Jones, D. D., & Hanna, M. A. (2009). Thermochemical Biomass Gasification: A Review of the Current Status of the Technology. *Energies*, 556-581.

Kuo, P.-C., Wua, W., & Chen, W.-H. (2014). Gasification performances of raw and torrefied biomass in a downdraft fixed bed gasifier using thermodynamic analysis. *Fuel*, 1231-1241.

Lee, S., Speight, J. G., & Loyalka, S. K. (2014). *Handbook of Alternative Fuel Technologies.* CRC Press.

Li, H., Liu, X., Legros, R., Bi, X. T., Lim, C., & Sokhansanj, S. (2012). Torrefaction of sawdust in a fluidized bed reactor. *Bioresource Technology*, 453-458.

Malaysian Timber Council. (n.d.). *MTC Wood Wizard - report 103*. Retrieved from MTC Wood Wizard: http://mtc.com.my/wizards/mtc_tud/items/report(103).php

Malaysian Timber Council. (n.d.). *MTC Wood Wizard - report 123*. Retrieved from MTC Wood Wizard: http://mtc.com.my/wizards/mtc_tud/items/report(123).php

Malaysian Timber Council. (n.d.). *MTC Wood Wizard - report 22*. Retrieved from MTC Wood Wizard: http://mtc.com.my/wizards/mtc_tud/items/report(22).php

Malaysian Timber Council. (n.d.). *MTC Wood Wizard - report 54*. Retrieved from MTC Wood Wizard: http://mtc.com.my/wizards/mtc_tud/items/report(54).php

Malaysian Timber Industry Board. (2012). Malaysian Timber Statistics 2009-2011,.

Masiá, A. T., Buhre, B., Gupta, R., & Wall, T. (2007). Characterising ash of biomass and waste. *Fuel Processing Technology*, 1071-1081.

Matali, S., Rahman, N., Idris, S., Yaacob, N., & Alias, A. (2016). Lignocellulosic Biomass solid Fuel Properties Enhancement via Torrefaction. *Procedia Engineering*, 671 – 678.

McKendry, P. (2002). Energy production from biomass (part 2): conversion technologies. *Bioresource Technology*, 47-54.

Medic, D., Darr, M., Shah, A., Potter, B., & Zimmerman, J. (2012). Effects of torrefaction process parameters on biomass feedstock upgrading. *Fuel*, 147–154.

Miranda, M., Arranz, J., & S. Rojas, I. M. (2009). Energetic characterization of densified residues from Pyrenean oak forest. *Fuel*, 2106-2112.

Morley, R. J., Pisupati, S. V., & Scaroni, A. W. (2017, August 24). *Coal utilization* . Retrieved from Encyclopædia Britannica : https://www.britannica.com/topic/coal-utilization-122944

Munawar, S. S., & Subiyanto, B. (2014). Characterization of Biomass Pellet made from Solid Waste Oil Palm Industry. *Procedia Environmental Sciences*, 336-341.

Na, B.-I., Kim, Y.-H., Lim, W.-S., Lee, S.-M., Lee, H.-W., & Lee, J.-W. (2013). Torrefaction of oil palm mesocarp fiber and their effect on pelletizing. *Biomass and bioenergy*, 159-165.

Nhuchhen, D. R., & Salam, P. A. (2012). Estimation of higher heating value of biomass from proximate analysis: A new approach. *Fuel*, 55-63.

Nhuchhen, D. R., Basu, P., & Acharya, B. (2014). A Comprehensive Review on Biomass Torrefaction. *International Journal of Renewable Energy & Biofuels*, 1-56.

Nikoo, M. B., & Mahinpey, N. (2008). Simulation of biomass gasification in fluidized bed reactor using ASPEN PLUS. In *Biomass and Bioenergy* (pp. 1245-1254).

Pala, L. P., Wang, Q., Kolb, G., & Hessel, V. (2017). Steam gasification of biomass with subsequent syngas adjustment using shift reaction for syngas production: An Aspen Plus model. *Renewable Energy*, 484-492.

Parikh, J., Channiwala, S., & Ghosal, G. (2005). A correlation for calculating HHV from proximate analysis of solid fuels. *Fuel, 84*, 487-494.

Parr Instrument Company. (2018, March 19). Retrieved from Instruction manual - Parr Instrument Company: https://www.parrinst.com/download/37709/

Petrucci, R., Harwood, W., Herring, F., & Madura, J. (1993). *General Chemistry* (9th ed.). New Jersey: Pearson.

Phanphanich, M., & Mani, S. (2011). Impact of torrefaction on the grindability and fuel characteristics of forest biomass. *Bioresource Technology*, 1246-1253.

Pimchuai, A., Dutta, A., & Basu, P. (2010). Torrefaction of agriculture residue to enhance combustible properties. *Energy Fuels*, 4638–4645.

Prins, M. J., Ptasinski, K. J., & Janssen, F. J. (2006). Torrefaction of wood Part 2. Analysis of products. *Journal of Analytical and Applied Pyrolysis*, 35-40.

Qing, C., Song, Z. J., Jun, L. B., Feng, M. Q., & Yang, L. Z. (2011, May). Influence of torrefaction pretreatment on biomass gasification technology. *Chinese Science Bulletin*, pp. 1449-1456.

Repellin, V., Govin, A., Rolland, M., & Guyonnet, R. (2010). Energy requirement for fine grinding of torrefied wood. *Biomass and Bioenergy* , 923-930.

Rodrigues, R., Muniz, A. R., & Marcilio, N. R. (2016). Evaluation of Biomass and Coal Co-gasification of Brazillian Feedstock Using a Chemical Equilibrium model. *Brazilian Journal of Chemical Engineering* , 401-414.

Rousset, P., Aguiar, C., Labbé, N., & Commandré, J.-M. (2011). Enhancing the combustible properties of bamboo by torrefaction. *Bioresource Technology*, 8225-8231.

Ruoppolo, G., Miccio, F., Brachi, P., Picarelli, A., & Chirone, R. (2013). Fluidized Bed Gasification of Biomass and Biomass/Coal Pellets in Oxygen and Steam Atmosphere. *Chemical Engineering Transactions*, 595-600.

Saadon, S., Uemura, Y., & Mansor, N. (2014). Torrefaction in the Presence of Oxygen and Carbon Dioxide: The Effect on Yield of Oil Palm Kernel Shell. *Procedia Chemistry 9*, 194-201.

Sabil, K. M., Aziz, M. A., Lal, B., & Uemura, Y. (2013). Effects of torrefaction on the physiochemical properties of oil palm empty fruit bunches, mesocarp fiber and kernel shell. *Biomass and Bioenergy*, 351-360.

Saleh, S., Hansen, B., Jensen, P., & Dam-Johansen, K. (2013). Efficient fuel pretreatment: Simultaneous torrefaction and grinding of biomass. *Energy Fuels* , 7531-7540.

Schuster, G., Loffler, G., Weigl, K., & Hofbauer, H. (2001). Biomass steam gasifcation - an extensive parametric modeling study. *Bioresource Technology*, 71-79.

Shafie, S. M., Othman, Z., & Hami, N. (2017). Potential Utilisation of Wood Residue in KEDAH: A Preliminary Study. *Journal of Technology and Operations Management*, 60-69.

Sheng, C., & Azevedo, J. (2005). Estimating the higher heating value of biomass fuels from basic analysis data. In *Biomass and Bioenergy* (Vol. 28, pp. 499-507).

Siedlecki, M., Jong, W. d., & Verkooijen, A. H. (2011). Fluidized Bed Gasification as a Mature And Reliable Technology for the Production of Bio-Syngas and Applied in the Production of Liquid Transportation Fuels—A Review. *Energies*, 389-434.

Sluiter, A., Hames, B., Ruiz, R., Scarlata, C., Sluiter, J., & Templeton, D. (2008). *Determination of Ash in Biomass* . National Renewable Energy Laboratory.

Sreekala, M. S., Kumaran, M. G., & Thomas, S. (1997). Oil palm fibers: Morphology, chemical composition, surface modification, and mechanical properties. *Journal of Applied Polymer Science*, 821-835.

Sukiran, M. A., Abnisa, F., Daud, W. M., Bakar, N. A., & Loh, S. K. (2017). A review of torrefaction of oil palm solid wastes for biofuel production. *Energy Conversion and Management*, 101-120.

Sumathi, S., Chai, S., & Mohamed, A. (2008). Utilization of oil palm as a source of renewable energy in Malaysia. *Renewable and Sustainable Energy Reviews*, 2404-2421.

Suwatthikul, A., Limprachaya, S., Kittisupakorn, P., & Mujtaba, I. M. (2017). Simulation of Steam Gasification in a Fluidized Bed Reactor with Energy Self-Sufficient Condition. *energies*, 1-15.

Tapasvi, D., Kempegowda, R. S., Tran, K.-Q., Skreiberg, Ø., & Grønli, M. (2015). A simulation study on the torrefied biomass gasification. *Energy Conversion and Management*, 446-457.

The Japan Institute of Energy. (2008). *The Asian Biomass Handbook*.

Then, Y. Y., Ibrahim, N. A., Zainuddin, N., Ariffin, H., Yunus, W. M., & Chieng, B. W. (2014). The Influence of Green Surface Modification of Oil Palm Mesocarp Fiber by Superheated Steam on the Mechanical Properties and Dimensional Stability of Oil Palm Mesocarp Fiber/Poly(butylene succinate) Biocomposite. *International Journal of Molecular Sciences*, 15344-15357.

Thran, D., Witt, J., Schaubach, K., Kiel, J., Carbo, M., Maier, J., . . . Schipfer, F. (2016). Moving torrefaction towards market introduction - Technical improvements and economic-environmental assessment along the overall torrefaction supply chain through the SECTOR project. *Biomass and Bioenergy*, 184-200.

Tran, K.-Q., Trinh, T. N., & Bach, Q.-V. (2016). Development of a biomass torrefaction process integrated with oxy-fuel combustion. *Bioresource Technology*, 408-413.

Tumuluru, J. S., Sokhansanj, S., Wright, C. T., Boardman, R. D., & Hess, J. R. (2011). Review on Biomass Torrefaction Process and Product Properties and Design of Moving Bed Torrefaction System Model Development. *Industrial Biotechnology*, 384-401.

Uemura, Y., Matsumoto, R., Saadon, S., & Matsumura, Y. (2015b). A study on torrefaction of Laminaria japonica. *Fuel Processing Technology*, 133-138.

Uemura, Y., Omar, W. N., Jamaludi, J. I., Yusup, S. B., Tsutsui, T., & Subbarao, D. (2010). Torrefaction of woody biomass in Malaysia. *SCEJ 42nd Autumn Meeting*, 853.

Uemura, Y., Omar, W. N., Tsutsui, T., & Yusup, S. B. (2011). Torrefaction of oil palm wastes. *Fuel*, 2585–2591.

Uemura, Y., Omar, W., Othman, N. A., Yusup, S., & Tsutsui, T. (2013). Torrefaction of oil palm EFB in the presence of oxygen. *Fuel*, 156-160.

Uemura, Y., Saadon, S., Osman, N., Mansor, N., & Tanoue, K.-i. (2015a). Torrefaction of oil palm kernel shell in the presence of oxygen and carbon dioxide. *Fuel*, 171-179.

Vamvuka, D., Kakaras, E., Kastanaki, E., & Grammelis, P. (2003). Pyrolysis characteristics and kinetics of biomass residuals mixtures with lignite. *Fuel*, 1949–1960.

van der Stelt, M., Gerhauser, H., Kiel, J., & Ptasinski, K. (2011). Biomass upgrading by torrefaction for the production of biofuels: A review. *Biomass and Bioenergy*, 3748-3762.

Veerasamy, R., Rajak, H., Jain, A., Sivadasan, S., Varghese, C. P., & Agrawal, R. K. (2011). Validation of QSAR Models - Strategies and Importance. *International Journal of Drug Design and Disocovery*, 511-519.

Vélez, J. F., Chejne, F., Valdés, C. F., Emery, E. J., & Londoño, C. A. (2009). Co-gasification of Colombian coal and biomass in fluidized bed: An experimental study. In *Fuel* (Vol. 88, pp. 424-430).

Wahid, F. R., Harun, N. H., Rashid, S. R., Samad, N. A., & Saleh, S. (2017). Physicochemical Property Changes and Volatile Analysis for Torrefaction of Oil Palm Frond. *Chemical Engineering Transactions, 56*, 199-204.

Wannapeera, J., Fungtammasan, B., & Worasuwannarak, N. (2011). Effects of temperature and holding time during torrefaction on the pyrolysis behaviors of woody biomass. *Journal of Analytical and Applied Pyrolysis*, 99-105.

Yin, C.-Y. (2011). Prediction of higher heating values of biomass from proximate and ultimate analyses. *Fuel*, 1128–1132.

Yusoff, S. (2006). Renewable energy from palm oil - innovation on effective utilization of waste. *Journal of Cleaner Production* , 87-93.

Zaccariello, L., & Mastellone, M. L. (2015). Fluidized-Bed Gasification of Plastic Waste, Wood, and Their Blends with Coal. *energies*, 8052-8068.

Zogała, A. (2014). Equilibrium Simulations of Coal Gasification – Factors Affecting Syngas Composition. *Journal of Sustainable Mining*, 30-38.

APPENDIX A
LIST OF PUBLICATIONS

A – 1 Journals

Harun, N. H., Wahid, F. R., Saleh, S., & Samad, N. A. (2017). Effect of Torrefaction on Palm Oil Waste Chemical Properties and Kinetic Parameter Estimation. *Chemical Engineering Transactions, 56*, 1195-1200.

Wahid, F. R., Harun, N. H., Rashid, S. R., Samad, N. A., & Saleh, S. (2017). Physicochemical Property Changes and Volatile Analysis for Torrefaction of Oil Palm Frond. *Chemical Engineering Transactions, 56*, 199-204.

Wahid, F. R., Muslim, M. B., Saleh, S., & Samad, N. A. (2016). Integrated Gasfication and Fuel Cell Framework: Biomass Gasification Case Study. *ARPN Journal of Engineering and Applied Sciences*, 2673-2680.

Wahid, F. R., Saleh, S., & Samad, N. A. (2017). Estimation of Higher Heating Value of Torrefied Palm Oil Wastes from Proximate Analysis. *Energy Procedia*, 307-312.

A – 2 Conferences (Oral Presentation)

Muslim, M. B., Wahid, F. R., Saleh, S., & Samad, N. A. (2015). Application of Integrated Biomass Gasification and Proton Exchange Membrane Fuel Cell for Power Production. *28th Symposium of Malaysian Chemical Engineers.*

Wahid, F. R., Harun, N. H., Saleh, S., & Samad, N. A. (2017). Effect of Torrefaction on Forestry Residue Physicochemical Properties. *Alternative Energy in Developing Countries and Emerging Economies (AEDCEE 2017).*